ORGANELLAR RIBONUCLEASES AND POLY(A) POLYMERASES IN *CHLAMYDOMONAS REINHARDTII*

A Dissertation

Presented to the Faculty of the Graduate School

of Cornell University

In Partial Fulfillment of the Requirements for the Degree of

Doctor of Philosophy

by

Sara Lana Zimmer

August 2008

ORGANELLAR RIBONUCLEASES AND POLY(A) POLYMERASES IN *CHLAMYDOMONAS REINHARDTII*

Sara Lana Zimmer Ph. D.

Cornell University 2008

RNA catabolism occurs in multiple cellular compartments. This study used the unicellular photosynthetic eukaryote *Chlamydomonas reinhardtii* to identify a small suite of putatively organellar, nucleus-encoded prokaryotic-like ribonucleases and poly(A) polymerases (PAPs) that may participate in this process. Other related genes encoded putative exosome components, but no nucleus or cytosol-specific exosome activating factors. A surprisingly large family of nine non-canonical PAPs were hypothesized to play a regulatory role in RNA degradation.

The well-studied *E. coli* poly(A)-mediated RNA degradation pathway was the model used to predict and test the roles of candidate genes in chloroplast RNA catabolism. The pathway initiates with an endonucleolyic cleavage event, followed by polyadenylation of the resultant 3' end, which stimulates 5'→3' exoribonucleolytic degradation. Unlike *E. coli*, *Chlamydomonas* has no RNase E and thus utilizes another enzyme, possibly RNase J1, as an endonuclease. Transient depletion of *RNJ1* mRNA showed a very mild effect on chloroplast transcripts. As in *E. coli*, one hydrolytic (RNB2) and one phosphorolytic (Polynucleotide phosphorylase: PNPase) exoribonuclease may play a role in RNA decay. PNPase depletion caused an

increase in *RNB2* expression, but no profound alterations in the processing or steady state level of chloroplast RNA that would be expected if it were the sole exoribonuclease. Thus, it was concluded that there is likely to be some functional redundancy between these enzymes. PNPase depletion also revealed unique functional aspects, since it resulted in defects in acclimation to phosphate limitation, and was shown to be responsible for both polyadenylation and poly(A) tail degradation in the chloroplast.

Comparative analysis of *Arabidopsis* and *Chlamydomonas* nucleotidyltransferases suggested that *Chlamydomonas* PAP4 but not PAP3 is likely to be mitochondrially localized. Recombinant PAP4 has polyadenylation activity, and when expressed in *E. coli* can partially complement a PAP1 (*pcnB*) mutant. Although PAP4 appeared to be mitochondrially targeted, its depletion affected neither mitochondrial poly(A) nor novel U-rich tails.

Taken together, these studies have identified candidate genes encoding ribonucleases and poly(A) polymerases, elucidated some of the functions of PNPase in the chloroplast, characterized the biochemical activity of PAP4, and characterized polynucleotide tails in the mitochondria of *Chlamydomonas reinhardtii*.

BIOGRAPHICAL SKETCH

Sara Zimmer was born in St. Cloud, Minnesota to Rose Ann and Allen Zimmer. Her first interest in science was revealed when she checked every book on astronomy out of her grade school library. In the eighth grade, the topic of genetics was first introduced, and it was her new knowledge of this subject that began her relationship with the genetic code and its expression that would be the subject of her future work. She attended Michigan Technological University in Houghton, Mi, and in 1996 received dual Bachelors of Science degrees in Biological Sciences and Chemical Engineering. During her undergraduate years, she completed internships with the Wisconsin Department of Natural Resources, 3M Company, and most importantly, Promega Corporation, where she acquired her first skills at the laboratory bench. After graduation she pursued a Nordic ski racing career at the national level for five years, and was ranked as high as ninth nationally and third on the ski marathon circuit. During this time she continued to develop her laboratory skills as a technician in the laboratory of Dr. Benjamin Clarke at the University of Minnesota Duluth School of Medicine. She resumed her education in 2002, moving to Ithaca, New York with her husband to begin graduate school at Cornell University, where she joined the laboratory of Dr. David Stern. During her graduate work, she had two sons and traveled to Israel to collaborate with Dr. Gadi Schuster. In 2008 she received her Ph.D. in Biochemistry, Molecular and Cell Biology.

To my family: even when you don't understand what I do, you always support my endeavors. Thank you.

ACKNOWLEDGMENTS

I would like to thank David Stern for his mentorship and enthusiasm for this research endeavor. I am grateful to all members of the Stern Laboratory for the numerous ways they have helped me. I will specifically mention Shlomit Yehudai-Resheff and Yoshiki Nishimura, with whom my collaborations resulted in published material. Tom Bollenbach helped me both with research advice and manuscript revision. I am indebted to Gadi Schuster and Aleks Schein at Technion University for their help and expertise in enzyme purification. Zhangjun Fei at the Boyce Thompson Institute provided guidance and data for the bioinformatic portion of this dissertation. The technical expertise and teaching skills of Helene Javot, manager of the Plant Cell Imaging Center (PCIC) at the Boyce Thompson Institute was vital for the generation of the microscopy data in this dissertation. The PCIC is funded by an award from the TRIAD Foundation, and microscopes were purchased with an award from the NSF (NSF DBI-0618969). My participation in this work was funded by an NIH training grant from 2002-2004, followed by grants from the United States-Israel Binational Agricultural Research and Development Fund (BARD IS-3605-04CR), NSF (9975765, DBI-0211935, and 0646350), and the Binational Science Foundation (2005184) to D. B. S. and Gadi Schuster.

TABLE OF CONTENTS

LIST OF FIGURES

LIST OF TABLES

CHAPTER 1
INTRODUCTION

RNA processing is essential for the expression of a genome. It is required for the conversion of transcripts to their mature forms, the decay of aberrant transcripts, and RNA turnover, all of which are facets of gene regulation. Because defects in RNA decay can lead to disease phenotypes in all organisms, understanding the regulation of decay is an important focus of study. Before regulation can be adequately addressed, however, the basic mechanisms and enzymes involved must be elucidated. This work focuses on an RNA degradation pathway and its constituent enzymes in the chloroplast of the model organism *Chlamydomonas reinhardtii*.

OVERVIEW OF CHLAMYDOMONAS

Chlamydomonas is a single-celled aquatic and soil alga. It can be cultured in the laboratory on both solid agar and in liquid medium. The ease of its laboratory propagation, and a doubling time of as little as eight hours under ideal conditions, are both reasons it has become a model organism. The alga is motile by virtue of its two flagella, and responds to light with positive phototaxis, and many laboratories use it as a model for the study of motility. Significant for the purposes of this dissertation, its single large chloroplast and its ability to grow either photoautotrophically or heterotrophically, facilitate the use of *Chlamydomonas* as a model for studies of photosynthesis.

Historically, researchers of chloroplast function and gene expression have taken advantage of the genetic properties of *Chlamydomonas*. The

haploid alga will undergo gametogenesis under nutrient starvation, and mating of *Chlamydomonas* results in a diploid zygote that eventually sporulates, yielding four haploid progeny. Mating can be utilized to establish linkage and generate strains with multiple mutations, and indeed genetics has long been employed in the analysis of chloroplast function. Finally, the nuclear, chloroplast and mitochondrial genomes can all be stably transformed, and a near-fully sequenced nuclear genome has completed a set of tools facilitating reverse as well as forward genetic studies.

THE CHLOROPLAST GENOME UNDER NUCLEAR CONTROL

The chloroplast originated from an endosymbiotic event in which a cyanobacterial-like ancestor was engulfed by a larger cell. Over time, much of the genetic material of the endosymbiont was transferred to the nuclear genome, and now the plant or algal chloroplast contains only a small remnant of the original genome. Chloroplast genomes contain approximately 120 genes encoding enzymes of the photosynthetic pathway, a full complement of tRNAs and several genes required for transcription and translation, including the core components of a eubacterial-like RNA polymerase. The chloroplast, however, contains over 2,000 proteins, most of which are nucleus-encoded and targeted to the chloroplast by virtue of an N-terminal transit peptide, for diverse functions ranging from gene expression to central metabolism.

Regulatory factors are an important subset of these proteins. Examples of these are a sigma^{70}-like factor regulating the plastid-encoded RNA polymerase (Bohne *et al.*, 2006), ribosomal proteins that regulate the core chloroplast translational apparatus (Marin-Navarro *et al.*, 2007), and factors

such as those that regulate splicing of *psbA* (reviewed in Herrin and Nickelsen, 2004). The regulatory role of these factors is indicated by their involvement in the expression of only one or a small subset of chloroplast genes, or their participation in chloroplast responses to environmental or developmental cues (Barkan and Goldschmidt-Clemont, 2000). By maintaining genes encoding regulatory proteins in the nucleus, the control of chloroplast activities remains under the sphere of influence of the whole cell.

STABILITY OF CHLOROPLAST RNA

Global changes in chloroplast transcription occur during chloroplast differentiation in plants (Deng and Gruissem, 1987), and are associated with circadian rhythms in *Chlamydomonas* (Hwang *et al.*, 1996; Salvador *et al*, 1993); however, transcriptional regulation of individual plastid genes is not typical. Rather, gene regulation tends to take place at the post-transcriptional level (Monde *et al.*, 2000; Herrin and Nickelsen, 2004; Marín-Navarro *et al.*, 2007). For example, there are numerous examples of translational regulation of chloroplast proteins. A well-studied case is the D1 subunit of the photosystem II reaction center, which is unstable under photoinhibiting light. D1 undergoes rapid replacement synthesis under these conditions, but abundance of the encoding *psbA* mRNA does not change (Schuster *et al.*, 1988). A mechanism applicable to many chloroplast protein complexes is CES (Control by Epistasy of Synthesis). Here, the absence of a member of a protein complex attenuates the rate of synthesis of another subunit in the complex. The subunit whose synthesis is assembly-dependent is called a CES

protein, and at least one CES protein has been observed in photosystem I, photosystem II, ATP synthase, and the cytochrome *b6f* complex in chloroplasts (Choquet and Wollman 2002). In another example of CES, the rate of synthesis of the chloroplast-encoded large subunit of Rubisco is dependent on the amount of nucleus-encoded small subunit, while large subunit mRNA levels remain unaffected (Khrebtukova and Spreitzer, 1996; Rodermel *et al.*, 1999; Wostrikoff and Stern, 2007).

Regulation of RNA stability is another way chloroplast gene expression is controlled, and it is the major focus of this study. Chloroplast RNA (cpRNA) stability, as measured by transcript half-life, varies widely. For example, mRNA half-lives in barley chloroplasts were found to range from 6 to over 40 hours (Kim *et al.*, 1993). In *Chlamydomonas, tufA* mRNA has a half-life of less than 2 hours, while *rbcL* has a much longer half-life of 21 hrs under the same growth conditions (Salvador *et al.*, 1993). The same study showed that relative rates of transcript decay vary under different conditions; the half-life of *rbcL* mRNA increases by over five-fold in darkness versus light, while the *tufA* half-life merely doubles.

Although global *cis*-acting stability factors such as 3' stem-loops have been found to stabilize most chloroplast mRNAs (Stern and Gruissem, 1987), and some nucleus-encoded *trans*-acting factors have been identified or predicted, much needs to be done to characterize the activities and functions of these factors. For example, although the nucleus-encoded protein MCD1 that stabilizes *Chlamydomonas petD* RNA (Drager *et al.*, 1998) has been identified and the corresponding gene cloned (Murakami *et al.*, 2005), its mechanism of action is still poorly understood. In the *Arabidopsis* mutant *hcf145*, the tricistronic *psaA-psaB-rps14* transcript is destabilized. Although

the gene has been mapped to the upper arm of chromosome 5, the mutant protein causing this destabilization has yet to be identified (Lezhneva and Meurer, 2004). Some protein families, such as the RNA-binding pentatricopeptide repeat proteins, are expanded in plants hypothetically because of their involvement in chloroplast gene expression including RNA stability, but have only limited functional characterization (Saha *et al.*, 2007).

As with chloroplast RNA stability factors, the identification of roles played by the core chloroplast RNA degradation machinery described in this dissertation is still in its early stages. An anticipated result of studying the basic components of cpRNA decay is that once our understanding of these enzymes increases, the mechanisms by which *cis* and *trans* factors either enhance or attenuate the actions of the core machinery might be elucidated.

E. COLI *AS A MODEL SYSTEM FOR POLY(A)-MEDIATED RNA DECAY*

A reverse genetic approach is the mode I chose to study cpRNA degradation enzymes. By using this method, I took advantage of current knowledge of decay pathways and enzymes in other relevant organisms. Since the chloroplast genome has prokaryotic ancestry, it is not surprising that many enzymes and aspects of chloroplast RNA degradation are similar to those of the well-characterized *E. coli* pathway, which is described here.

Degradation begins in *E. coli* with endonucleolytic cleavage of an mRNA, thought to occur in the translation initiation region, followed by additional cleavages in AU-rich stretches of other parts of the transcript by RNase E (Kushner, 2002). Transcript 3' untranslated regions (UTRs) end in an

inverted repeat that can fold into a stable stem-loop structure, protecting the transcript against digestion by processive exoribonucleases (Stern *et al.*, 1984). However, after RNase E cleavage, the newly-generated 3' ends are vulnerable to 3'-5' exonucleolytic degradation by RNase II and/or the reversible enzyme polynucleotide phosphorylase (PNPase; Regnier, 2000; Carpousis, 2007). Both of these enzymes are inhibited by secondary structure (Coburn and Mackie, 1996; Yehudai-Resheff and Schuster, 2000). While PNPase or RNase II mutants are viable, a PNPase/RNase II double mutant will transiently accumulate high levels of cleavage intermediates before the cell dies, suggesting that these are the primary enzymes responsible for the 3'-5' exonucleolytic degradation of mRNA (Donovan and Kushner, 1986). Finally, RNase II and PNPase are unable to completely degrade the intermediates. The last two to five nucleotides are degraded by oligoribonuclease (Ghosh and Deutscher, 1999).

One prominent feature of eubacterial RNA degradation is the destabilizing influence of poly(A) tails. In *E. coli*, poly(A) polymerase (PAP I) is predominantly (75-95% of total activity) responsible for polyadenylating the 3' terminus following endonucleolytic cleavage, with PNPase being responsible for the remaining activity (Mohanty and Kushner, 2000a). Polyadenylated RNA is the preferred substrate for PNPase, and a 20nt poly(A) tail is a sufficient toe-hold for PNPase or the degradosome, a multiprotein complex that contains PNPase (Carpousis, 2007), to begin processive degradation (reviewed in Littauer and Soreq, 1982). When PNPase reaches a region of RNA secondary structure, local melting may allow one or two nucleotides in the terminus of the structured region to be degraded before PNPase falls off the transcript. PAP I can then readenylate this transcript, again providing a platform for PNPase

degradation, which this time progresses slightly further before requiring another cycle of polyadenylation. This process would also likely include the activity of RhlB, a helicase of the degradosome, to facilitate the degradosome's processing of secondary structure. Eventually, when all significant secondary structure has been removed on a decay intermediate, fully processive degradation by PNPase and RNase II can begin (model reviewed in Coburn and Mackie, 1999; Régnier and Arraiano, 2000).

The pathway described above is supported by the fact that PAP I is necessary *in vitro* for degradation of at least one 3' terminus, the 147-residue RNase E cleavage product of the *rpsT* mRNA, and at least some of its internal degradation intermediates are polyadenylated as well (Coburn and Mackie, 1999). It should be noted that *E. coli* PAP I is unable to add tails to transcripts with terminal stem-loops *in vitro* unless two to six unpaired nucleotides are added to the end of a stem-loop (Yehudai-Resheff and Schuster, 2000), which may appear incongruent with a model where this enzyme is supposed to generate an unstructured platform on the end of a structured region of RNA. It is also possible that the main role for a polyadenylated tail is only to make the overall process of catabolizing RNA decay intermediates more efficient, or to direct the degradation machinery to cleavage products rather than mature, active transcripts. Interestingly, RNase II can actually play an inhibitory role in degradation at the 3' terminus (Hajnsdorf *et al.*, 1994; Pepe *et al.*, 1994), and in overall transcript stability (Mohanty and Kushner, 2003), possibly by preventing the more processive degradosome from accessing the 3' ends (Mohanty and Kushner, 2003).

While *E. coli* is a well-studied model, it is not representative of all prokaryotes. For example, the only PAP-like enzyme in *Bacillus subtilis* is

actually a CCA nucleotidyltransferase (Raynal *et al.*, 1998). Additionally, *B. subtilis* lacks RNase E, but instead possesses two other endoribonucleases, RNases J1 and J2, thought to be paralogues (Even *et al.*, 2005). Although *E. coli* lacks a 5' → 3' exonuclease, and this seems to be a common feature of prokaryotic RNA degradation, 5' → 3' exonuclease activity has also been attributed to RNase J1 (Mathy, 2007; Deikus *et al.*, 2008). Another example of differences in enzyme roles can be found in *Synechocystis*, a relative of the chloroplast progenitor. Inactivation of either PNPase or RNase II in *Synechocystis* is lethal (Rott *et al.*, 2003), suggesting that both enzymes have essential functions, rather than being partially redundant as in *E. coli*. Additionally, there is no degradosome complex in *Synechocystis* (Rott *et al.*, 2003). The diversity in prokaryotic RNA degradation mechanisms raises the question of which aspects have been retained in the chloroplast, and whether aspects of chloroplast RNA decay are consistent among species.

OVERVIEW OF CHAPTER ORGANIZATION

In Chapter 2 I will outline a model for chloroplast poly(A)-mediated RNA degradation that is based on the *E. coli* pathway described in this Introduction, and will identify the putative enzymes involved in each step of the pathway in *Chlamydomonas*. Results of experiments designed to define the roles of the putative ribonucleases will also be shown. Chapter 3 contains experiments that investigate potential polyadenylation enzymes of the cpRNA decay pathway, and also show that polyadenylation appears to play a role in mitochondrial RNA degradation. Chapter 4 is a genomic analysis of

ribonucleases and poly(A) polymerases on the whole-organism scale. Finally, I will close with a vision for the directions this research could take in the future.

CHAPTER 2

THE ENZYMOLOGY OF CHLOROPLAST RNA DECAY IN *CHLAMYDOMONAS*, WITH AN EMPHASIS ON POLYNUCLEOTIDE PHOSPHORYLASE *

ABSTRACT

Modulation of transcript stability is an important way in which chloroplast gene expression is controlled. Mechanisms of this regulation, evidenced by transcripts of varying half-lives, appear to differ in organelles and microbes with a similar basic RNA degradation pathway. Understanding the core machinery of chloroplast (cp) RNA degradation will help to elucidate how control of this process is implemented.

Chloroplast RNA degradation occurs at least in part via a poly(A)-mediated pathway. The *Chlamydomonas* nuclear genome encodes homologues of each of the known plant chloroplast endonucleases CSP41a and b and RNase J1, a poly(A) polymerase (PAP), two hydrolytic exonucleases RNB1 and RNB2, and the phosphorolytic exonuclease polynucleotide phosphorylase (PNPase). Notably, RNase E, which initiates RNA decay in *E. coli* and is found in plant and some algal chloroplasts, is not

* Data from Nishimura, Y., Kikis, E. A., Zimmer, S. L., Komine, Y., and Stern, D. B. (2004) Antisense transcript and RNA processing alterations suppress instability of polyadenylated mRNA in *Chlamydomonas* chloroplasts. Plant Cell **16**: 2849-2869 are included in this chapter.

Also parts of this chapter are data and some text from Yehudai-Resheff, S., Zimmer, S. L., Komine, Y., and Stern, D. B. (2007) Integration of chloroplast nucleic acid metabolism into the phosphate deprivation response in *Chlamydomonas reinhardtii*. Plant Cell **19**: 1023-1038. Text contributed by other authors is enclosed in quotation marks.

encoded in *Chlamydomonas*. I tested certain of these proteins for (1) the likelihood of being located in the chloroplast; (2) the impact of their depletion on chloroplast transcripts; and (3) in the case of PNPase, the effect of its depletion during phosphate limitation and its likely quaternary structure.

Confocal microscopy of tomato protoplasts expressing putative ribonuclease transit peptides fused to GFP demonstrated that RNB2 but not RNB1 was likely to reside in the chloroplast. Although silencing of RNB2 was not successful, a PNPase RNAi strain contained 10% of the wild-type PNPase level and in this strain, *RNB2* expression increased. Transient RNase J1 depletion appeared to result in the accumulation of RNA decay intermediates. A lack of significant changes in the sizes or abundance of transcripts resulting from PNPase depletion suggested that RNB2 and PNPase are redundant for bulk RNA accumulation and 3' end processing. However, PNPase depletion did stabilize a reporter transcript ending in 28 adenosines, suggesting a specialized function in the decay of polyadenylated RNA. The PNPase depleted strain also exhibited a lack of accumulation of cpRNA normally observed upon phosphate limitation, suggesting that under some conditions it is rate-limiting for cpRNA decay. Finally, analysis by gel filtration suggests that at least some of PNPase may exist as a homotrimer in *Chlamydomonas*. Taken together, these data suggest that some the RNA decay factors and/or their functions in *Chlamydomonas* chloroplasts differ from those in plant chloroplasts and in *E. coli*.

INTRODUCTION

Expression of chloroplast gene products is tightly linked to plant growth and development, and is essential for plant and algal survival. Since components of photosynthetic complexes are encoded in both nuclear and chloroplast genomes, their coordinated expression and accumulation requires precise regulation of chloroplast gene expression. This regulation occurs to some extent at the level of RNA stability. In Chapter 1, I discussed the *E. coli* poly(A)-mediated RNA decay pathway. A related pathway also utilizing the steps of endonucleolytic cleavage, polyadenylation, and 3'→5' exonucleolytic degradation is thought to function in chloroplast RNA decay, and is a probable target of regulation by RNA stability.

The focus of this chapter is on ribonucleases that ultimately determine the stabilities of chloroplast transcripts. These ribonucleases in *Chlamydomonas* were originally identified from gene models, which are software-generated putative proteins from potential gene loci generated across the entire genome by the Joint Genome Institute (Walnut Creek, CA). The silencing of putative chloroplast ribonucleases and analyses of the effects was a major goal of this research. The second goal of this chapter was a more thorough investigation into the activity of PNPase, and particularly how effects of phosphate (P) limitation on chloroplast RNA stability may be conveyed though this enzyme.

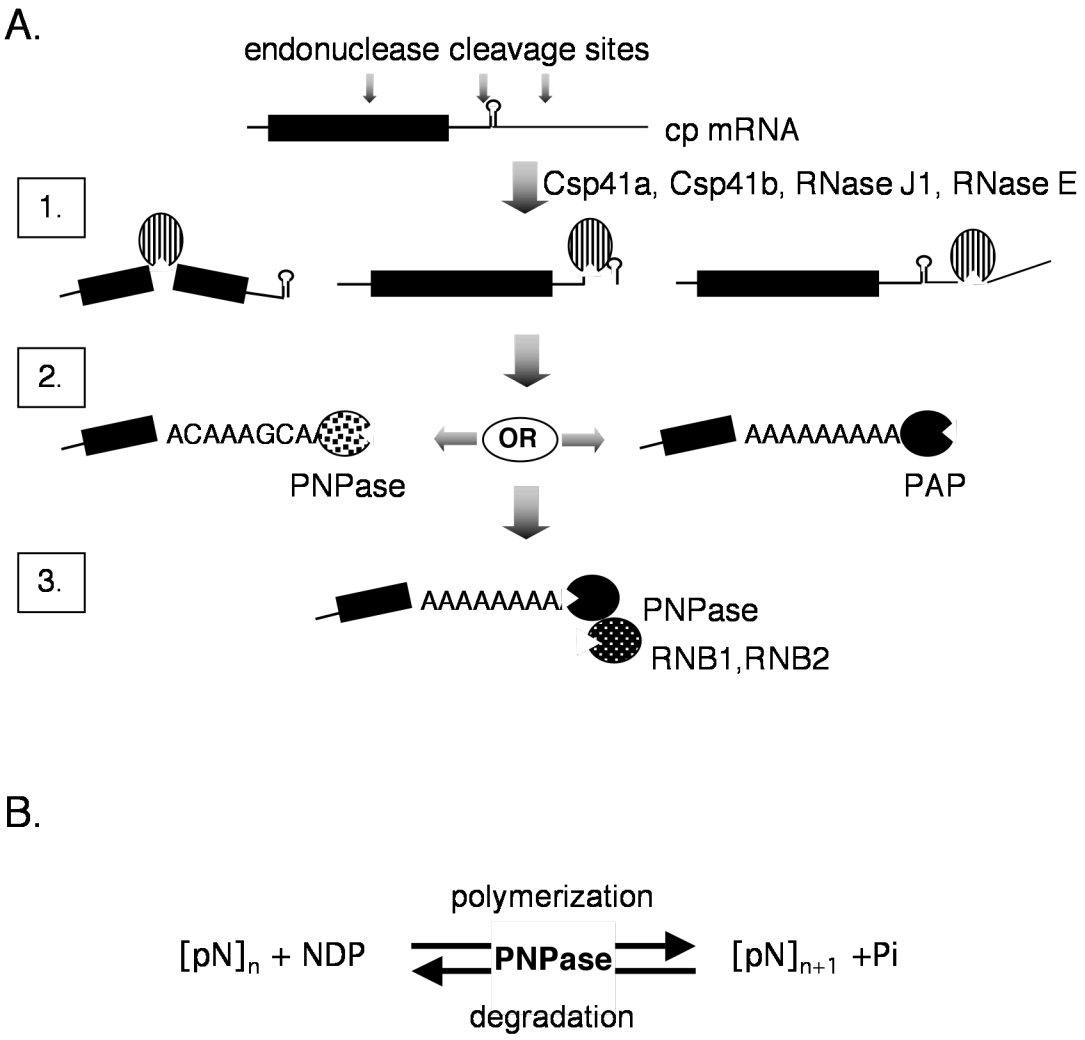

Figure 2.1: Possible roles of enzymes in cpRNA decay.
A. An overview of the degradation process and the enzymes that could potentially act at each step. The pathway initiates with endonucleolytic cleavages such as those shown in Step 1, followed by polyadenylation (Step 2) to mediate exonucleolytic decay (Step 3). Since PNPase has two demonstrated activities, it could act in more than one step of the pathway. B. The readily-reversible reaction catalyzed by PNPase.

Chloroplast poly(A)-mediated RNA decay

Genes encoding putative and known enzymes involved in chloroplast RNA degradation have been identified, but relatively little is known about their substrate specificity, regulation, or relative contribution to decay *in vivo*. The candidate enzymes are shown in Figure 2.1A. Although a degradosome complex is not present in spinach chloroplasts (Baginsky *et al.*, 2001), RNase E homologues appear to exist in all higher plants, and a truncated version of *Arabidopsis* RNase E was found to have activity similar to that of the *E. coli* enzyme (Schein *et al.*, 2008). Another endonuclease, CSP41a, was found to be chloroplast-targeted in spinach (Chen *et al.*, 1995; Yang *et al.*, 1996). CSP41a preferentially cleaves at stem-loops (Yang and Stern, 1997), unlike RNase E, which is specific to single-stranded RNA. Like RNase E of bacteria, however, it has been demonstrated to initiate mRNA turnover (Bollenbach *et al.*, 2003). A homolog of CSP41a, CSP41b, is also chloroplast-targeted and is currently being studied in our laboratory. Both of these enzymes in *Chlamydomonas* have been associated with ribosomes but not with their individual subunits (Yamaguchi *et al.*, 2003), provoking speculation that either these enzymes are necessary to hold complete ribosomes together prior to activation, or that these enzymes are important for correct mRNA processing, which then facilitates or permits translation. CSP41b has also been implicated in rRNA maturation in *Arabidopsis* chloroplasts (Beligni and Mayfield, 2008). An additional endonuclease candidate is RNase J1, since homologues of the *Bacillus* enzyme are encoded in plant and algal genomes.

Putative polyadenylation enzymes and exonucleases that could function in *Chlamydomonas* cpRNA decay were identified in the genomic analysis described in Chapter 4. These include PAP4 and PNPase as potential PAPs,

and PNPase, RNB1 and RNB2 as exonucleases. Plants encode homologues of each of these enzymes, but some differences are apparent. For example, the chloroplast RNase II/R family member in *Arabidopsis*, RNR1, appears to act primarily in rRNA processing (Bollenbach et al., 2005), whereas I hypothesize below that *Chlamydomonas* RNB2 but not RNB1 has a role in RNA turnover. Finally, a nuclease domain corresponding to that of oligoribonuclease, which is presumably necessary to degrade RNA intermediates down to the single nucleotide level, was found in the *Chlamydomonas* genome (Chapter 4), but the gene model, ORN1, is incomplete.

The potential role for phosphate in modulation of cpRNA decay

Phosphate deficiency is a problem in many of the world's soils, often existing in amounts lower than other required ions (Vance *et al.*, 2003). Plants and algae have evolved mechanisms to maintain phosphate homoeostasis. This includes things such as activating P transporters, releasing phosphatases into the extracellular environment, and mobilizing intracellular stores of phosphate (Grossman, 2000; Misson *et al.*, 2005). Since one pool of intracellular phosphate is nucleic acid, it is possible that the action of exoribonucleases and RNA decay might play a role in a cell's response to fluctuating levels of P in the environment. RNA degradation by a hydrolytic exonuclease such as RNB2 might be a first step in the release of phosphate from this source (Green, 1994). The phosphorolytic PNPase also could play a role in P mobilization, but in this case, a cessation of its catabolism is necessary to preserve P.

This apparent paradox is explained by the readily-reversible reaction catalyzed by PNPase, shown in Figure 2.1B. Since PNPase utilizes P in RNA degradation, its activity in this direction would not be desired when P was scarce. However, when the reaction proceeds in the opposite direction, PNPase uses nucleotide diphosphates (NDPs) to extend the nucleotide chain, releasing P as a product. Therefore, cells could potentially utilize the regulation of PNPase as a way to respond to P starvation.

RESULTS

Identification of potential enzymes of the poly(A)-mediated degradation pathway

My study of *Chlamydomonas* cpRNA decay initiated just after the first draft of the sequenced genome became available. Work performed in my capacity as an annotator of the genome increased my familiarity with the tools and techniques used to analyze computer-generated gene models available on the genome browser. Annotation categories assigned to me and David Stern included: snRNAs, RNA binding proteins, tetratricopeptide repeat (TPR) proteins, RNA processing and splicing proteins, and the location of rRNA genes. Our contributions are included in Merchant *et al.* (2007).

Sequence information and a genome browser coupled with an improved method to silence genes by RNAi (Rohr *et al.*, 2004), provided a way to investigate cpRNA degradation in *Chlamydomonas*. Analysis of the first draft of the genome revealed candidate genes of a poly(A)-mediated degradation pathway, summarized in Table 2.1. The table also delineates the level to which I was able to study each of them. One enzyme apparently not encoded

in *Chlamydomonas* was RNase E. A protein BLAST search using the *Arabidopsis* RNase E produced one hit in the moss *Pyscomitrella patens* and one in the primitive alga *Ostreococcus tauri* but none in *Volvox*, a close relative of *Chlamydomonas*, suggesting that the absence of a chloroplast RNase E is more an exception than a rule. This also suggests that initiation of transcript decay in *Chlamydomonas* chloroplasts may be catalyzed by factors different from those of most chloroplast systems.

Table 2.1: Summary of enzymes studied in Chapter 2.

Enzyme type	*C.r.* gene	Protein	My contribution
Endoribonuclease	*CSP41a*	Csp41a (RAP41)	Evaluated expression.
	CSP41b	Csp41b (RAP38)	Evaluated expression.
	RNJ1	RNase J1	Evaluated expression, supervised cDNA sequencing and antibody production, transiently silenced and evaluated the impact on chloroplast transcripts.
Nucleotide Polymerase	*PAP4*	PAP4	See Chapter 3.
	PNP1	PNPase	Evaluated expression, supervised the sequencing of the cDNA, made the antibody, silenced the gene, determined the role of PNPase in the chloroplast *in vivo*. Determined size of native PNPase complex.
Exoribonuclease	*PNP1*	PNPase	Listed above.
	RNB1	Rrp44	Evaluated expression, determined localization.
	RNB2	RNase II/R	Evaluated expression, supervised sequencing, determined localization, and transiently silenced.
	ORN1	Oligoribo-nuclease	Not evaluated

Many of the genes in Table 2.1 needed to be fully sequenced before studying them further. Due to the high GC content of the genome, this was not always straightforward. With the assistance of Steve MacKinnon, who was a Univ. Waterloo (Canada) intern in the laboratory, cDNAs encoding PNPase, RNB2, RNase J1 and PAP4 were sequenced in preparation for further analysis.

Candidate gene expression in Chlamydomonas *cultures of different cell densities*

One way to approach the control of cpRNA stability is to investigate the expression levels of decay enzymes in conditions where RNA stability may be altered, such as light/dark conditions, varying nutrient levels and during different phases of culture growth. In bacteria, growth phase effects on RNA stability are well-known (Bernstein *et al.*, 2004). Furthermore, *Chlamydomonas* cells grown in +P and –P, studied in later experiments, attain different cell densities due to variable growth rates. As we were comparing expression of ribonuclease-encoding genes at these times, it was important to know if any of the changes in mRNA or protein level of various factors as a result of P limitation can also be ascribed to altered cell density, irrespective of P concentration. If such phenomena were found, I would be required to tease apart these two possibly interrelated influences. I analyzed expression levels of the genes listed in Table 2.1, with the exception of *ORN1*, during different phases of cell density. Figure 2.2 shows that for the most part, the density of cells in a culture could not be correlated with any expression pattern for the genes of interest. Most genes showed consistent expression at the RNA level

from early log phase (1 x 10^6 cells/ml), to a five day-old culture that has likely been in stationary phase for 24-48 hours.

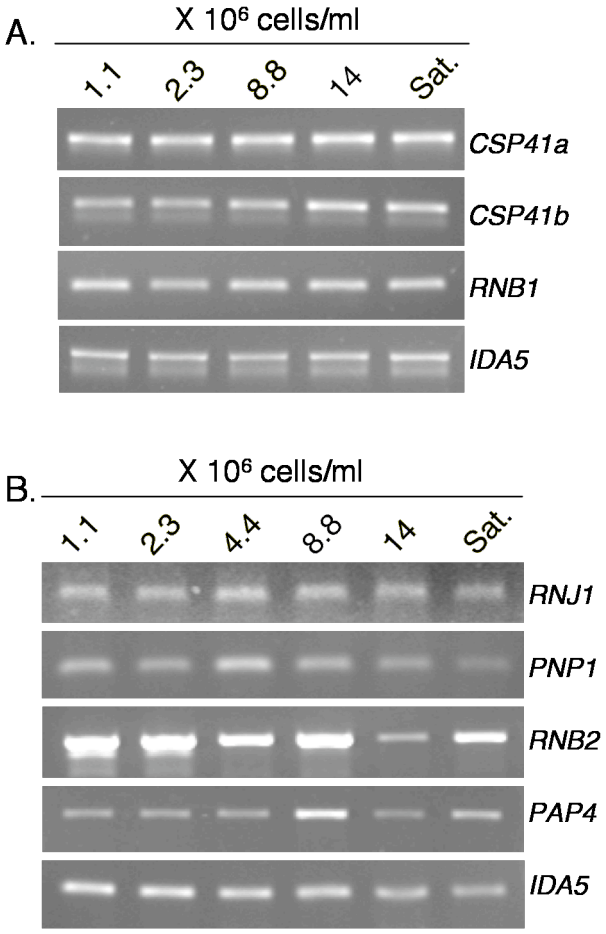

Figure 2.2: Selected nuclear genes show little change in expression at the RNA level during growth of a *Chlamydomonas* culture.
A. RT-PCR was performed on RNA from cultures at the cell densities listed B. The same RT-PCR but with an additional concentration of 4.4x10^6 cells/ml (lane 3). In both groups, amplification of the actin gene (*IDA5*) is used as a loading control. "Sat." indicates a saturated culture.

An exception is *PNP1*, which showed a slight decrease in expression at the final two culture densities in several repetitions. Cultures in the +P and –P studies were likely harvested before achieving this density, so this result was not pursued further. Another enzyme that possibly saw a change in expression

over the course of cell growth in culture was *RNB2*, but of all the expression profiles this one was the most variable. A more consistent increase or decrease during the course of the experiment could point to an effect of cell density on expression, but what was observed here could be experimental variability.

Localization of candidate proteins

Table 2.2: Predicted and actual locations of *Chlamydomonas* proteins potentially involved in chloroplast RNA decay.

Protein	Predicted localization[1]			Location in other organisms[1]	Empirical location[1]
	TargetP	Predotar	iPSORT		
Csp41a	mt	mt	mt	cp (Spinach)	cp (proteomics)
Csp41b	cp	cp	mt	cp (Spinach)	cp (proteomics)
RNase J1	cp	neither	cp	cp (*Arabidopsis*), unpublished data	
PAP4	cp	cp	mt		mt
PNPase	cp	neither	mt	Higher plants have two paralogues: chloroplast and mitochondrial	cp
RNB1	cp	neither	neither	Homologues in *Arabidopsis* are either not organellar, or are dual-targeted	neither
RNB2	cp	cp	mt		cp

[1]cp: chloroplast; mt: mitochondrial; neither: program did not predict localization to either organelle.

Csp41a and Csp41b are already known to be chloroplast-localized in *Chlamydomonas* (Yamaguchi *et al.*, 2003), and the *Chlamydomonas* PNPase more closely resembles the chloroplast than the mitochondrial PNPase of

higher plants. The laboratory also has unpublished evidence of chloroplast localization of *Arabidopsis* RNase J1. This left the locations of RNB1, RNB2, and PAP4 as unknown. Table 2.2 summarizes protein targeting predictions for each of these proteins.

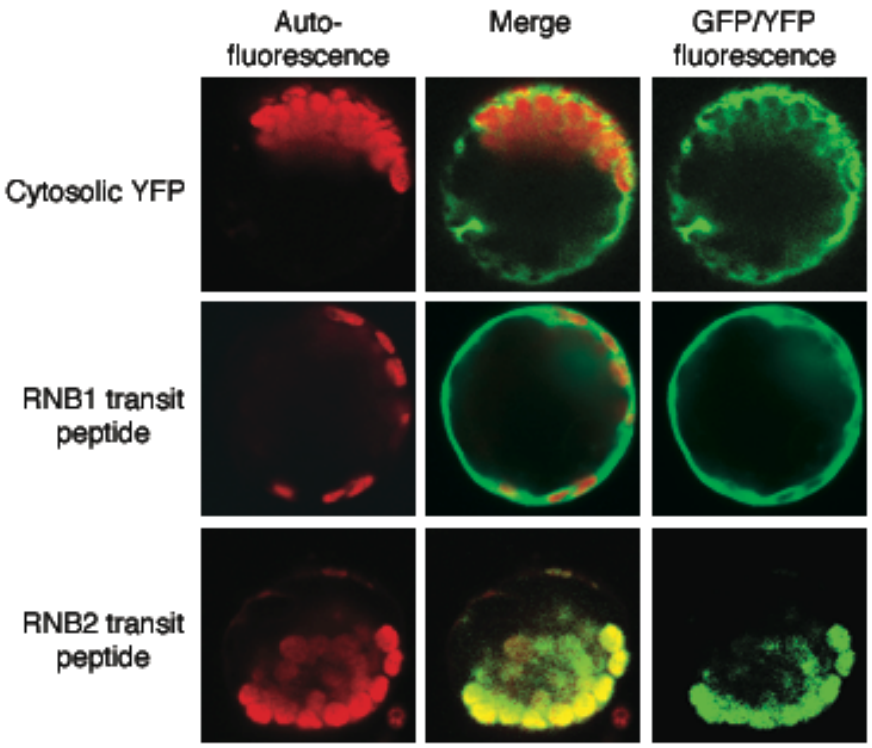

Figure 2.3: Tomato protoplasts transformed with transit peptide/GFP fusions.
Each panel shows a single protoplast containing multiple chloroplasts that can be visualized due to their autofluorescence (first column). With cytosolic YFP and RNB1 transit peptide fusion-transformed protoplasts, signals from GFP and autofluorescence do not co-localize. Co-localization is apparent in the protoplast transformed expressing the RNB2/GFP fusion.

Microscopic techniques were employed to obtain empirical evidence of chloroplast localization for either RNB1 or RNB2. cDNAs encoding the N-

terminal 189 amino acids (RNB1) or 115 amino acids (RNB2) were fused to a green fluorescent protein (GFP)–encoding gene, and the proteins were expressed transiently in tomato protoplasts. As shown in Figure 2.3, a cytosolic version of yellow fluorescent protein (YFP) generated fluorescence throughout the cell, except the large vacuole. RNB2 fusions were clearly targeted to the chloroplasts, because chlorophyll autofluorescence colocalized with the GFP signal. The localization of the RNB1 fusion was similar to that of the cytosolic control. This data suggests that RNB2 very likely encodes a chloroplast RNase II but that RNB1 encodes a nuclear or cytosolic RNase II family protein, possibly the exosome-associated Rrp44 homologue (see Chapter 4). However, since the size of the RNB1 fusion was not confirmed by immunoblotting, protein cleavage of the fusion resulting in an unmodified GFP protein cannot be ruled out. Targeting of PAP4 is covered in Chapter 3.

The empirical evidence of location is summarized in Table 2.2 along with the predictions. In no instance did all three protein predictors agree with the empirical evidence of cellular location. This was not unexpected, and there are several reasons why predictors fare poorly with *Chlamydomonas* proteins. (1) Since sequence similarity of transit peptides is poor between organisms, we must rely entirely on gene modeling software to generate a correct transit peptide on a gene model, which I have already discovered in my sequencing of PAP4 and RNB2 does not always occur. This, however, is not the case with the proteins in Table 2.2, because their encoding cDNAs have been fully sequenced. (2) *Chlamydomonas* proteins were not among those utilized in the training sets that generated the prediction algorithms. This possibly contributed to the results I obtained. I conclude that while the predictors may have some merit for predicting whether a *Chlamydomonas*

protein is or is not organellar, when trying to distinguish between mitochondrial and chloroplast targeting, the programs have little or no value.

Strategy to elucidate the roles of RNB2, RNase J1, and PNPase

Since the chloroplast localization of RNB2, RNase J1, and PNPase was directly or indirectly verified, I wanted to know whether silencing one of these endo- or exonucleases might result in changes to the size or quantity of chloroplast transcripts. Given the current model of chloroplast RNA turnover, silencing an RNase II-like enzyme should lead to accumulation of degradation intermediates. I would expect that polyadenylation of RNA would increase, or tails would increase in length if one of the genes responsible for degrading these tails decreased in abundance. For example, in *E. coli* strains where PNPase is silenced, the homopolymeric PAP-generated tails are more abundant and longer, and therefore much easier to observe (Mohanty and Kushner, 2000b).

I utilized a modified version (see Methods) of the vector described in (Rohr *et al.*, 2004) for this work, and a schematic of the relevant portion is found in Figure 2.4A. Briefly, an inverted repeat of a region of the gene to be silenced is inserted between arms of inverted repeat 3' UTR sequence of the tryptophan synthase gene *MAA7*. This vector expressed a chimeric inverted repeat of *MAA7* and the gene of interest. Transformed cells are selected on plates containing 5-fluoroindole (5-FI) and tryptophan (Trp); 5-FI being converted by tryptophan synthase into the toxic 5-fluorotryptophan, so that cells are only able to survive with reduced amounts of the *MAA7* gene product. The selection in this case is linked to the activation of RNAi for *MAA7* and presumably, the gene of interest as well.

RNB2 transformants were identified by growth on 5-FI+Trp, and RNA was extracted as soon as enough material was generated for collection (approximately 4 weeks from the appearance by eye of the first transformed colonies). RT-PCR was performed on two of the RNAi lines, RNBi1 and i2, and these had reduced expression of *RNB2* and the co-silenced *MAA7*. However, the level of silencing at the protein level was unknown. As a preliminary screen for a possible photosynthetic defect caused by alterations in cpRNA metabolism, RNBi1 and i2 were transferred to a minimal medium plate lacking a reduced carbon source, where growth would be compromised or not

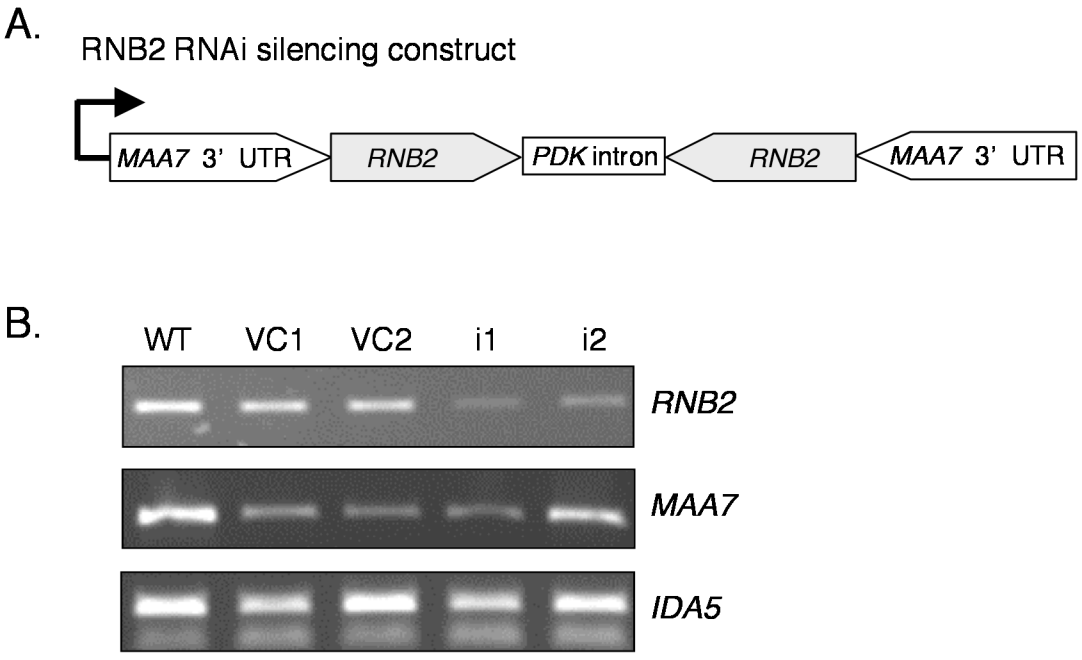

Figure 2.4: Silencing of *RNB2*.
A. Diagram of the construct used to generate silenced strains. Transcription of the tandem *MAA7/RNB2* hairpin activates the RNAi pathway to downregulate both genes. UTR, untranslated region. PDK intron, *Arabidopsis* pyruvate orthophosphate dikinase intron B. RT-PCR shows that transformants i1 and i2 have reduced levels of *RNB2* RNA compared to WT and Vector Control (VC), and that *MAA7* mRNA is reduced in VC and at least one *RNB2* RNAi strain. *IDA5* encodes actin and is used as the control.

possible with a photosynthetic deficiency. However, these transformants grew at a similar rate as compared to the progenitor strain, indicating that their photosynthetic machinery was still functional. Unfortunately, maintaining silencing in RNBi1 and i2 was difficult and subsequent analysis revealed a suppression of silencing.

cpRNA from transiently silenced RNase J1 strains show alterations in minor bands from WT on RNA gel blots.

Since *Chlamydomonas* chloroplasts lack RNase E, another endonuclease must fulfill its role in triggering RNA decay. When J1/J2 were discovered in *B. subtilis*, it became evident that homologues were encoded in plastid-containing organisms, including *Chlamydomonas*. Thus, it was an interesting candidate for RNAi-mediated silencing. After performing the transformation by the same strategy as with *RNB2*, I obtained enough RNA from transformants to test both whether *RNJ1* had been downregulated, and to investigate chloroplast transcript size and abundance. Figure 2.5A shows by RT-PCR that *RNJ1* RNAi transformants had reduced expression of *MAA7* and *RNJ1*. Like the *RNB2* RNAi transformants, the *RNJ1*-downregulated strains were able to grow like the WT on minimal medium.

The same RNA samples and others collected near the same time were used for RNA gel blot analysis of various chloroplast transcripts (Figure 2.5B). Since transcription termination is inefficient in *Chlamydomonas* chloroplasts (Rott *et al.*, 1996), many transcripts are initially polycistronic, and subsequently processed to mature species. While the *psbA* and *petD* mRNAs show little or no change in size or abundance, in *atpH*, *atpI*, *rps19* and 16S, secondary bands disappeared in the *RNJ1* silenced lines when the entire blot was

Figure 2.5: Partial silencing of *RNJ1* and its effect on chloroplast transcripts.
A. RT-PCR shows silencing of *RNJ1* RNAi transformants at the RNA level compared to WT and Vector Control (VC), a strain transformed with only the *MAA7* hairpin. The panel showing *RNJ1* mRNA reduction was provided by BMCB rotation student Wade Heller. *IDA5*, encoding actin, is used as a control. B. RNA gel blot analysis of chloroplast transcripts. The top panel is the RNA gel blot with 10 μg total RNA per lane, the bottom panel is the ethidium bromide-stained gel before transfer, and serves as the loading control. Top row: RNA gel blots of transcripts showing no differences upon *RNJ1* silencing. Bottom row: RNA gel blots of transcripts exhibiting minor bands, indicated with arrows, that appear in WT but not in the *RNJ*-silenced strains. The *rps19* blot was re-probed with *atpI* for this figure, so the same loading control is used.

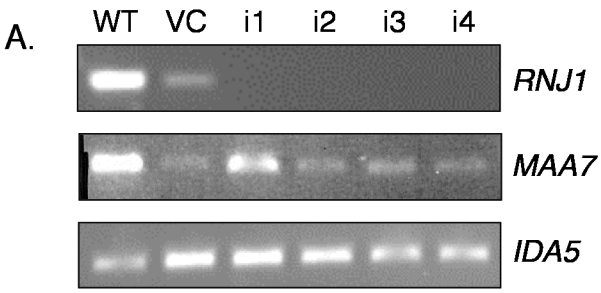
A.
WT VC i1 i2 i3 i4
RNJ1
MAA7
IDA5

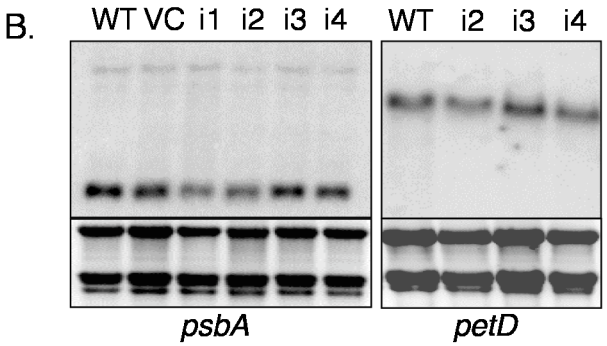
B.
WT VC i1 i2 i3 i4
WT i2 i3 i4
psbA
petD

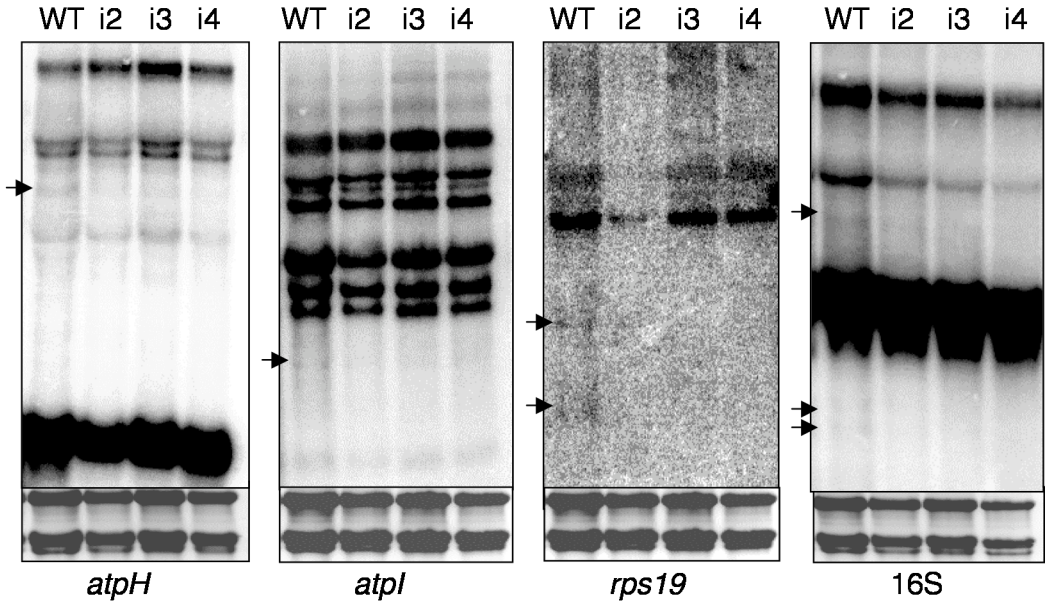
WT i2 i3 i4
WT i2 i3 i4
WT i2 i3 i4
WT i2 i3 i4
atpH
atpI
rps19
16S

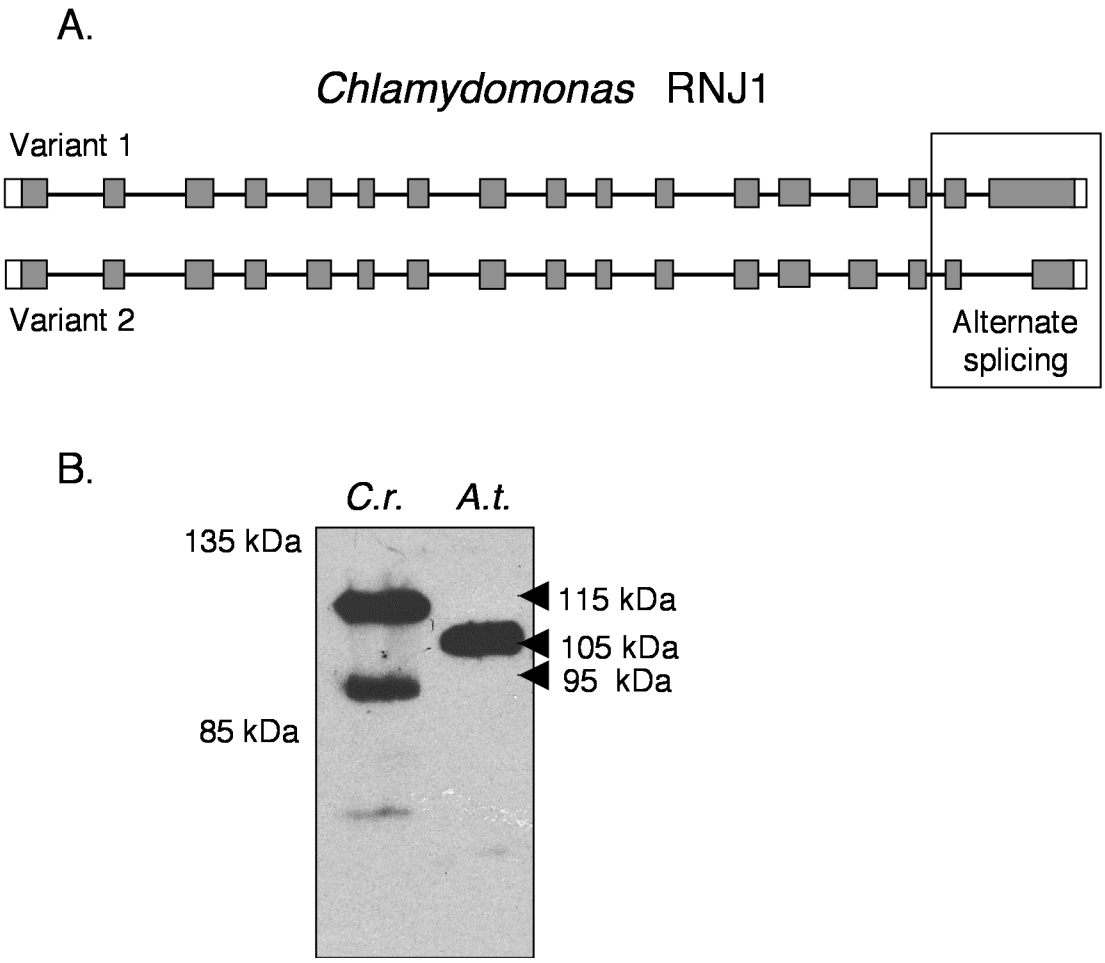

Figure 2.6: Alternative splicing of RNase J in Chlamydomonas
A. The two splice variants of *RNJ1*. Boxes represent exons, grey indicates coding sequence and white is untranslated sequence. B. The antibody detects two isoforms of *Chlamydomonas (C.r.)* RNase J1 at apparent molecular weights of 115 kDa (predicted 95 KDa) and 95 kDa (predicted 80 kDa), while there is only one protein in *Arabidopsis (A.t.)* at an apparent molecular weight of 105 kDa (predicted 93 kDa). Predicted sizes exclude the transit peptide predicted by TargetP. Generation of the RNase J1 antigen and immunoblotting was performed by Steve MacKinnon.

compared with a vector control (VC) or wild-type (WT) cells. The missing bands of the 16S transcript, especially those of a larger size than the mature 16S, were of particular interest, because *B. subtilis* RNase J1 has been implicated in the processing of its 16S rRNA (Britton *et al.*, 2007).

Our cDNA sequencing revealed alternative splicing *Chlamydomonas RNJ1* gene due to different splice junctions for the last two exons, 16 and 17 (Figure 2.6A). This is not the case for the *B. subtilis* enzyme, where there are two RNase J1 isozymes arising from two loci, or *Arabidopsis*, where only one transcript is observed. The *Chlamydomonas* transcripts are both translated, as revealed by immunoblot analysis (Figure 2.6). The experiment was performed on *Chlamydomonas* and *Arabidopsis* total proteins using an antibody raised against a region of RNase J1 with high amino acid sequence similarity between the two organisms. Two bands were observed in the *Chlamydomonas* lane, but only one for *Arabidopsis*. The apparent relative molecular weights of the three proteins are in agreement with their predicted sizes, although all of the proteins migrate more slowly than what is predicted based solely on amino acid sequence.

The RNase J1 antibody was next used to investigate the degree of silencing in *RNJ1* RNAi lines at the protein level, using cells revived from frozen stocks. It was then discovered that the silenced lines had reverted to WT in their levels of RNase J1, both at the RNA and protein levels (results not shown).

PNPase degrades polyadenylated RNA in vivo.

As a first step towards elucidating the function of PNPase in the chloroplast, I utilized an existing laboratory strain with a polyadenylated

reporter transcript. This heteroplasmic strain, spa19, contains a chloroplast genome (designated “PS- “) containing a reporter *atpB* gene, required for photosynthesis and originally engineered to generate a transcript terminating with a polyadenylated (A_{28}) sequence (Komine *et al.*, 2002). In spa19, the *atpB* transcript would be rapidly degraded but for the existence of a small mini-genome (designated “PS+”), acquired as a result of a genetic suppressor screen, containing *atpB* in an orientation resulting in expression of a complementary 3’ *atpB* sequence that stabilizes the *atpB* mRNA transcribed from the PS- genome and allows its expression. The *spa19* strain is thus photosynthetic.

To see if the PS+ genome was necessary for photosynthesis when RNA decay via PNPase was repressed, I crossed spa19 (mt+) with the strain Ap6 (mt-), which is reduced in PNPase expression due to *PNP* antisense RNA expression, as described in Methods. 34 zygotes were dissected and the progeny separated on medium containing the antibiotic zeocin. This was done to select for progeny reduced in PNPase expression, since only cells that inherited the *PNP* antisense cassette would grow on this medium. 23 of the 34 tetrads had two surviving progeny as expected, and these were tested for the ability to grow on minimal medium, which revealed that 100% of these surviving progeny were photoautotrophic. Previous genetic analysis showed that the PS+ genome is poorly transmitted, inherited by only 21% of complete tetrads from the cross (spa19 mt+ x WT mt-; Nishimura *et al.* 2004). Therefore, a likely reason for the photosynthetic nature of most of the strains was that the reduced level of PNPase permitted photoautotrophic growth even without the PS+ genome.

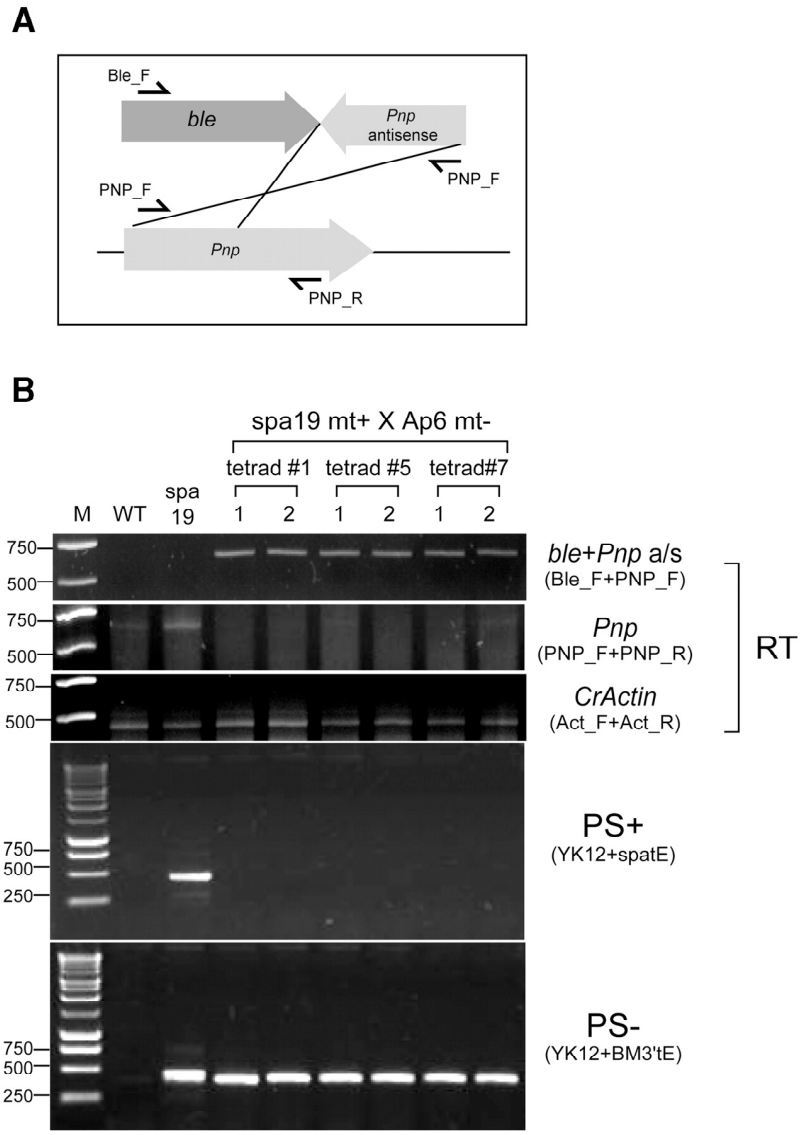

Figure 2.7: Analysis of spa19 (mt+) x PNPase (Ap6) antisense (mt-) progeny.
A. Locations of primers used in (B). The *ble* gene confers resistance to zeocin and is fused transcriptionally to a 365-bp segment of the *PNP* gene in the reverse orientation. B. Spa19 was crossed to the antisense strain Ap6, and the zeocin-resistant members of each tetrad were analyzed; three representative sets are shown here. The top panel is RT-PCR to detect *ble*-anti-*PNP* cotranscripts, and the second panel is RT-PCR to detect *PNP* sense transcripts. *PNP* transcripts accumulate to very low levels even in wild-type cells; hence, the PCR product is not abundant. The third panel shows amplification of actin cDNA as a control for RNA amounts. The bottom two panels show PCR analysis to assess the presence or absence of the PS+ or PS– genome in the progeny. The primer sets used are indicated at the right. M, 1 kb ladder. Figure and legend from Nishimura *et al.* (2004).

To verify this, a collaborating postdoctoral associate, Yoshiki Nishimura, analyzed the photosynthetic progeny by PCR and demonstrated that they no longer contained the PS+ genome that had been necessary for stabilizing the polyadenylated transcript in the presence of wild-type amounts of PNPase (Figure 2.7). Furthermore, the polyadenylated *atpB* transcript was able to accumulate, as shown by RT-PCR. This result indicates that PNPase destabilizes polyadenylated transcripts in the *Chlamydomonas* chloroplast.

PNPase levels are reduced in multiple RNAi strains

While the level of *PNP* suppression in the Ap6 strain was sufficient to see an effect on *atpB* mRNA decay in the above experiment, subsequent analysis of levels of depletion at the protein level were found to be 25-50% of WT. Therefore, a strain with more strongly reduced levels was desirable for further studies. I utilized the RNAi vector to generate PNPase-silenced strains in two cell wall-deficient strains, CC-406 and CC-849. Before performing the transformation, I had generated an antibody against PNPase that I could use to determine which transformants were reduced in PNPase at the protein level. This antibody usually recognizes a doublet. Figure 2.8A shows that all of the silenced strains analyzed had reduced levels of PNPase. The silencing in CC-406 transformant #3, called PNPi3, was more accurately quantified in an immunoblot by postdoctoral associate Shlomit Yehudai-Resheff (Figure 2.8B), and found in multiple assays to have about 10% of the WT level. The same figure presents the level of silencing for two antisense strains, including Ap6 that was utilized in the above cross.

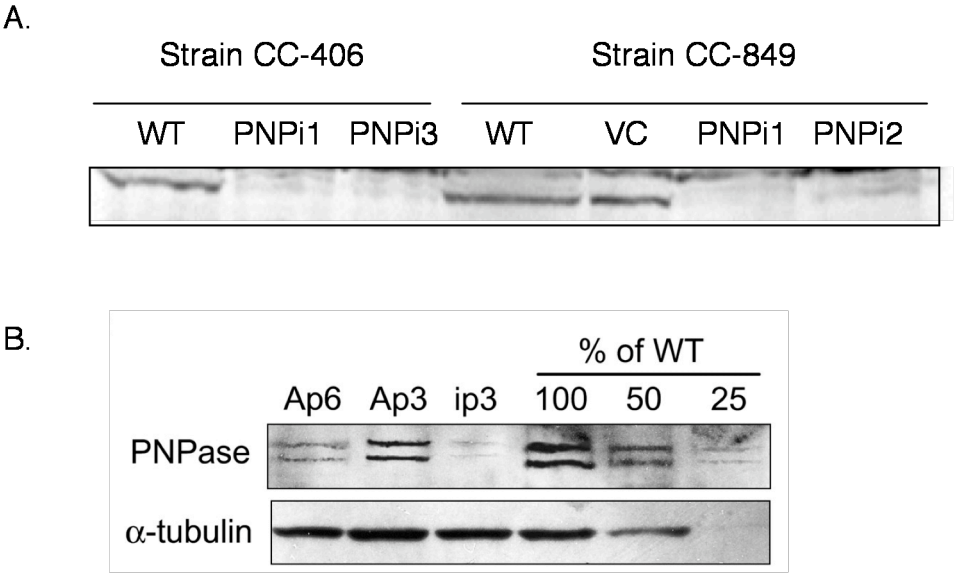

Figure 2.8: Evidence of PNPase depletion in RNAi strains.
A. Immunoblot with total *Chlamydomonas* protein probed with the *Chlamydomonas* PNPase antibody. B. Representative immunoblot with the PNPase RNAi strain PNPi3 (ip3) (derived from CC-406), and antisense strains Ap3 and Ap6 used to quantify the reduction in expression of PNPase. Figure was modified from Yehudai-Resheff *et al.* (2007).

Effects of phosphate starvation on chloroplast transcript abundance are mediated through PNPase.

As demonstrated *in vitro* in Yehudai-Resheff *et al.* (2001), and diagrammed in Figure 2.1B, Pi and NDPs are a substrates or products of the readily-reversible reaction catalyzed by PNPase. If conditions arise such that the availability of free P in the cell, and especially the chloroplast, decreases, it is possible that the ratio of Pi to NDPs would be altered enough to drive the reaction from degradation to polymerization.

Since PNPase can clearly act as an exoribonuclease in the poly(A)-mediated decay pathway, the next question was whether P availability affects the degradation capacity of PNPase *in vivo*. To that end, cpRNA levels were measured after P depletion and compared in WT and PNPi3 strains in experiments performed by Shlomit Yehudai-Resheff and described in the following text, adapted from Yehudai-Resheff *et al.* (2007):

"Wild-type or PNPi3 cells were first grown in the presence of P, then the culture was divided into two portions, one with P and one without. Samples were taken over a 48-h time course and at the end, the starved culture was transferred back to P-containing medium for 2 h. Figure 2.9A shows a representative gel blot that reveals that in WT cells, accumulation of the *petD* and *tufA* chloroplast transcripts increased substantially under P limitation. This increase is most evident at the 24- and 48-hr time points and was fully reversed 2 hr after P was restored (Figure 2.9A, lanes +2). This accumulation is consistent with diminished PNPase catabolic activity along with continued transcription, and the 24 h delay in the manifestation of the phenomenon could be explained as the time taken for the Pi concentration in the chloroplast to change under P starvation.

This phenomenon was not observed in PNPi3 cells (Figure 2.9A, right panel). In –P conditions, chloroplast mRNA levels remained constant, reacting to neither P depletion nor the readdition of P to the culture. This finding implicates decreased PNPase exonucleolytic activity as being responsible for cpRNA accumulation in wild-type cells acclimating to P deficiency; in PNPi3, the initial PNPase level is low, so minimal activity changes might be expected under P limitation."

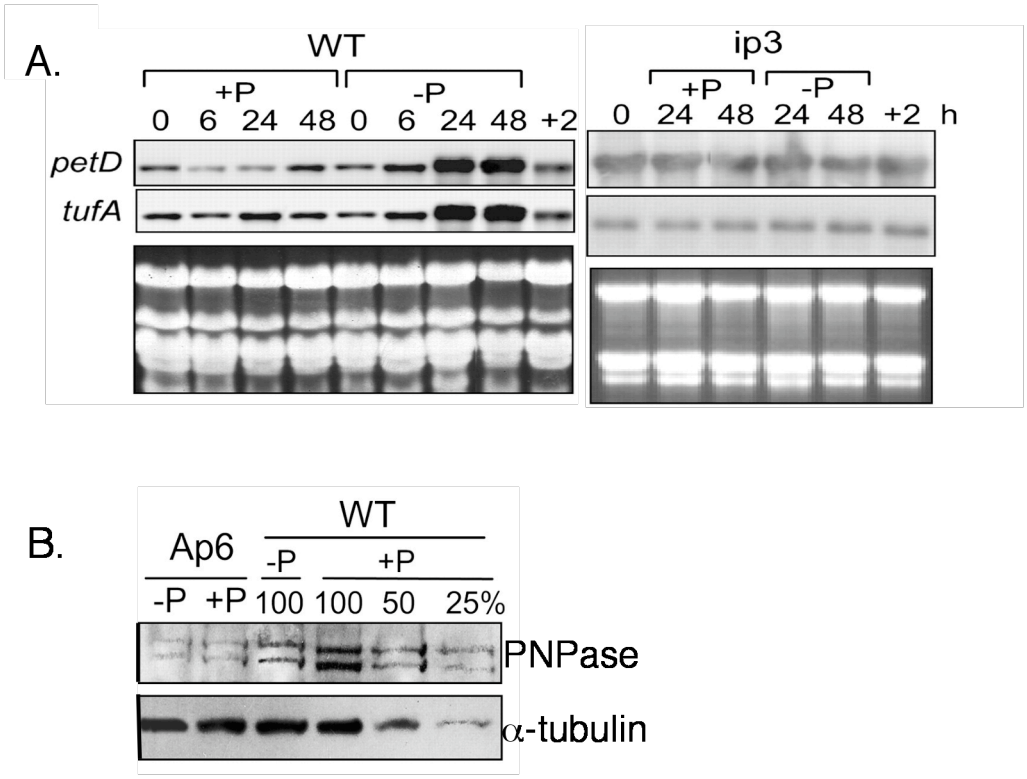

Figure 2.9: Effects of phosphate limitation.
A. Chloroplast RNA accumulation under P limitation. Wild-type and PNPi3 (iP3) cells were grown to early log phase in TAP medium, then collected and resuspended in TAP (+P) or TA (–P) medium. Total RNA was isolated immediately (0) or after 6, 24, or 48 hr. An additional sample was obtained from cells in TA, after they were transferred to TAP medium for an additional 2 hr (+2). A total of 3 μg of RNA was loaded in each lane, and blots were hybridized with the experimental probes listed at left. To demonstrate the equality of loading, gels were stained with ethidium bromide. B. Immunoblot analysis of a dilution series of wild-type total protein from cells grown under +P conditions, compared with total protein from wild-type or Ap6 cells starved for phosphate for 48 hr, using an anti-PNPase antibody. A tubulin antibody was used as a loading control. Figure and legend were modified from Yehudai-Resheff *et al.* (2007).

Furthermore, as presented in Figure 2.9B, P limitation unexpectedly induced changes in the abundance of PNPase. Immunoblot analysis performed by Shlomit Yehudai-Resheff showed an approximately 2-fold reduction of PNPase after cells were incubated 48 hours in medium without phosphate, and she observed consistent changes in the *PNP1* RNA level (not

shown). Since neither culture upon harvest was at a cell density where reductions in PNPase were observed (Figure 2.2), stage of growth of the culture was unlikely to be a factor in this observation. However, since P amounts are likely to be reduced in a saturated culture, it may be this reduction that is the cause of the decreased *PNP1* mRNA expression observed in Figure 2.2.

In addition to the effects of P limitation on RNA that are dependent on the presence of PNPase, other physiological responses to P limitation are also impacted by PNPase depletion. Cell survival in the absence of P, and the P depletion-inducing destabilization of chloroplast DNA are two of these (Yehudai-Resheff *et al.*, 2007). Since my contributions to these results were minimal, they are not included in this dissertation.

Chloroplast transcripts in PNPase RNAi strains appear to be largely unaffected.

Since decreased PNPase exonucleolytic activity is likely responsible for cpRNA accumulation during P limitation, it follows that under full nutrient conditions, cpRNA levels would be higher in strains with reduced amounts of PNPase. I expected to see these changes on RNA gel blots as we did with the P starvation experiments. Furthermore, an *Arabidopsis* strain with reduced chloroplast PNPase caused by cosuppression has altered 3' end maturation of 23S rRNA, as well as 3' extensions on *psbA* and *rbcL* transcripts (Walter *et al.*, 2002). These should also be readily visible on gel blots.

I probed *Chlamydomonas* RNA gel blots for nine chloroplast transcripts using RNA from WT and PNPase reduced strains, in an attempt to observe altered trascript quantities or sizes. In these blots, shown in Figure 2.10, I

utilized several PNPase RNAi lines, because minor differences could be more easily confirmed with multiple samples. I observed some differences in quantity between the untransformed strains and the PNPase silenced lines, such as the decrease in abundance of *psbA*, *tufA*, and *rbcL* in the PNPase-depleted strain i2 in the CC-849 background. However, these differences were not observed in the CC-406 background, and the analysis was not repeated sufficiently to confirm this finding. The increase in *petD* abundance in PNPase-depleted strains in Figure 2.10 was not reproducible. For only one of the probes, *rps19*, was I able to observe any difference consistent among all PNPase depleted strains. In these strains, there is an additional band among the *rps19* transcripts in various processed states. This may be a transcript that after an endonucleolytic cleavage, would primarily utilize PNPase to trim its 3' end to become the more abundant form that migrates more quickly. This band is minor in abundance, however, and therefore does not represent a major processing defect. Viewing these results together, the significant, reproducible effect of dramatically increased cpRNA levels under conditions of P limitation, or the altered cpRNA maturation seen in *Arabidopsis* were not observed when PNPase was depleted by the mechanism of RNAi silencing.

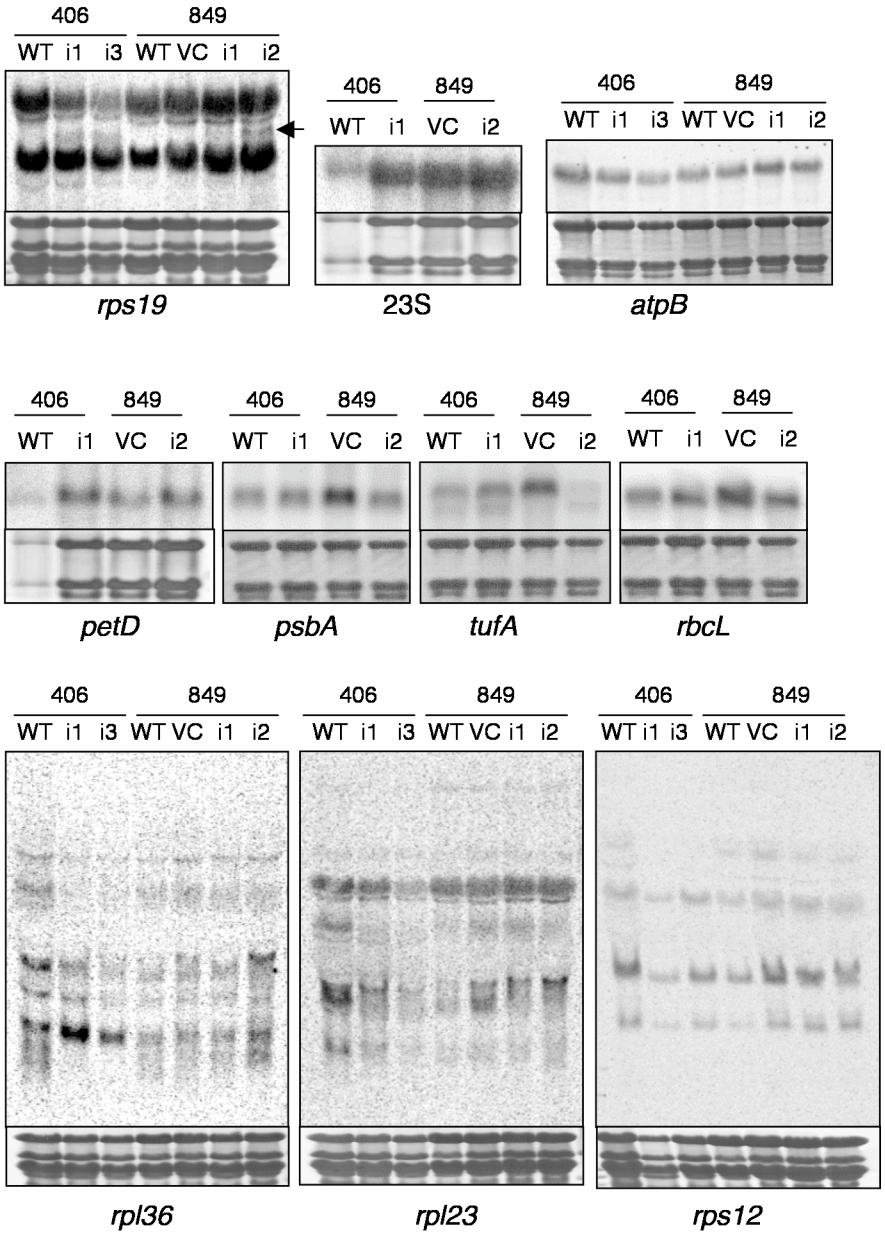

Figure 2.10: Chloroplast transcripts in PNPase RNAi strains.
The top panels are RNA gel blots of 20 μg (*rpl23*, *rpl36*, *rps12*, and *rps19*) or 5 μg (all others) total RNA from the indicated strains. The bottom panels are loading controls; ribosomal RNA detected by either gel staining with ethidium bromide before transfer (*atpB*), or methylene blue staining of the membranes (all others). The arrow on *rps19* shows the location of an additional band in the PNPase RNAi strains.

Expression of RNB2 Is Increased in PNPi3.

The apparent ability of PNPase to limit mRNA accumulation under P limitation in the wild type raises the question of why PNPi3 or antisense PNPase strains do not overaccumulate cpRNAs under +P conditions (Figure 2.9A). Furthermore, it was unexpected that there were not more defects in the processing of cpRNAs in the RNAi strains, especially since certain defects in *Arabidopsis* mutants are obvious. One explanation is that other exoribonucleases such as RNB2 might mask the depletion of PNPase. PNPase and RNase II are partly redundant in *E. coli*, and the RNase II homolog RNR1 is known to have a key role in chloroplast rRNA maturation in *Arabidopsis*, as mentioned in the Introduction. Furthermore, PNPase depletion in *E. coli* results in increases in RNB activity and in increased amounts of the RNase II transcript, *rnb*, while PNPase overexpression has the reverse effect (Zilhao *et al.*, 1996; Bernstein *et al.*, 2004). Therefore, I explored whether *Chlamydomonas RNB2* mRNA levels might be upregulated by PNPase depletion as it appears to be in *E. coli*.

Expression of *RNB1* and *RNB2* mRNA was analyzed in cells growing in +P or –P conditions, as shown in Figure 2.11. In multiple experiments, *RNB2* mRNA was found at increased levels in PNPi3 compared with CC-406 or VC under both +P and –P conditions. This increase was not quantified, but examination of the gels in Figure 2.11, and other experiments, were consistent with a two- to three-fold difference when normalized to the actin control, an increase similar to that observed in the *E. coli* PNPase-depleted strain (Zilhao *et al.*, 1996). Predictably, there was no change in the levels of *RNB1*, which does not encode a chloroplast exonuclease. If the increase in *RNB2* mRNA reflects an increase of RNase II–like activity in PNPi3 chloroplasts, this might

account for the lack of increased cpRNA when cells are grown under nutrient-replete conditions, and may explain my failure to observe other differences in chloroplast transcripts.

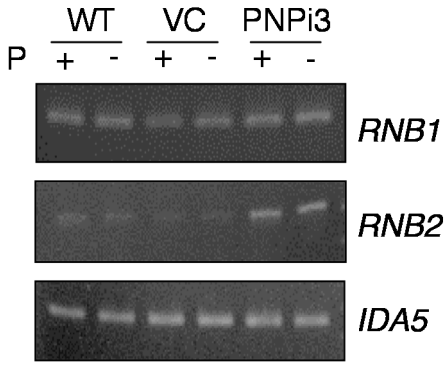

Figure 2.11: *RNB2* expression.
RT-PCR analysis for the strains shown across the top (WT, recipient strain CC-406; VC, vector control in CC-406) from cells grown under +P or –P conditions. The vector control was transformed with the RNAi vector targeting only *MAA7*. The genes are listed at right (*IDA5* encodes actin), with RT-PCR performed as described in Methods. Figure and legend are from Yehudai-Resheff *et al.*, (2007).

***PNPase may exist in both trimeric and monomeric forms in* Chlamydomonas.**

Another aspect of PNPase activity is its state of interaction with other molecules. Is PNPase acting as the homotrimer observed by others, in either its degradative or polymerizing capacities, or can PNPase function in a different complex, or act as a monomer? To answer this question in part, I obtained total soluble protein in native form from *Chlamydomonas* and separated them using gel filtration. I analyzed fractions by immunoblotting with the PNPase antibody, as shown in Figure 2.12. Based on protein size standards, PNPase eluted in fractions centered at 300 and 100 kDa. The 100 kDa value likely corresponds to a monomeric form. One possibility for the

identity of the 300 kDa complex is a PNPase homotrimer. Although the size of the spinach chloroplast PNPase was consistent with a monohexamer (Baginsky *et al.*, 2001; Yehudai-Resheff *et al.*, 2001), and the PNPase from *Streptomyces antibioticus* purified as a dimer of trimers (Symmons *et al.*, 2000), the physiologically active form of bacterial PNPase is thought to be trimeric (Littauer and Soreq, 1982). While it is certainly possible that PNPase exists and may even be active in the monomeric form, I cannot rule out that it appears in the monomeric fractions due to disassociation of the complex during purification or gel filtration, or that the chloroplast harbors an inactive fraction of PNPase. Indeed, the crystal structure suggests that assembly into a trimer creates the channel for the single stranded RNA substrate (Symmons *et al.*, 2000).

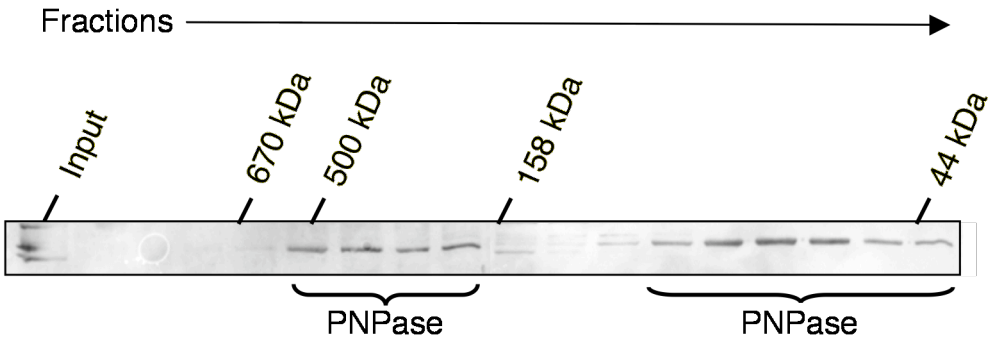

Figure 2.12: FPLC analysis of PNPase.
Total soluble *Chlamydomonas* protein was loaded on a Superdex 200 HR 10/30 column and 0.5 ml fractions were collected, precipitated, and 1/3 of each fraction was analyzed by SDS-PAGE. After transfer to nitrocellulose, the blot was probed with the PNPase antibody.

DISCUSSION

Analysis of silencing using current RNAi technology in Chlamydomonas

Three genes were targeted for silencing by RNAi. Ultimately, only *PNP1* was stably silenced. *PNP1* is also one of the few genes, in the experience of the laboratory, whose expression could be reliably reduced by the preceding antisense-based technology (Schroda *et al.*, 1999). Although transient silencing of *RNJ* and *RNB2* was observed at the RNA level, PNPase silencing was mainly observed at the protein level for PNPi3, where strains showing silencing by immunoblotting all showed close to normal levels of the *PNP1* RNA (results not shown). In contrast, the antisense Ap6 strain does show a reduction in *PNP1* mRNA (Figure 2.7), though the protein is present in greater amounts than in PNPi3 (Figure 2.8B). In my hands, is not the only situation where the RNAi vector has produced this result. In Chapter 3 I will show that depletion of PAP4 protein by RNAi is likewise not accompanied by a corresponding depletion in mRNA (Schroda, 2006). Mechanisms of gene silencing involving complementary RNA are known to operate at the translational level, as well as by inducing RNA degradation (Filipowicz *et al.*, 2008). My data suggest that *Chlamydomonas* may possess both of these silencing mechanisms. The multiple examples of gene silencing in *Chlamydomonas* are likely to provide insights into these processes over the next few years (Schroda, 2006).

RNase J1 as a possible chloroplast endoribonuclease

One of the transiently-silenced genes, *RNJ1*, encodes a protein with two isoforms. Alternate forms of proteins may be targeted to different cellular

compartments if the variation lies within the transit peptide. Additionally, since 3' UTRs of yeast play a role in mitochondrial targeting (Gonsalvez *et al.*, 2005), changes in the 3' UTR of *RNJ1* mRNA may alter location as well. However, the alternative splicing of the *RNJ1* mRNA affects only the last two exons and occurs within the coding region, so it is unlikely that these isoforms are targeted to different locations in the cell. The sequence absent from the shorter version of RNase J1 is repetitive with no recognizable motifs. One may hypothesize, therefore, that the presence or absence of this repetitive region is neutral, so that both isoforms are tolerated by the cell. Since transient RNase J1 silencing was correlated with some minor modifications to chloroplast transcripts, it may be worth repeating the silencing, especially given that an RNase J1 antibody is available to monitor silencing at the protein level.

The role of RNase J1 is worth exploring in *Chlamydomonas* for two reasons. First, unlike higher plants, *Chlamydomonas* appears to lack an RNase E homologue, the primary endonuclease of poly(A)-mediated decay in *E. coli*. Therefore, the likelihood that RNases J1 and/or CSP41 fulfill this role is increased. Secondly, 5' to 3' RNA decay in *Chlamydomonas* has been documented on the *petD* transcript (Drager *et al.*, 1999), and on the *atpB* transcript as part of the 3' processing pathway (Hicks *et al.*, 2002). Since RNase J1 has recently been shown to participate in 5' to 3' decay in *B. subtilis* (Mathy *et al.*, 2007), it is possible that RNase J1 may be acting in this capacity in *Chlamydomonas* chloroplasts. An importance for RNase J1 is also suggested indirectly by the fact that homozygous knockouts are embryo-lethal in *Arabidopsis*, and a heterozygous knockout has a significant growth phenotype (C. Marchive, Stern laboratory, unpublished results).

One hypothesis for the existence of additional minor cpRNA bands in RNase J1 RNAi strains (Figure 2.5) is that transcript processing is less efficient. Steady exoribonucleolytic degradation of transcripts rather than cleavage/degradation cycles may be necessary when levels of RNase J1 are lowered. This might result in the disappearance of discrete intermediates if RNase J1 normally cleaves at specific positions to initiate decay.

RNB2 as a chloroplast exoribonuclease

Little was elucidated from transient silencing of *RNB2*, except that no major defect in photosynthesis occurred, under the assumption that silencing occurred at the protein level as well. The upregulation of RNB2 upon depletion of PNPase was an unexpected finding (Figure 2.11). In *E. coli*, levels of the *rnb* transcript increase upon PNPase depletion due to a direct feedback mechanism. This mechanism stems from the fact that PNPase normally targets the *rnb* mRNA, thus in *pnp* mutants it is turned over at a slower rate (Zilhao *et al.*, 1996). While I observed the same net effect in *Chlamydomonas*, the mechanism has to be different, as PNPase acts in the chloroplast, but *RNB2* is nucleus-encoded. PNPase could exert its influence on *RNB2* mRNA levels through either transcriptional regulation in the nucleus, or by RNA stability in the cytosol. In either case, some sort of chloroplast retrograde signal would be a likely way for chloroplast PNPase depletion to be signaled back to the nucleus. Examples of such signals include reactive oxygen species, inhibition of plastid protein synthesis, and redox state changes of chloroplast proteins (Beck, 2005). In *Chlamydomonas*, intermediates of tetrapyrrole synthesis were found to affect transcription of the heat shock factor gene *HSP70* (Beck, 2005).

While the lack of a chloroplast protein might itself be the signal for increased transcription of a nuclear gene, an alternate possibility is that the level of RNA decay intermediates are strictly regulated, and an increase in these by-products might be a signal to increase the transcription or stabilization of an exonuclease mRNA until RNA decay intermediates are again cleared. Furthermore, our laboratory has preliminary evidence that an *Arabidopsis* Csp41b mutant also lacks Csp41a protein in leaves over 15 days old (T. J. Bollenbach, unpublished results), suggesting that signals from the cpRNA decay pathway might be affecting nuclear transcription or cytosolic stability of particular mRNAs.

The effects of PNPase activity in the chloroplast

The similarity of abundance and size of chloroplast transcripts in PNPi3 and WT strains was unexpected, especially considering the strong phenotype observed in response to P limitation. One explanation for my failure to observe differences in chloroplast transcripts may be that PNPase is not fully silenced and the residual activity of the enzyme is sufficient to maintain transcript abundance. However, since the response to P deprivation is so altered in the deficient strain, including a lethal phenotype (Yehudai-Resheff *et al.*, 2007) not discussed in this chapter, an alternative explanation is more likely, namely that the activity of another enzyme, possibly RNB2, is redundant with PNPase. In *Arabidopsis*, where sizes of transcripts are altered in the *pnp* mutants (Walter *et al.*, 2002), the activity of the chloroplast RNase II/R family protein, RNR1, seems exclusive to rRNA processing (Kishine *et al.*, 2004; Bollenbach *et al.*, 2005). In the choice of its substrate, RNR1 tends to resemble *E. coli* RNase R rather than the mRNA-targeting RNase II. However, RNase R in an *rnb* mutant

did hydrolize some mRNA (Deutscher, 1993). RNB2 may resemble RNase II in its substrate preference, and RNR1 may be more similar to RNase R. This could explain why the absence of PNPase appears masked in *Chlamydomonas* compared to *Arabidopsis*. One way to assess the ability of PNPase and RNB2 to substitute for each other would be the generation of a double mutant. If such a mutant is inviable as with the *E. coli pnp*/*rnb* mutant (Donovan and Kushner, 1986), this would suggest that the enzymes do have redundant functions.

Chlamydomonas *cpRNA decay: how closely does it follow other models of decay?*

The overall pathway of poly(A)-mediated degradation of RNA appears well conserved in most living organisms, with a few exceptions (Portnoy and Schuster, 2008). However, the assumption that the ribonucleases of the *E. coli* pathway are operational in other organisms is perhaps only a good starting point from which to begin studies in these systems. For instance, *Chlamydomonas* likely uses RNase J1, Csp41a and/or Csp41b to initiate cpRNA turnover, lacking a homologue of RNase E that is required for viability in *E. coli*. The *Chlamydomonas* chloroplast may be more similar to *E. coli* and less similar to the higher plant chloroplast in that its phosphorolytic and hydrolytic exonucleases may be partially redundant. In a lot of ways, it is the less-studied *B. subtilis* that has more in common with *Chlamydomonas* chloroplasts regarding RNA decay: including the RNase J1 enzyme, evidence of a 5'-3' decay pathway, and the lack of RNase E and PAP1 (shown in Chapter 3).

METHODS

***Chlamydomonas* growth conditions**: For the growth phase experiment, cell wall-deficient CC-849 cells were taken from a culture in mid-log phase. The cells were diluted to 0.25 x 10^6 cells/ml in Tris-acetate-phosphate (TAP) medium (Harris, 1989) and grown under continuous light at 25°C. Cells were collected at the time points indicated in Figure 2.2. Cultures for collection of RNA and protein to determine the degree of silencing and for tail analysis were initiated from solid media and grown to between 4 and 7 x 10^6cells/ml.

Cell wall-deficient *Chlamydomonas* CC-849 and CC-406 cultures for transformation were initiated from TAP plus 1% sorbitol plates under continuous light at 25°C and grown for several days until mid-log phase. They were then kept growing continually for five more days in early to mid log phase by dilutions every 48 hr, and were used for transformation at a concentration between 1 and 2 x 10^6 cells/ml.

To perform crosses, strains spa19[mt+] and Ap6[mt-] were transferred from TAP plates to N10 plates (containing one-tenth the normal concentration of nitrate) for 48 hours before incubating under light for three hours in water. The two strains were mixed and allowed to mate for four hours before transfer to TAP and dark conditions. After five days, zygotes were collected and transferred to TAP + 2 μg/ml zeocin for selection of progeny maintaining the PNPase antisense construct. To select for photosynthetic growth, surviving tetrad progeny were transferred to minimal medium plates + 4 μg/ml zeocin and maintained under continuous light.

Strains CC-849 and CC-406 were obtained from the *Chlamydomonas* Stock Center (St. Paul, MN).

Sequencing: The sequencing of *RNB2* and both *RNJ1* cDNAs was performed by Steve MacKinnon using protein predictions from the *Chlamydomonas reinhardtii* genome (version 3.1) at the Joint Genome Institute (http://genome.jgi-psf.org/chlre3/) as a guide, designing primers to amplify across gaps in sequence. Overlapping portions of cDNA were amplified, sequenced, and the full length coding sequence (cds) compiled using Sequencher version 4 (Gene Codes Corp.). The EST clone AV631068 that contains the full coding sequence (cds) of *PAP4* was obtained from the Kazusa DNA Research Institute (Asamizu *et al.*, 1999).

Prediction of localization: To predict potential mitochondrial or plastid targeting, Predotar (http://urgi.versailles.inra.fr/predotar/predotar.html; (Small *et al.*, 2004), TargetP (http://www.cbs.dtu.dk/services/TargetP/; (Emanuelsson *et al.*, 2000), and iPSORT (http://hc.ims.u-tokyo.ac.jp/iPSORT/; (Bannai *et al.*, 2002) were used.

RNA extraction and gel blotting: Cells were stored directly in Tri-Reagent (Molecular Research Center), and flash frozen in liquid nitrogen. RNA was then extracted according to the manufacturer's instructions, but an overnight isopropanol precipitation step at -20°C was included. Quantitation was performed by measuring A_{260}, and RNA quality was checked by agarose gel electrophoresis of 1 μg of RNA. Gel electrophoresis and blotting followed by hybridization to DNA probes shown in Table 2.3 were performed as previously described (Drager *et al.*, 1998). Images were obtained from intensifying screens using a Storm 840 Phosphorimager.

Table 2.3: Primers for probes used for RNA gel blotting.

Gene	Primer	
	f/r[1]	Sequence (5'→3')
16S	f	GTAACGCGTAAGAACCTACCTATCGGA
	r	GCGGCTGCTGGCACAGAGTTAG
23S	f	GGGGCAGCGGTAACGATGAACT
	r	CAAACCCAATTCCAAGATACATGCAAG
atpB	f	TGTGTAATTAAAATAAATTGGCTC
	r	GGGGCATATTAATTCCACTTA
atpH	f	AGGAAATACAATGAACCCTATCGT
	r	AAGATTCCATGAAAGCGAAACT
atpI	f	ATGTAGTTGGCAGTTATTCTAAAT
	r	GGTTATGAATTACACGGTCA
petD	f	AAACCTGATTTAAGCGATCCAGT
	r	AGGGAATGTTGAACCAATACCTAAC
psbA	f	GTTCTCTTCTTTACGGTAAC
	r	GAAACCCATGTAGCAGT
rbcL	f	TGAGTGAAGTAAATACCACGGCTACGG
	r	GTACATGGACTACAGTATGGACTGACGGTT
rps12	f	ACACGAAGACAAATACCACG
	r	AGCCATAGCTTACATTTAAAAATCT
rpl23	f	TTAACAAGTTCTCCATCAGCAGTT
	r	GGTACCGCCACTGCCTATTT
rpl36	f	ATAAAGATGCACCCTCAAACTGTCAG
	r	GCAACTGCCACTGACGTCCAC
rps19	f	TACAGCTTTAGCCATTATTAT
	r	AGAGCTGCAAGACAACAAGT
tufA	f	TATCCGAATGTTAATGCTTAGT
	r	ATTTTATACCCAAACTGTAATAGTTAT

[1] "f" indicates forward and "r" indicates reverse primer.

RT-PCR: For results shown in Figure 2.2, reverse transcription was performed on 1 μg DNase-treated RNA using random hexamers and SuperScript III Reverse Transcriptase (Invitrogen) in a 20 μl reaction according to the

manufacturer's instructions, with the addition of betaine to a final concentration of 1M. PCR was performed with GoTaq polymerase (Promega) using 1.5 μl of the cDNA in a 25 μl reaction with the gene-specific primers shown in Table 2.4. Betaine was included in each reaction to a final concentration of 1M.

Table 2.4: Primers used to analyze expression in Figure 2.2.

Gene	Primer		Temp[2]	Cycles[3]
	f/r[1]	Sequence (5'→3')		
CSP41a	f	CGTGTGGCGGGTGGTGCTC	62°C	35
	r	CAGGTCCTTGCCGTTGTTGTCATA		
CSP41b	f	GCACAGGTCAAGGTCTCTGCTCG	60°C	27
	r	CATGCGGTCTCCCTGGATGTGC		
PAP4	f	CTATCCTCGGCTTCATGTGTGCG	57°C	35
	r	GGCTGTAGCATCGCAGCGTTATG		
PNP1	f	CCGCTTGCGTGACTGCAAATGC	60°C	23
	r	CATCCGACGCAGCGATGTCC		
RNB1	f	CTGTACCGGCCTGGTGGACGAG	60°C	32
	r	GCGAGCCGCGTATCCAGCAGG		
RNB2	f	GCCGCAACTTCCGCCACC	62°C	28
	r	GAGGACTTGACGGCGTGCA		
RNJ1	f	GTCGTAGCTCAGGCGGATAA	60°C	23
	r	GGCGTCAATGACCACGTATC		
IDA5[4]	f	AATCGTGCGCGACATCAAGGAGAA	60°C	23-24
	r	TTGGCGATCCACATTTGCTGGAAGGT		

[1] "f" indicates forward and "r" indicates reverse primer.
[2] annealing temperature of the PCR.
[3] indicates number of cycles in PCR necessary for amplification of each gene.
[4] *IDA5* encodes Actin.

To verify silencing of *RNB2*, *RNJ1* and *PNP1*, The Access RT-PCR kit (Promega) with the addition of 1M betaine was used in a one-step amplification of *IDA5* and *MAA7*. 20 cycles was needed to amplify *IDA5*, 23 for *MAA7*. The *IDA5* primers in Table 2.4 were used, and the primer set for *MAA7* was 5'-TGAACATCACTGCCCCTACTC-3' and

5'-CCCAGCGAGTTGTTGATCTTA-3'. A two-step RT-PCR protocol was utilized for *RNB2* and *RNJ1* amplification as described above.

To investigate expression of *RNB1* and *RNB2* in PNPi3, cDNA was generated from 0.5 *μ*g of DNase-treated RNA (TAP-grown cells; PNPi3 and VC cultures contained 8 *μ*M 5-FI) and random hexamers using the SuperScript III kit (Invitrogen). One-tenth of the reaction was used in a 50-*μ*L PCR with Promega GoTaq polymerase with 1 M betaine for *RNB1* (37 cycles), *RNB2* (35 cycles), or *IDA5*, encoding actin (30 cycles). Intron-spanning primers for *RNB1* and *IDA5* are the same as those in Table 2.4, the primers for *RNB2* are: 5'-TCGTGGCTGCACGCGGCAC-3' and 5'-CAGGTAGCTGGCGGGCGAC-3'.

Targeting Experiment: The *RNB1* fragment encoding amino acids 1 to 189 was amplified from cDNA, inserted into the Gateway entry vector pENTR, and recombined into pMDC83 (Curtis and Grossniklaus, 2003), a vector designed for N-terminal fusions with GFP. The intronless *RNB2* fragment encoding amino acids 1 to 115 was amplified from genomic DNA and cloned in the same manner. The predicted RNB2 amino acid sequence differs from the gene model at the N terminus, based on cDNA sequencing by Steve MacKinnon (GenBank accession number EF431887). The expression cassette for the YFP cytosolic control was described previously (Bollenbach *et al.*, 2005). 20 *μ*g of the control and RNB2 vector, and 10 *μ*g of the RNB1 vector were used in polyethylene glycol–mediated transformation of tomato protoplasts as described (Xing *et al.*, 2001). Protoplasts were visualized at 24 h (20 hours for RNB1) after transformation by confocal microscopy on Leica TCS SP2 and TCS-SP5 confocal microscopes (Leica Microsystems, Exton, PA USA).

Generation of antisense and RNAi constructs: The *PNP1* antisense construct was based on plasmid pCB797 (Schroda *et al.*, 2002). Postdoctoral associate Yutaka Komine utilized PCR to amplify base pairs 158 to 522 of the *PNP1* coding region, with the addition of ClaI and EcoRI sites, and ligated the product into the same sites of pCB797. Nuclear transformants were generated by electroporation (Shimogawara *et al.*, 1998) with the linearized construct and selected on TAP medium containing 2 μg/mL zeocin after a 24 hour recovery period.

The RNAi construct was based on the vector containing the Maa7/X inverted repeat transgene from Rohr *et al.* (2004). To facilitate the insertion of an inverted repeat into this vector, modifications were performed to make it Gateway (Invitrogen) compatible, similar to pHELLSGATE (Helliwell and Waterhouse, 2003). The new vector was named pGwyRNAi and contains the *Arabidopsis* PDK intron in the spacer region. PCR was used to amplify coding region base pairs 277 to 522 of *PNP1*, 2600-2836 of *RNB2*, and 752 to 992 of *RNJ1*; these were inserted into pENTR. A double Gateway LR recombination was then used to insert this fragment in inverted orientations into pGwyRNAi. Transformation was performed as above, and after a 48 hour recovery period, PNPase RNAi transformants of the recipient strains CC-406 and CC-849 were selected on TAP medium containing 8 μM 5-fluoroindole, 10 μg/mL paromomycin, and 1.5 mM Trp on plates covered with a single layer of paper towels and under light. Only the recipient strain CC-849 was utilized for RNase J1 and RNB2 RNAi, and 10 μM 5FI and 1.5 mM Trp were used on the selection plate.

Generation of antibodies: To generate the anti-PNPase antibody, a cDNA fragment extending from position 172 to 522 of the coding region was inserted into pENTR. Gateway LR Clonase facilitated recombination of the fragment into the pDEST17 expression vector with an N-terminal His tag. BL21-AI cells carrying the vector grown to an OD_{600} of 0.44 were induced with 0.2% arabinose for 4.5 h at 25°C. The cells were pelleted and resuspended in lysis buffer (300 mM NaCl, 10 mM imidazole, and 50 mM Tris, pH 8). After the cells were passed two times through a French press, it was determined that the overexpressed antigen was in the insoluble fraction. The insoluble pellet was resuspended in urea buffer (10 mM Tris, 100 mM sodium phosphate, 50 mM NaCl, and 8 M urea) and clarified before mixing with nickel–nitrilotriacetic acid agarose slurry (Qiagen) for 1.5 h at room temperature and transferring to a column. After washing, the protein was eluted with 100 mM NaH_2PO_4, 10 mM Tris HCl, and 8 M urea, pH 4.4. A total of 2.5 mg of the eluted polypeptide was excised from a polyacrylamide gel and sent to Lampire Biological Laboratories for antibody production in rabbits using their Express-line protocol.

I supervised Steve MacKinnon in the generation of the RNase J1 antigen. A cDNA fragment extending from 715 to 1059 of the coding region was inserted into pDEST17 as described above. BL21-AI cells carrying the vector grown to an OD_{600} of 0.62 were induced with 0.1% arabinose for 3 h at 37°C. Again, the peptide was mainly insoluble, so it was prepared for antibody production as described above, and 1.5 mg of the protein was sent for antibody production.

FPLC analysis: CC-849 cells were lysed using a French press in HEPES I buffer (25 mM HEPES pH 7.5, 5 mM $MgCl_2$, 0.3 M sucrose). Samples were

centrifuged at 14,000 x g for 30 minutes at 4°C to remove insoluble material. 100 μl of the protein at a concentration of 3.5 mg/ml was loaded on a Superdex 200 HR 10/30 column and eluted with co-IP buffer (150 mM NaCl, 20 mM Tris pH 8.0, 1 mM EDTA). 0.5 ml fractions corresponding to molecular weights from > 670 to < 44 kDa were collected, TCA-precipitated, and compared to peaks emerging at 670, 158, and 44 kDa from a gel filtration standard (BioRad).

CHAPTER 3

POLYNUCLEOTIDE PHOSPHORYLASE POLYADENYLATES IN *CHLAMYDOMONAS* CHLOROPLASTS, BUT MITOCHONDRIAL POLY(A) AND POLY(U)-RICH TAILS ARE UNAFFECTED BY ITS DEPLETION

ABSTRACT

RNA decay-facilitating polyadenylation occurs in *Chlamydomonas* chloroplasts, but it is not known whether addition of poly(A) to decay intermediates is a part of the RNA degradation pathway in algal mitochondria. A reverse genetic analysis was performed in the search for enzymes responsible for adding poly(A) tails to organellar transcripts. Three candidates, nucleotidyltransferase family members PAP3 and PAP4, and polynucleotide phosphorylase (PNPase) all have this potential. Comparisons to the nucleotidyltransferase family in *Arabidopsis* and the nature of a signature amino acid residue suggest that PAP3 is a CCA transferase, an enzyme that acts exclusively on tRNA and is not likely to polyadenylate in either organelle. PAP4 was shown biochemically to be a poly(A) polymerase, with the unusual ability to add NDPs as well as NTPs to an RNA substrate. Furthermore, compositional analysis of tails in a PAP4-transformed *E. coli* PAP1 (*ΔpcnB*) mutant demonstrated that PAP4 polyadenylates RNA *in vivo*. However, depleting PAP4 in *Chlamydomonas* did not alter the character of tails in either the chloroplast, or in the mitochondria where they were also found. In contrast, a PNPase-depleted strain was almost entirely lacking in chloroplast tails, while mitochondrial tails appeared unaffected by PNPase depletion. Unexpectedly, by using an oligo(dC)(dT)-adaptor primer on G-tailed RNA, I was able to detect

not only polyadenylated mitochondrial *cox1* mRNA, but also *cox1* transcripts bearing tails composed primarily of U and A nucleotides. These two tail types were distributed in similar locations on *cox1*, leading to speculation that at least two as-yet unknown enzymes are required to polymerize tails in *Chlamydomonas* mitochondria.

INTRODUCTION

Addition of an oligonucleotide tail as part of the process of RNA decay occurs in virtually every organism (Dreyfus and Regnier, 2002; Kushner, 2004) (Slomovic *et al.*, 2006b; Slomovic *et al.*, 2006a; West *et al.*, 2006; Vanacova and Stef, 2007), in contrast to the stabilizing function of poly(A) tails in the eukaryotic cytosol.

It was demonstrated in Chapter 2 that polynucleotide phosphorylase (PNPase) is required for degradation of an artificially polyadenylated reporter gene mRNA in *Chlamydomonas* chloroplasts. This suggests that one function of this protein in chloroplasts resembles its major role in *E. coli*, namely to act as a 3'→5' exoribonuclease in a polyadenylation-mediated mRNA decay pathway (Cheng and Deutscher, 2003; Carpousis, 2007). However, both the *E. coli* and chloroplast enzymes are readily reversible, being capable of both degradation and polymerization under conditions of biological relevance (Mohanty and Kushner, 2000a; Yehudai-Resheff, 2001), and thus, PNPase might also act as a poly(A) polymerase (PAP) in the chloroplast as well.

It is unclear whether the tails naturally found on chloroplast mRNAs (Komine *et al.*, 2000) are added by PNPase, by a prokaryotic-type PAP orthologous to *E. coli* PAP1 (Mohanty and Kushner, 1999), or by both. In *E.*

coli, PAP1 is the major polyadenylating enzyme, but PNPase generates tails in *pcnB* mutants; *pcnB* encodes PAP1 (Mohanty and Kushner, 2000a). The bacterial PNPase adds heterogeneous tails composed of ~75% A, whereas PAP1 synthesizes largely homogeneous A tails. *Chlamydomonas* chloroplast tails are of this latter class, which suggests that they are generated by a PAP. Furthermore, as described in more detail in Chapter 4, the *Chlamydomonas* nucleus encodes three enzymes of the nucleotidyltransferase (NTR) family, and nine members of a novel oligonucleotide-adding family belonging to the same superfamily, called the non-canonical poly(A) polymerases (ncPAPs). All of these are potential polynucleotide and oligonucleotide adding enzymes.

In comparison to our knowledge of *Chlamydomonas* chloroplast RNA degradation, less is known about the process of mitochondrial RNA decay. Mitochondrial oligonucleotide tails are known to be involved in degradation in plant and human mitochondria, but paradoxically, tails are also necessary to stabilize some human mitochondrial transcripts (Gagliardi *et al.*, 2004; Slomovic *et al.*, 2006a). Addition of tails in these two mitochondrial systems is also catalyzed by PNPase and/or a PAP. Since oligonucleotide tails have not yet been described in *Chlamydomonas* mitochondria, this issue was also investigated. Given this study's focus on PNPase, mitochondrial tails are especially relevant since unlike higher plants, which separately encode mitochondrial and chloroplast PNPases, the *Chlamydomonas* genome appears to contain a single gene. This raises the question of whether PNPase is absent in *Chlamydomonas* mitochondria, or is dually targeted.

This question of which enzymes catalyze tail addition to a given substrate must be addressed in order to better understand how tail addition affects the rate and regulation of RNA decay. Here, I have focused on

determining which enzymes are responsible for tail addition in chloroplasts and mitochondria of the green alga *Chlamydomonas reinhardtii.* PNPase and the NTR family members PAP3 and PAP4 have been identified as likely organellar polyadenylating enzymes. While *Chlamydomonas* PNPase has a known catabolic function and has also been implicated in the cellular response to phosphorus deprivation (Chapter 2), the effect of PNPase depletion on organellar oligonucleotide tails had not been examined. The results reported here suggest that PNPase is the major enzyme generating poly(A) tails in the chloroplast, but has little or no mitochondrial activity. I also found that PAP3 is most likely a tRNA CCA-transferase (CCAtr), and that while PAP4 possesses polyadenylation activity and may be mitochondrially localized, its partial depletion does not measurably affect mitochondrial oligonucleotide tails.

RESULTS

PAP3 is likely to be a CCA transferase but PAP4 may be a poly(A) polymerase

PNPase has been previously characterized in *Chlamydomonas*, but PAP3 and PAP4 had not been studied. To obtain an indication of the type of activity these NTRs may possess, they were aligned with the three *Arabidopsis* NTRs (Figure 3.1), which based on their amino-terminal sequences, are predicted to be targeted to mitochondria or chloroplasts (Martin and Keller, 2004). This was done primarily so that our laboratory could better define the organellar NTRs in a collaborative effort with the laboratory of Dr. Gadi Schuster (Technion University, Haifa, Israel), where the *Arabidopsis* NTRs were being studied. All of these proteins belong to the Class II NTRs,

which in addition to the eubacterial-like PAPs, include CCAtrs that mature tRNAs by adding the non-encoded terminal CCA. In addition, the CCAtr activity in organisms such as *Synechocystis* sp., *Deinococcus radiodurans*, and *Aquifex aeolicus* is split between two enzymes, one that adds –CC and the other that adds a terminal –A (Tomita and Weiner, 2002).

Although it is difficult to assign an activity to a Class II NTR based on primary sequence, Martin and Keller (2004) identified Glu193 in *B. stearothermophilus* as a residue in the PAP domain that allows discrimination between CCAtrs and PAPs. This residue is Glu in all enzymes known to be capable of adding a cytosine to RNA, and is variable in other family members. Only one each of the *Arabidopsis* and *Chlamydomonas* proteins possess this Glu.

The relationships between the *Chlamydomonas* and *Arabidopsis* NTRs of interest are shown in Figure 3.1A. For convenience, I have used the name of the *Arabidopsis* chromosomal locus as a way of describing a putative or known protein product, while using “Cr” to designate *Chlamydomonas* proteins for comparative purposes. The two likely CCA transferases, At1g22660 and CrPAP3, cluster together with a high bootstrap value. Excluding the presumptive transit peptides, they are 38% identical and 54% similar at the amino acid level. The two remaining *Arabidopsis* proteins cluster together and may derive from a gene duplication event. They are 54% identical at the amino acid level, minus the probable transit peptides. At1g28090, predicted by Martin and Keller to be the chloroplast PAP, has an additional isoform due to alternative splicing, which differs by the absence of the first exon and begins at a start codon 15 bp upstream of the second exon (Figure 3.1B).

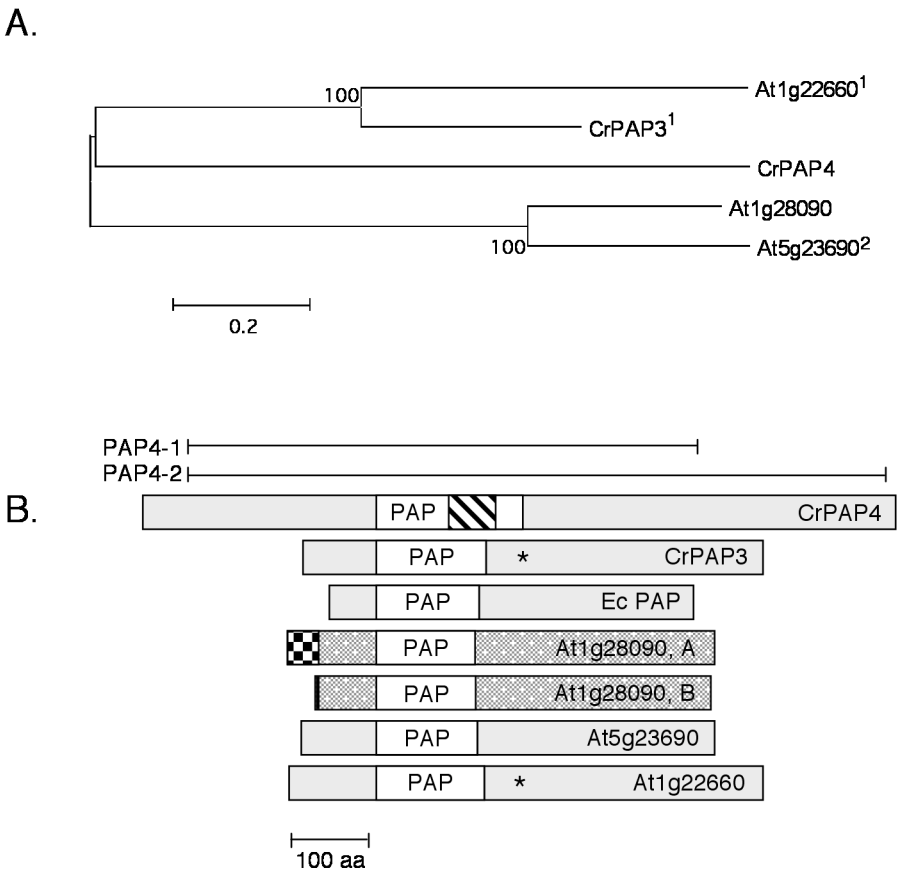

Figure 3.1: Comparison of putative organellar *Chlamydomonas* and *Arabdiopsis* NTRs

A: Phylogenetic analysis of *Chlamydomonas* and *Arabidopsis* Class II NTRs that are predicted to be organellar. The sequences, PAP3: *Chlamydomonas* genome version 3.1 protein ID 206563, PAP4 (EU311729), At1g28090 (NP_174130.2), At5g23690 (NP_197758.2), At1g22660 (NP_173680) were aligned and assembled on a phylogenetic tree using MEGA 3 http://www.megasoftware.net/, as in Chapter 1. [1]Sequences likely to encode CCA transferases. [2]Sequence is likely a PAP. B: Alignment of *Chlamydomonas* and *Arabidopsis* putative organellar Class II NTRs with *E. coli* PAP. The proteins are aligned from the beginning of the catalytic and conserved PAP head domain, pfam PF01703. Cr: *Chlamydomonas reinhardtii*; Ec: *Escherichia coli*. The lengths of the N- and C-terminal extensions in PAP4 can be observed from this to-scale drawing. The PF01703 domain in PAP4 is interrupted with extended intervening sequence (hatched). Asterisks mark the Glu residue that designates a likely CCAtr. Isoforms of the *Arabidopsis* putative PAP are presented, with the identical regions in grey with dots and the dissimilar N-termini in checks (isoform A) and black (Isoform B). Regions in grey have variable amounts of sequence similarity between proteins (described in text). The length of recombinant PAP4 proteins are shown along the top of the CrPAP4 schematic.

Initial data from the laboratory of Dr. Gadi Schuster suggest that At1g28090, but not At5g23690 possesses PAP activity *in vitro* (data not shown). CrPAP4, the remaining *Chlamydomonas* NTR, is on a separate branch from either the *Arabidopsis* PAP-like proteins or the CCAtrs, so little can be inferred about its activity from this tree.

At 960 aa, CrPAP4 is larger than all other known NTRs; a comparison of length with *E. coli* PAP and the three *Arabidopsis* NTRs discussed above is shown in Figure 3.1B. The location of the discriminating Glu mentioned above is indicated with an asterisk. All of the plant and algal proteins are longer on the N-terminus than *E. coli* PAP, and on this basis could encode transit peptides for mitochondrial or chloroplast localization. In addition, CrPAP4 has a long C-terminal extension. This region is highly repetitive both at the nucleotide and the amino acid level, and glutamine-rich. Another unusual feature of CrPAP4 is a region of unique sequence that interrupts its PAP domain.

Chlamydomonas *PAP4, like most of the* Arabidopsis *organellar NTRs, is probably mitochondrial.*

CrPAP4 and three of the *Arabidopsis* NTRs (At5g23690, At1g28090 Isoform A, and At1g28090 isoform B), could play a role in organellar polyadenylation. Several targeting predictors, namely TargetP (Emanuelsson *et al.*, 2000), Predotar (Small *et al.*, 2004), and iPSORT (Bannai *et al.*, 2002), suggested that all of these proteins were organellar. To obtain empirical evidence that the N-terminal regions of these proteins and that of the probable *Arabidopsis* CCAtr could act as transit peptides, the first 264 aa of CrPAP4, 100 aa of At1g22660, 100 aa of At5g23690, 100 aa of At1g28090 isoform A,

and 60 aa of At1g28090 isoform B were fused to GFP and expressed transiently in tomato protoplasts. Figure 3.2 shows that nearly all of the potential transit peptides, including PAP4, direct GFP to mitochondria, since the GFP signal is coincident with MitoTracker Red. This is in contrast with the control transformation of the RNB2 transit peptide-GFP fusion, which, as shown in Chapter 2, is localized to the chloroplast. The only non-mitochondrial NTR was At1g28090 isoform B, whose N-terminus did not target GFP to either organelle. I cannot exclude that the 60 aa fused to GFP constituted an incomplete transit peptide; however, a fusion using 100 amino acids was not expressed. Although the probable At CCAtr N-terminus directed GFP to the mitochondria, a slight signal from the chloroplasts in the GFP channel, almost indistinguishable from background, allows for the possibility of low level expression in the chloroplast as well. There are many instances of dual targeting of proteins, reviewed in (Millar *et al.*, 2006); for example, dual targeting of aminoacyl-tRNA synthetases is the rule rather than the exception in *Arabidopsis* (Duchene *et al.*, 2005).

Figure 3.2: Confocal microscopy images of tomato protoplasts expressing fusions of the N-termini of putative organellar NTRs fused with GFP.
Each image is a single protoplast within which chloroplasts can be visualized by their autofluorescence, and mitochondria by MitoTracker dye. In the last column, these two channels were overlayed with the GFP channel to show the location of the transit peptide/GFP fusion.

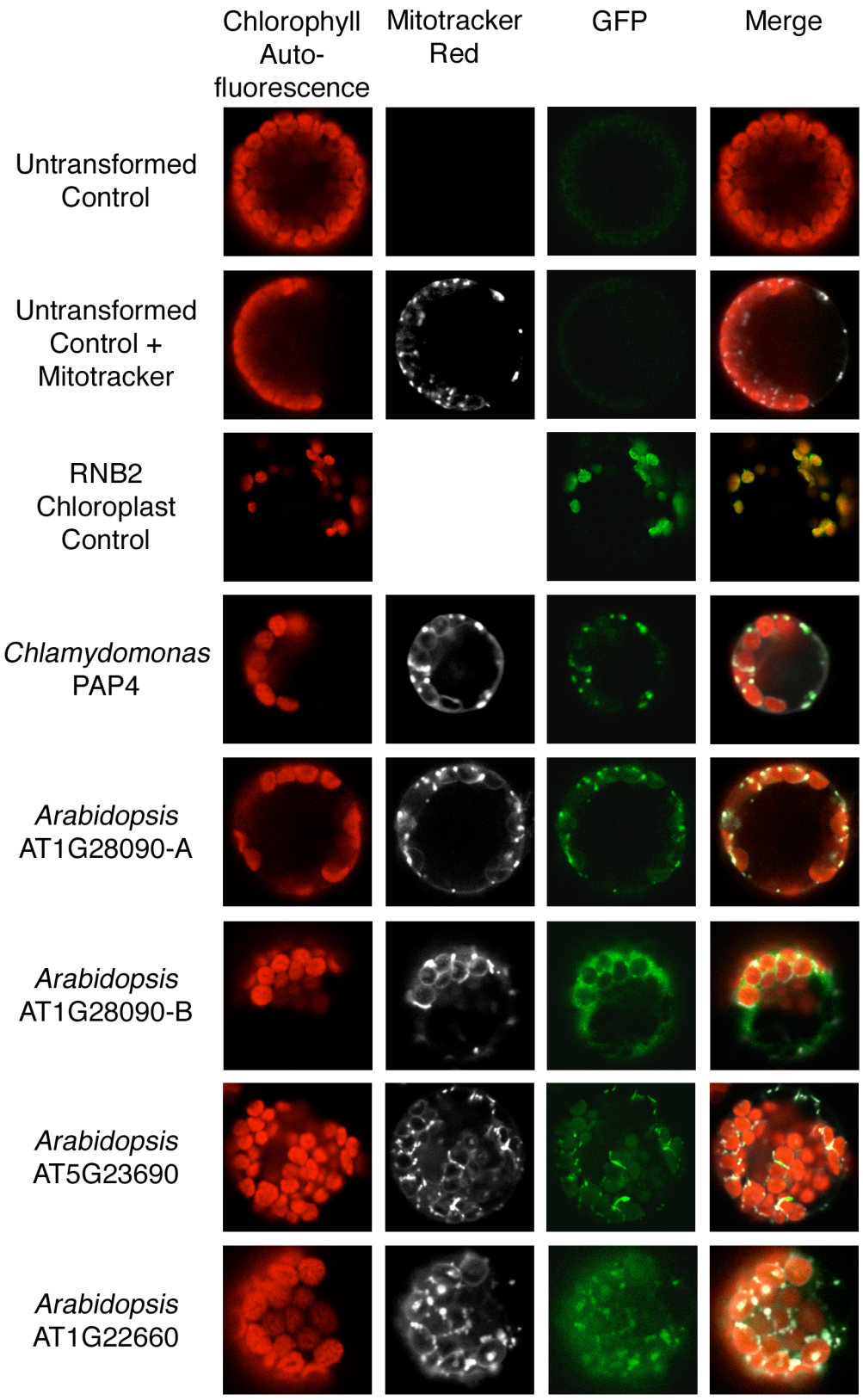
Chlorophyll Auto-fluorescence
Mitotracker Red
GFP
Merge
Untransformed Control
Untransformed Control + Mitotracker
RNB2 Chloroplast Control
Chlamydomonas PAP4
Arabidopsis AT1G28090-A
Arabidopsis AT1G28090-B
Arabidopsis AT5G23690
Arabidopsis AT1G22660

PAP4 recombinant expression

With the evidence that PAP4 is mitochondrial, at least based on fluorescent protein targeting in a heterologous system, I next asked if it had the ability to add a poly(A) tail to RNA. Recombinant PAP4 (shown above the cpPAP4 schematic in Figure 3.1B), lacking the predicted 58 aa transit peptide, was expressed in *E. coli* with an N-terminal thioredoxin tag and a C-terminal histidine (His) tag (PAP4-1). This protein also lacked the repetitive 259 aa C-terminus, which shares no sequence similarity with other PAPs. PAP4 was purified using the His tag, followed by two chromatography steps (see Methods), yielding the purity seen in Figure 3.3. After the first affinity purification step, a sample of partially purified PAP4-1 was analyzed by SDS-PAGE and immunoblotting with the antibody PAP4a, to verify that the main band observed was indeed PAP4 (Figure 3.3A).

Of concern was potential contamination by *E. coli* PNPase, which also exhibits polyadenylation activity under the assay conditions used. *E. coli* PAP1 could theoretically also contaminate the assay but is much less abundant. The level of contaminating PNPase was tracked during purification by immunoblotting and it is presented along with the purification in Figure 3.3B. I determined that the level of contaminating PNPase was below 0.04 ng/μl, only 0.3% of the amount of PAP4 in the assay. This was deemed acceptable, especially considering that the ATP used in subsequent assays is a relatively poor substrate for PNPase, compared to its preferred substrate ADP.

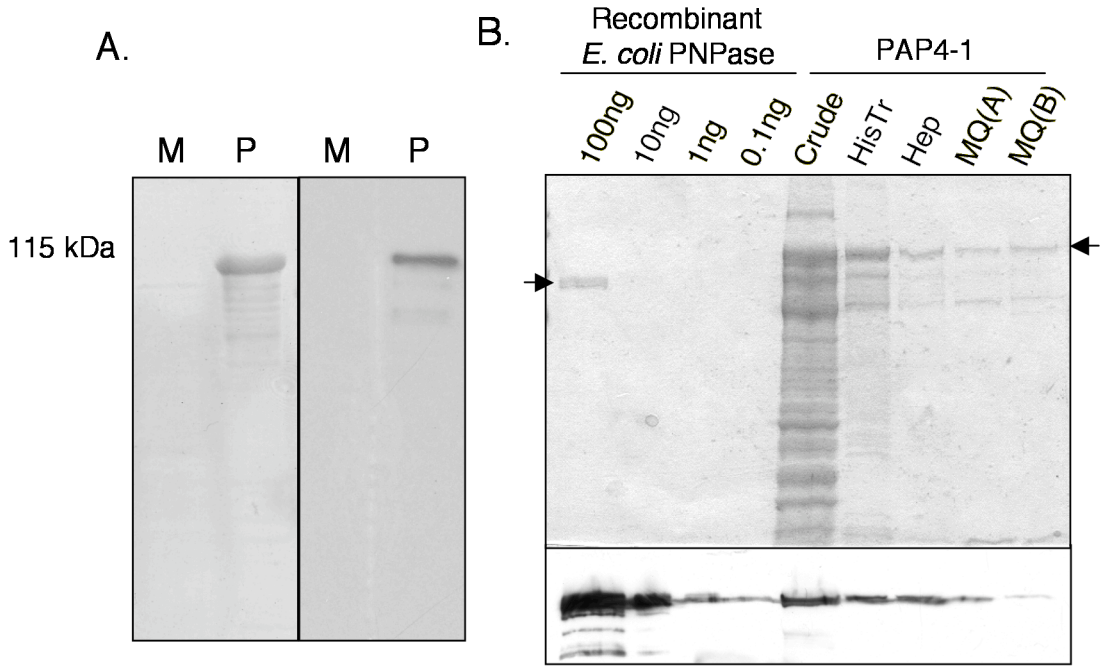

Figure 3.3: Purification of recombinant PAP4-1.
A: Partially purified thioredoxin and His-tagged PAP4-1 (P) eluted off a Nickel-NTA column is recognized by a PAP4a antibody as a band of an apparent weight of 115 kDa. The left panel shows a Coomassie stain (approximately 1 μg loaded) and the right panel, a nitrocellulose membrane with 0.01 μg of PAP4-1, probed with the PAP4a antibody at a 1:3000 dilution. The antibody does not recognize anything in a mock (M) purification of untransformed *E. coli*. B: Purification of PAP4-1. The top panel is Coomassie-stained gel showing purity of full-length protein indicated by the left-pointing arrow after HisTrap (HisTr), Heparin (Hep), and MonoQ (MQ) columns. A portion of MonoQ-eluted protein was concentrated before using in the assay (A), the other portion was dialyzed into the assay buffer D (B) and used directly. The bottom panel is an immunoblot showing the reduction of contamination by *E. coli* PNPase (indicted by right-facing arrow) over the course of the purification, to below the level of 0.1 ng per assay.

PAP4 activity

The ability of PAP4 to act as a CCAtr was tested first, in a comparative analysis with the probable *Arabidopsis* CCAtr At1g22660. The capacity of At1g22660 for this activity was demonstrated first. Recombinant At1g22660 (AtCCAtr) lacking the predicted 84 aa transit peptide was expressed in *E. coli* with an amino-terminal His tag, and purified as previously described (Portnoy

and Schuster, 2006) by Aleks Schein at Technion University. When utilized in a CCAtr assay, AtCCAtr added three terminal nucleotides to $tRNA^{Phe}$, demonstrated by migration of the radiolabeled $tRNA^{Phe}$ in a high-resolution polyacrylamide gel (Figure 3.4A). Since PAP4 lacks the Glu diagnostic of CCAtrs, it was unlikely to be a –CC or –CCA adding enzyme. It might, however, add a single –A to tRNAs instead of adding a polynucleotide tail. To test this possibility, an assay where the $tRNA^{Phe}$ substrate already possessed the terminal –CC was utilized. Figure 3.4B shows that while AtCCAtr is able to add the terminal nucleotide, PAP4 is not. Therefore, this recombinant version of PAP4 cannot act as any form of a tRNA maturation enzyme.

PAP4 was then tested for polyadenylation activity, using an A_{20} substrate and ATP. As shown in Figure 3.5A, this substrate could be rapidly and processively elongated to a high molecular weight product. After 5 min, the products tended to migrate as a discrete band rather than a smear, suggesting that the tails are long enough to remain in the exclusion zone of the gel. The recombinant PAP4 is inefficient, as 150 ng of the enzyme polyadenylated only a small amount of the substrate RNA, which was in approximately 10-fold molar excess, and its efficiency was not improved when the thioredoxin tag was cleaved (data not shown). The optimal ATP concentration for PAP4-catalyzed polyadenylation was between 0.2 and 1 mM (Figure 3.5B), a physiologically relevant concentration, since the ATP concentration has been estimated to be in the 0.1 mM range in actively respiring yeast mitochondria (Amiott and Jaehning, 2006).

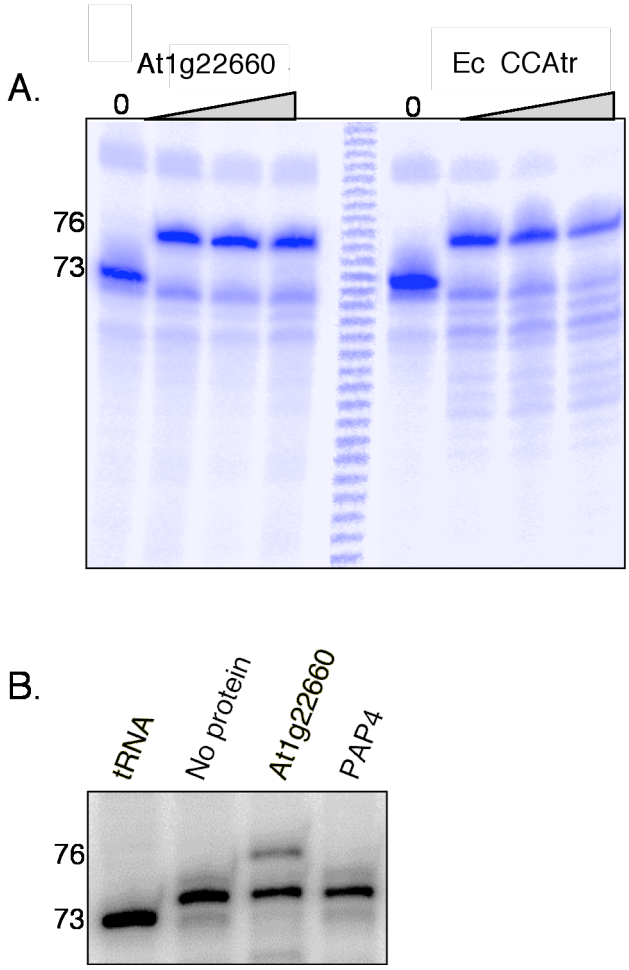

Figure 3.4: Testing –CCA and –A transferase activity of At1g22660 and PAP4.
A: Purified [^{32}P]-labeled tRNA^{Phe} was incubated with nucleotides and At1g22660, or recombinant *E. coli* CCAtr as a positive control. After incubation, the RNA was isolated and analyzed by high-resolution denaturating PAGE and autoradiography together with RNA ladder and size markers. Sizes of RNA molecules (in nucleotides) are indicated on the left. (Figure and legend adapted from the Ph.D. dissertation of Aleks Schein at Technion University.) B: A-transferase assay with PAP4-1. [^{32}P]UTP-labeled tRNA^{Phe} was incubated with At1g22660 and CTP in an initial reaction to generate a substrate for PAP4. The –C and –CCtRNA^{Phe} was then incubated with ATP and no protein (lane 2), At1g22660 (lane 3), or PAP4 (lane 4) for 15 minutes, and analyzed as in (A).

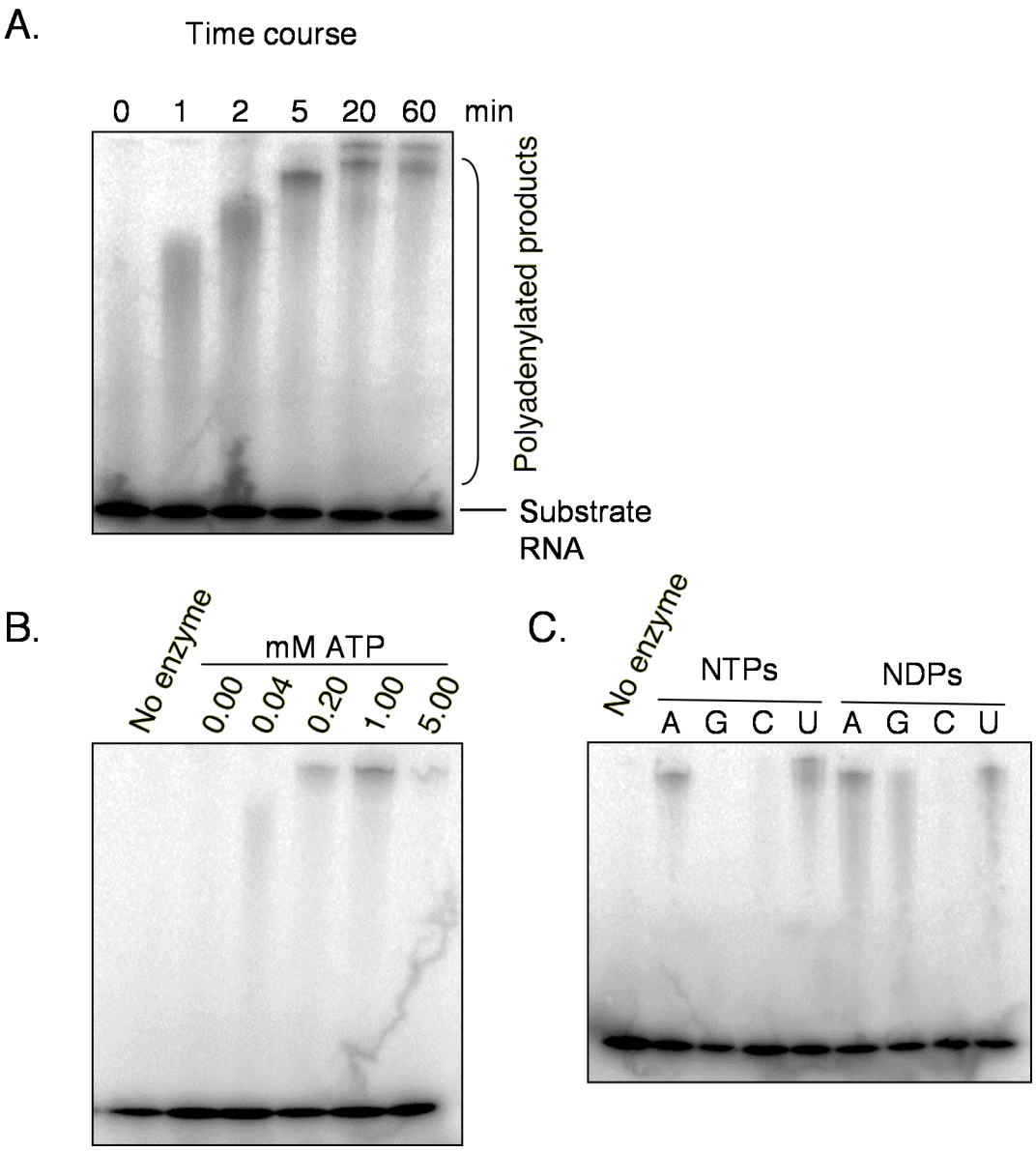

Figure 3.5: Polyadenylation assays.
A: PAP4-1 was incubated with radiolabeled A_{20} and 0.5 mM ATP at 25°C. Aliquots were removed at the times shown and RNA was isolated and analyzed by PAGE. B: The same assay shown in (A), except that the amount of ATP was adjusted in each reaction as indicated, and the reaction was allowed to proceed for 20 minutes. C: PAP4 was incubated for 20 minutes with the A_{20} substrate and 0.5 mM of each of the eight nucleotides shown, and treated as (A).

Finally, in light of the fact that *E. coli* PAP can only utilize nucleotide triphosphates (August *et al.*, 1962), while PNPase is able to utilize both nucleotide di- and triphosphates (Littauer and Kornberg, 1957; Grunberg-Manago *et al.*, 1956; Yehudai-Resheff *et al.*, 2001), PAP4's ability to incorporate various nucleotides was examined. Since ADP and other NDPs are the preferred substrate of PNPase, in this assay it was crucial that no *E. coli* PNPase contamination be present in purified PAP4. Therefore, PAP4 was prepared in a PNPase mutant strain, but overall yield was lower when this purification strategy was employed. Surprisingly, unlike *E. coli* PAP1, PAP4 is able to utilize ATP and ADP equally well, and also has the ability to utilize UTP and UDP *in vitro* (Figure 3.5C). A trace amount of activity was observed when GDP was provided.

***PAP4 alters the composition of nucleotide tails in* E. coli.**

To see whether PAP4 could act as a PAP *in vivo*, I attempted to complement an *E. coli* PAP1 deletion mutant (Δ*pcnB*) with the *Chlamydomonas* protein. Both N- and C-terminal truncated PAP4, equivalent to the moiety assayed in Figures 3.4-3.5, and a version including the unique C-terminus (PAP4-2), were used and are shown above the cpPAP4 schematic in Figure 3.1B. Expression of both PAP4 versions could be detected by immunoblotting 30 minutes after arabinose induction but surprisingly, protein accumulation subsequently decreased, and two hr post-induction no protein could be detected (Figure 3.6A).

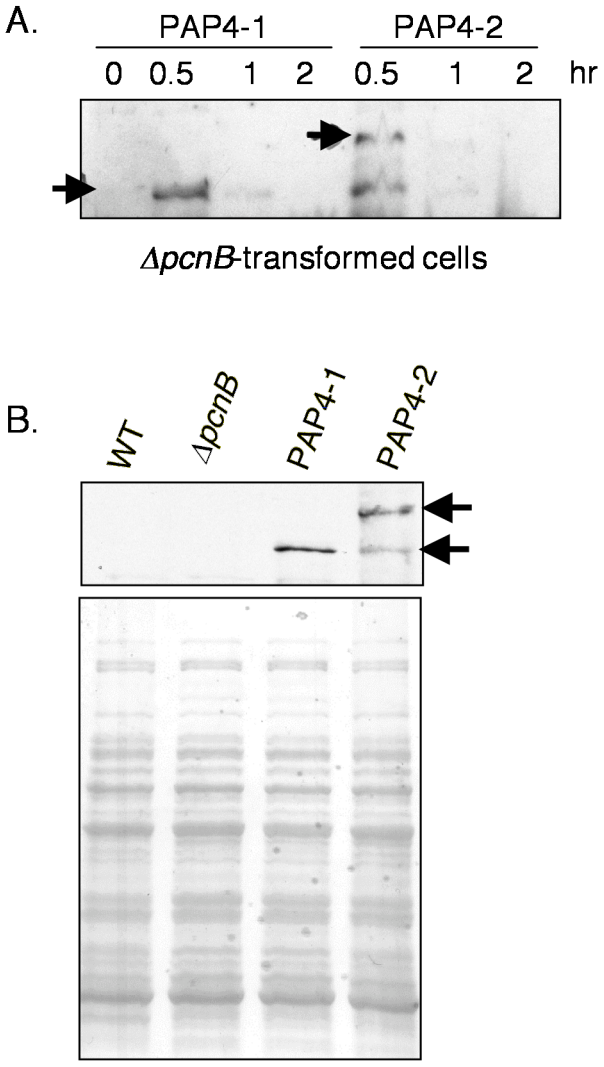

Figure 3.6: PAP4-1 and PAP4-2 Expression in *E. coli*
A: Time course of PAP4-1 and PAP4-2 expression. *E. coli ΔpcnB* was transformed with constructs expressing each version of PAP4. At the indicated times, cells were collected and protein from approximately 165 μl of cells at $O.D._{600}$ 0.5 was analyzed on an immunoblot challenged with anti-PAP4b. Arrows indicate the expressed protein. B: Protein from *ΔpcnB* transformed with one of several PAP4 constructs, using approximately 0.4 ml of cells at 0.3 $O.D._{600}$, was collected at the same time RNA was obtained for *lpp3* tail analysis. After running duplicate gels, one was Coomassie stained as a loading control (bottom panel), and the other was transferred to nitrocellulose and probed with a PAP4 antibody (top panel). Arrows indicate the expressed protein.

One phenotype of the *ΔpcnB* mutant is that transcripts including *lpp3*, which encodes outer membrane murein lipoprotein, lack the transient homogeneous A tails found in wild-type (WT) cells (Mohanty *et al.*, 2004). Instead, tails consisting of only 75% A are observed, and their presence has been attributed to the activity of PNPase. Therefore *lpp3* cDNAs were amplified using an oligo(dT)-adaptor primer from WT, mutant and PAP4-expressing strains. At the time of RNA collection, protein was also analyzed to verify that PAP4 was indeed expressed in the transformed strains (Figure 3.6B). The *lpp3* PCR products were separated in a 1.5% agarose gel, and the smear of fragments from 150 to 500 bp was excised, this being the range of probable products considering the transcript size. Purified products were cloned and sequenced.

Table 3.1: Composition of nucleotide tails added to *lpp3* transcripts in strains with and without PAP4 expression.
Results diagnostic of *ΔpcnB* are shaded. Transformed *ΔpcnB* is indicated with the plasmid in parentheses.

Strain	Total tails >10 nt	*lpp3* tails, percentage of total		
		Composition ≥90% A	Composition 75% > A > 90%	Composition <75% A
WT	30	67	3	30
ΔpcnB	17	0	18	82
***ΔpcnB*(pPAP4-1)**	22	27	23	50
***ΔpcnB*(pPAP4-2)**	8	13	12	75

Table 3.1 summarizes the tails obtained. 17 tails were analyzed for composition in *ΔpcnB*. Since none of these had a composition of >90% A, this was used as the benchmark for identification of tails likely to be a result of PAP activity. Thus, any tail with >90% A was inferred to be a PAP rather than PNPase product. Conversely, >80% of the *ΔpcnB* tails had ≤75% A, so this

was the benchmark of a PNPase-generated tail. The population of tails in WT, *ΔpcnB*, and both *ΔpcnB* PAP4 transformants were assigned into categories of ≤75% A, 75%-90% A, and >90% A. It is evident that in the WT, there is a mixture of tails generated by PNPase and PAP. While 62% of the tails were almost or totally homogeneous A, there was also a portion of <75% A. This is similar to the 70% homogeneous A tails observed previously in a WT strain (Mohanty *et al.*, 2004). When PAP4-1-expressing cells were analyzed, 27% of the tails were nearly homogeneous, whereas none were seen in untransformed *ΔpcnB*. This suggests that PAP4-1 has limited PAP activity in *E. coli*. While one homogeneous tail was obtained from PAP4-2-expressing cells, the low sample size does not allow us to draw any firm conclusions about the ability of PAP4-2 to complement *ΔpcnB*.

PNPase is responsible for polyadenylation in the chloroplast.

PNPase was shown to be entirely responsible for RNA tails in the cyanobacterium *Synechocystis* (Rott *et al.*, 2003), and the polyadenylation activity of spinach chloroplasts also co-purifies with PNPase (Yehudai-Resheff *et al.*, 2001). In both cases, the tails are A-rich and heterogeneous, in spinach being approximately 70% A. Tails previously described in *Chlamydomonas* chloroplasts were far more homogeneous (Komine *et al.*, 2000), suggesting that in the alga PNPase might not be responsible. Additionally, since non-encoded tails are also present in *Chlamydomonas* mitochondria, as shown below, either PNPase and/or PAP4 might generate them. To determine if either of these enzymes were required to generate tails in either organelle, I used RNAi to reduce expression of the two genes, and then analyzed tails on

mRNA from chloroplasts and mitochondria of the deficient strains, as compared to a strain containing only the silencing vector (Vector Control: VC).

In Chapter 2, I described the generation of a stable PNPase-deficient strain, PNPi3, estimated to express 10% of WT levels of PNPase. The same vector system was utilized to generate PAP4-silenced strains. Because of the difficulty in generating RNAi strains that did not eventually suppress PAP4 silencing, RNA and protein were collected from PAP4i transformants as soon as possible after they appeared on the selective medium. RNA from the three transformants showing the highest level of silencing at the protein level were combined and used in the analysis of tail composition, in a single experiment. After approximately 100 generations, the PAP4 depletion appeared to be suppressed, and no more RNA could be collected for experimental repetitions. Figure 3.7A demonstrates that although levels of *PAP4* mRNA are similar in VC and various transformants, the level of *MAA7* mRNA, whose silencing is necessary for survival of transformants on the selective medium, decreased as expected. However, Figure 3.7B shows that at the protein level, the amount of PAP4 is lower in transformants 1, 3 and 11, which were ultimately used for cDNA analysis. This situation was also observed with the PNPase RNAi mutants, and suggests that the silencing mechanism might be occurring at the translational level.

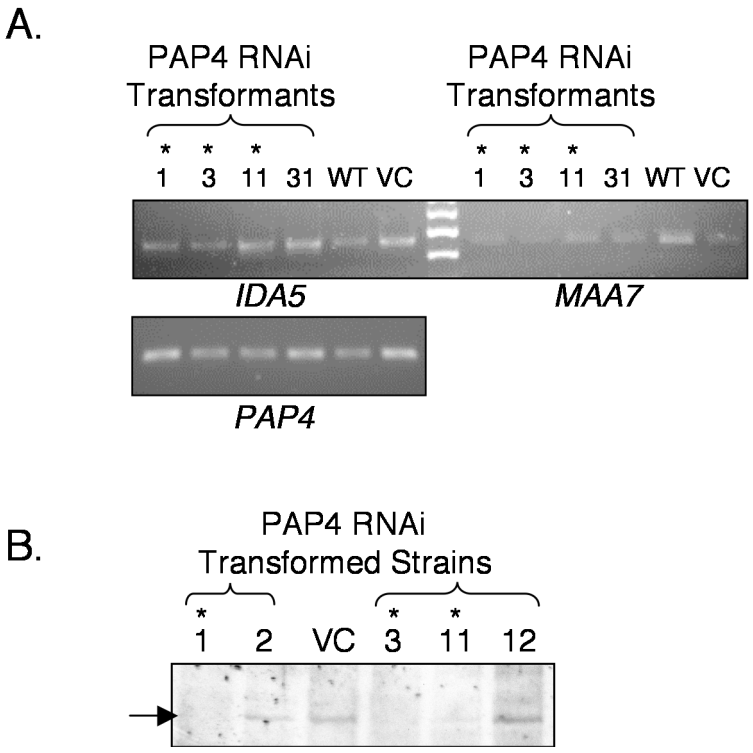

Figure 3.7: Depletion of PAP4 in *Chlamydomonas*.
A: RT-PCR analysis shows that the co-silenced *MAA7* transcript is reduced in all transformants, including three exhibiting PAP4 depletion at the protein level, as well as in the vector control (VC), when compared to levels in the untransformed strain (WT). The actin gene (*IDA5*) is used as a control. RNA from these three strains (indicated by asterisks) was used for analysis of polynucleotide tails in the chloroplast and mitochondria. B: The PAP4 antibody recognizes a protein of an apparent weight of 100 kDa, indicated by the arrow, in VC and transformed strains 2 and 12. This protein is barely detectable or undetectable in strains 1, 3 and 11.

For chloroplasts, I analyzed polynucleotide tails of the *atpB* transcript, for which previously obtained data were available from the WT (Komine *et al.*, 2002). To do so, total RNA was first G-tailed, and then I used a dC_5dT_8-adapter primer to promote cDNA synthesis from the very ends of polyadenylated transcripts. I then amplified *atpB* tails using nested primers (Figure 3.8, top, f1-f3). Results are shown in the lower part of Figure 3.8. The tails from the VC are shown in black and were for the most part homogeneous, although I did obtain some tails with more G, C, and U residues than was previously reported. The tails, located at or near the end of the mature transcript, were clustered around the endonucleolytic cleavage site, which was also consistent with previous results, although I did not see an additional spike in tail numbers at the mature end as seen previously. Tails from the PAP4i strain were similar in both location and composition (in red), suggesting that PAP4 does not have a major role in chloroplast polyadenylation. The 34 tails collected from these two strains ranged in length from 8 or less to 59 nt. This is also consistent with what was reported previously.

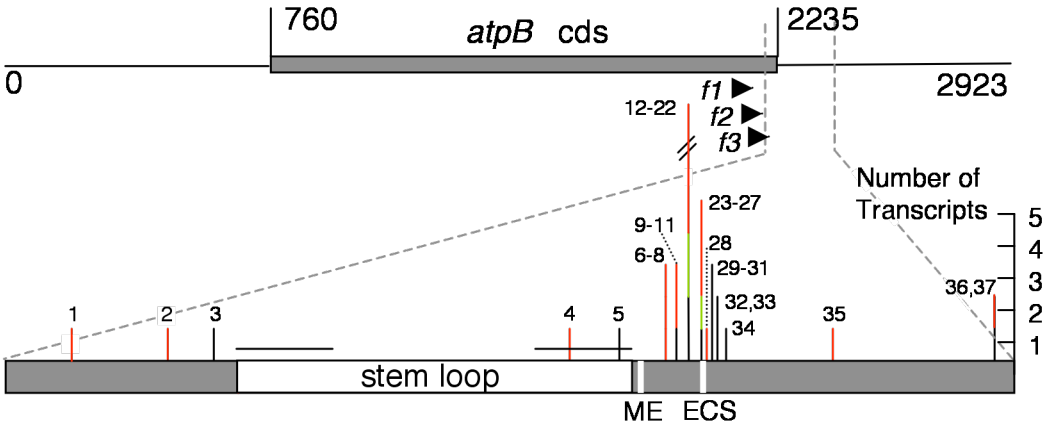

3. $GA_{17}GA_9$
5. $a_2A_9GA_{11}GGA_4GA_2GA_8$
11. A_8
19-20. A_8
24. aA_{14}
25. aA_{11}
26. $aA_{19}CA_{11}$
29. $aA_{12}CA_2GAGA_2GA_{12}$
30. $aA_2GA_5GA_{10}GA_{27}$
31. aA_6GA_{32}
32. GA_2UA_{16}
33. A_2CACA_{42}
34. $A_8GA_8CA_2GA_{24}$
37. A_8

1. $A_5GAGA_{21}GA_3UA_{25}$
2. $a_5A_5GA_2GA_{15}GA_5UA_6GA_6GA_8GA_{11}$
4. A_9
6. A_8
7. A_8
8. A_8
9. aA_{22}
10. aA_{14}
12. A_{13}
13. A_{25}
14. A_{19}
15. A_{14}
16. A_{19}
17. GCA_{13}

18. A_{15}
23. aA_4UA_{16}
28. aA_9
35. A_8
36. A_8
21. A_{16}
22. A_8
27. A_8

Figure 3.8: The location and composition of chloroplast *atpB* poly(A) tails.
The coding region of *atpB* is indicated, as are the features downstream of the stop codon, where a majority of the tails are added. ME: mature end of transcript; ECS: endonucleolytic cleavage site. “f1” and ”f2” are the primers used to amplify the tails (f2 is nested); the “f3” primer was used to screen colonies for those that contained *atpB* sequence-containing vectors (Figure 3.9 and Results). Tails colored black are from the Vector Control (VC), red tails are from PAP4i, and green tails are from PNPi3. Adenine (A) nucleotides in lower case (a) are ambiguous; the nucleotide may be part of the *atpB* sequence or it may have been added by the polymerase. The shortest tails (8 nt) are equivalent to the number of T’s in the dT-adaptor primer, the actual tail may be shorter.

For PNPi3, I was not able to obtain nearly as many clones corresponding to polyadenylated *atpB* mRNA. When the secondary (f2-adapter) cDNA products were inserted into pCR2.1 and transformed into *E. coli*, colonies were obtained for all strains. However, when the third nested primer (f3) was used to analyze colonies for those containing polynucleotide-tailed *atpB* sequences, for PNPi3 most of these colonies were negative (did not yield a PCR product of the expected size), indicating that the colony contained no *atpB* cDNA, and most likely harbored empty vector. The results are summarized in Table 3.2, and a representative sample of the PCR reactions is shown in Figure 3.9.

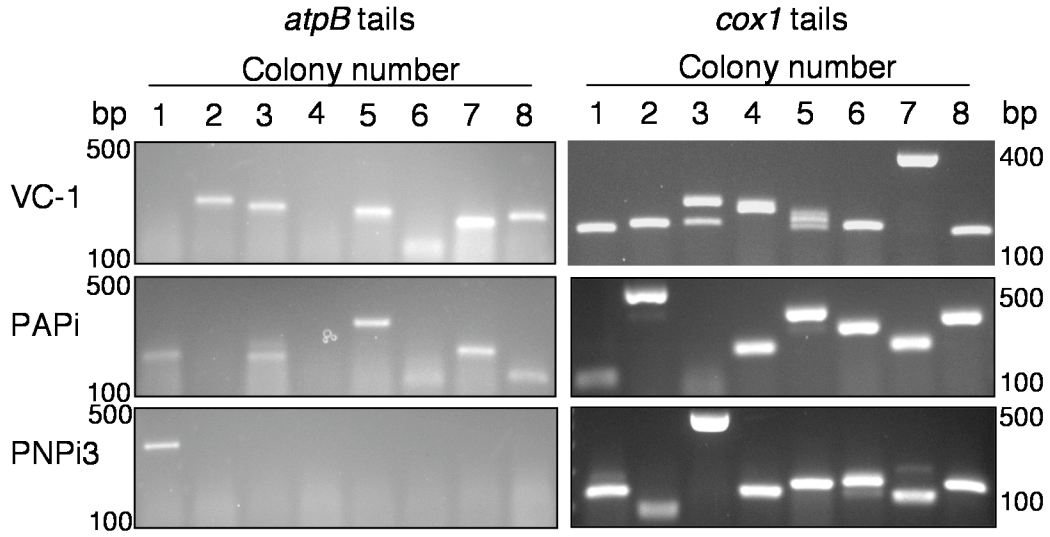

Figure 3.9: PCR screen to identify colonies with *atpB* or *cox1* transcript-containing clones.
Colony PCR was performed with f3 and adapter primers at the annealing temperatures shown in Table 3.3 in Methods, for 22-25 cycles. Representative screens of each of the experiments are shown.

Table 3.2: Summary of nucleotide tails.
Chloroplast (*atpB*) and mitochondrial (*cox1*) transcripts obtained from the same pools of cDNA primed with either a dT-adapter oligonucleotide (dT cDNA) or a dCdT-adapter oligonucleotide (dCdT cDNA) following G-tailing of the RNA. Results for *atpB* in the PNPase-deficient strain are highlighted. VC-1 is the vector control.

	atpB **dCdT cDNA**			***cox1*** **dT cDNA**			***cox1*** **dCdT cDNA**		
Strain	VC-1	PAP4i	PNPi3	VC-1	PAP4i	PNPi3	VC-1	PAP4i	PNPi3
Colonies Screened[1]	48	48	96	32	17	17	38	16	45
Positive Clones[2]	19	23	12	32	16	16	30	14	41
Polynucleo-tide Tails[3]	11	14	1	16	15	11	13	6	31
% Colonies w/ Tail Seq.	23	29	1.0	50	88	65	34	38	69

[1]Individual colonies possibly containing polyadenylated *atpB* sequence in vectors were screened by colony PCR using an internal *atpB* primer and the 3' adapter primer used in the initial amplifications.

[2]Each colony that yielded a single discrete product over 100 bp in colony PCR was considered a positive clone, and sequenced.

[3]Tails counted here are those that exceed the length of the primer.

Of the 96 PNPi3 colonies screened, only 12 were judged "positive". When DNA from these positive clones was sequenced, most contained *atpB* sequence that terminated within an AT-rich region of *atpB*, usually downstream of the 3' stem loop and endonucleolytic cleavage site that is the predominant region of polyadenylation for VC and PAP4i. I hypothesize that for most of the *atpB* sequences obtained for PNPi3, the reverse primer annealed to regions of AT-rich sequence within the *atpB* mRNA during reverse transcription, rather than to a polyadenylated tail. The three tails that were not found in positions where internal priming was highly probable are colored

green in Figure 3.8. An additional tail was found in the extreme 3' UTR at position 2469, and is not shown in the figure. Only one tail longer than the poly(A)$_8$ sequence corresponding to the primer binding region was obtained from the 96 colonies screened. This contrasts with a rate of 23% of clones containing *atpB* tails longer than 8 A's in the VC and 29% of clones when RNA from PAP4i was examined (Table 3.2). I conclude that my lack of ability to find polyadenylated *atpB* transcripts in this strain was due to the reduced levels of PNPase.

To eliminate the possibility that the RNA from the PNPi3 strain was inferior in quality, RNA quality was checked by analyzing the sharpness of ribosomal RNA bands in an agarose gel (data not shown). Furthermore, the same pool of PNPi3 cDNA was utilized to analyze mitochondrial tails, and an equivalent amount of *cox1* tails were obtained in PNPi3, VC, and PAP4i, as discussed below. I concluded that RNA from PNPi3 is of equivalent quality to those purified from VC and PAP4i, and that the lack of *atpB* tails cannot be attributed to a degradation of the PNPi3 RNA sample. The *cox1* screening results are also included in Table 3.2 and Figure 3.9.

Both A- and U-rich tails are observed in mitochondria

The *cox1* transcript, encoding cytochrome oxidase subunit 1, was utilized to investigate mitochondrial polyadenylation. As for *atpB*, I used the dCdT-adapter-primer and three nested upstream primers, but since the transcript is longer, PCR products up to 600 bp were collected. The results obtained were unexpected. Although I did sequence several poly(A) tails, many more U-rich tails were observed and shown in Figure 3.10B for VC (black), PNPi3 (green), and PAP4i (red). U-rich tails were defined as having a

combination of A and U nucleotides, and an arbitrary cutoff of ≥50% U in a given tail yielded the percentage of U-rich tails as 75%, 90% and 83% in the three strains, respectively. These tails had been added apparently stochastically throughout the part of the coding region analyzed, presumably to RNA degradation intermediates. They were comprised of 69% U, but A made up 28% of the composition, with G and C making up the remaining 3%. Typically, A's in groups of 1-4 nt would punctuate groups of 3-5 U's. There was no obvious strain-specific pattern either in terms of addition site, tail length or tail sequence. Uridine-containing tails have recently been discovered in several other contexts (see Discussion).

I interpret the prevalence of cDNAs corresponding to U-rich tails in this experiment to the additional hydrogen bonding between the five G's of the reverse primer to U's in the tail as compared to a pure poly(A) tail, where only the T's in the primer would anneal. In other words, the 5' end of the cDNA primer may be partially anchored by G-U bonds, enough to favor an initial cDNA product containing U's. If this is the case, the true length of the tails is especially uncertain given that the reverse primer could bind anywhere along the tail. Excluding the length of the primer, 7 nt, a range of 1 to 26 nt was observed.

Figure 3.10 Nucleotide tails on the *cox1* transcript.
"f1" and "f2" are the primers used to amplify the tail-containing RNA (f2 is nested). "f3" is the primer used for screening colonies to identify those containing vectors with *cox1* cDNA. Tails colored black are from the Vector Control (VC), red tails are from PAP4i, and green tails are from PNPi3. Lower case nucleotides are ambiguous, they could be derived from the *cox1* sequence or added by the polymerase. A. Tails with an elevated "A" composition, primarily obtained using a dT-adaptor primer. The shortest tails (10 nt) are equivalent to the number of T's in the dT-adaptor primer, the actual tail may be shorter. B. Tails with 50% or more U, primarily obtained using a dCdT-adapter primer on G-tailed RNA. Sequences shown for the U-rich tails do not include the nucleotides corresponding to the primer binding location (8 nt), because its composition cannot be determined.

A. poly(A) tails

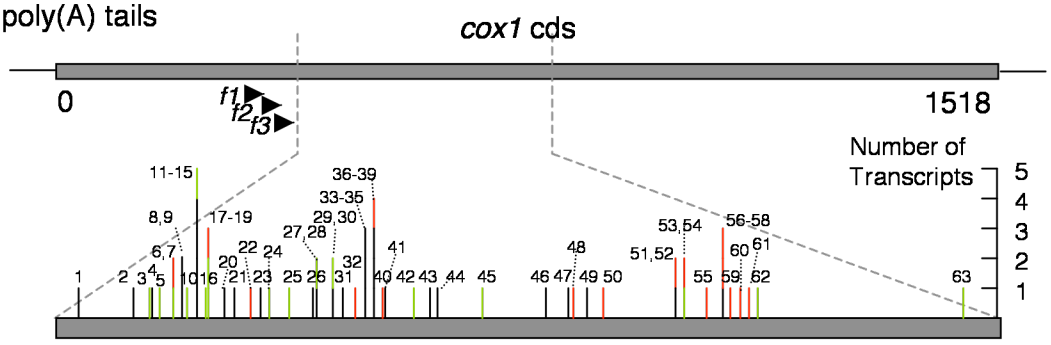

1. UA_{14}
2. $aA_{11}GA_2GA_2GCA_{10}$
4. A_{10}
8. aA_{10}
9. A_{10}
12. A_{10}
13. aA_{15}
14. A_{10}
15. aA_{10}
20. A_{12}
21. A_{25}
23. A_{10}
26. aA_8
28. $A_{12}CA_{10}CA_{12}$
30. $AUUA_{12}$
31. GA_{10}
33. A_{10}
34. A_{10}
35. A_{16}
37. A_{10}
38. A_{10}
39. A_{10}
41. A_{11}
43. A_{10}
44. A_{19}
46. A_{15}
47. $A_{15}UA$
49. A_{10}
52. A_{10}
58. A_{11}
7. A_{42}
19. aaA_{11}
22. A_{12}
32. A_{25}
36. aA_{10}
40. A_7UUA_{10}
48. A_{10}
50. A_2UUA_{14}
51. aA_{12}
54. A_{11}
55. aA_{34}
56. aA_3CA_{12}
57. aA_{18}
59. A_{10}
60. A_{15}
61. A_{11}
3. aA_{14}
5. AUA_2UA_{17} CC_AUA_{21}
6. A_{14}
10. A_2CA_{15}
11. aA_{10}
16. A_{10}
17. A_{10} x2
24. A_{10}
25. A_{12}
27. A_{32}
29. A_{11}
42. A_{15}
45. aA_{22}
53. A_{11}
62. A_{25}
63. A_{13}

B. U-rich tails

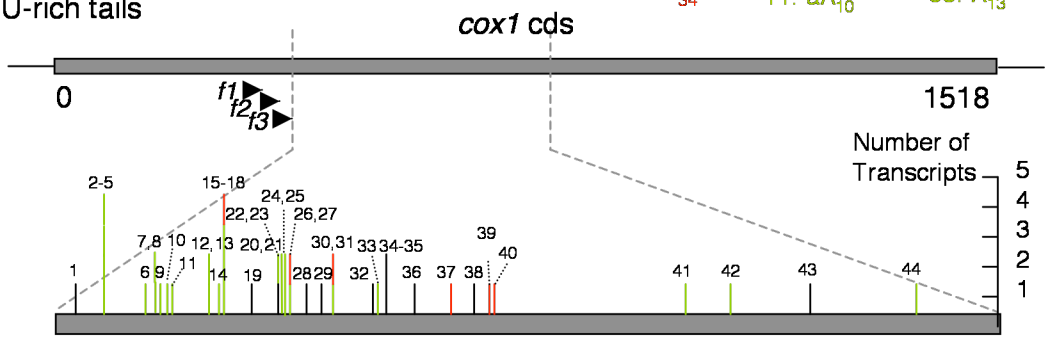

1. UUA
19. auuuu
20. $a_2UUUUUA_2U$
28. UUUUU
29. $uUUA_3UUUU$
32. $a_2UUUUUA_2U$
34. uuU
35. uuUUU
36. AU
38. G
43. $uUUUUA_2$
15. uuuUU
26. $uuA_2CAUUUUU$
30. UUA_2
37. auuAUUUU
39. A_3UA_3UUUUU
40. uUAUUUAUU
2. UUUU
3. aUUUU
4. a_2UUUU
5. a_2UUU
6. uU
7. $CGUUUUA_4UUUA$
8. auuu
9. $UUUUUUUCAN_7$
10. uaCUUUU
11. $uauuA_2UUU$
12. aUUAUUUUU
13. aaUUUUU
14. u
16. uuuAUUU
17. uuuAUUU
18. uuuAUAUUU
21. UUUUU
22. $GUUUGUA_3UUUUGAGAGA_8$
23. $aUUAUUUA_2UUU$
24. auUU
25. auUUU
27. $UUCA_2U$
31. AUUUUAUUUU
33. $uAUUUUA_3UUU$
41. UUUUUU
42. aUUUU
44. uuuUU

In an experiment that favors the preceding interpretation, when I utilized a dT_{10}-adapter primer to synthesize cDNA before amplifying *cox1*, the resultant tails were nearly homogeneous A (Figure 3.10A). Taking data from all three strains together, U-rich tails were only 7.3% of the population in this experiment. As for the U-rich tails, there was very little difference between results from VC, PNPi3, and PAP4i, leading me to conclude that neither PNPase nor PAP4 are responsible for mitochondrial tails. The only exception was that the median poly(A) tail location along the transcript for PAP4i was about 150 nt 3' to the median tail location in the other two strains. While this might have some significance, it is likely to be minimal, since the location of all the tails is within a 1,518 nt coding region.

DISCUSSION

PAP4 possesses a weak template-independent polyadenylation activity and unusual nucleotide specificity.

PNPase and PAP4 are enzymes that might be responsible for chloroplast and/or mitochondrial polyadenylation in *Chlamydomonas*. While PNPase activity had been previously investigated, the activity of PAP4 needed to be verified biochemically. I demonstrated that PAP4 has polyadenylation activity but cannot act as a tRNA –CCA or –A transferase. While recombinant PAP4 was processive, it was also quite inefficient, since very little of the substrate RNA became polyadenylated even after a one hr incubation (Figure 3.5A). Several reasons may underlie this observation. First, PAP4 contains a

repetitive region that was excluded from the recombinant protein, due to concern that it would cause aggregation in *E. coli*. This region could have functional significance; for instance in allowing PAP4 to dissociate from the transcript and initiate polyadenylation on a different molecule. The fact that full length PAP4 did not appear to complement *ΔpcnB* any differently than the truncated version makes this possibility less likely. A second and related possibility is that too much of the N-terminal region remained in the recombinant protein, where normally it would have been cleaved off during translocation. Also, the protein carried two epitope tags, which could interfere with folding or catalysis. Finally, PAP4 may require an accessory factor(s) for optimal activity.

Recombinant PAP4 differs from other prokaryotic-like PAPs because it is able to utilize ADP as well as ATP to extend a nucleotide chain. Although it is possible that a given sample of ATP might become contaminated with ADP due to decay by contaminating dephosphorylases, it is unlikely that the ADP stock is contaminated with ATP, and it is the utilization of ADP that was unexpected. Although the structural data available for yeast and mammalian PAPs have helped to define the active site and ATP position during catalysis (Balbo and Bohm, 2007; Martin *et al.*, 2004), no prokaryotic-like PAP has been crystallized, so the ability to compare binding pockets of a bacterial PAP and PAP4 to explain why PAP4 could accept a wider range of nucleotides is limited. The crystal structure of a CCA transferase is available (Li *et al.*, 2002), but this enzyme differs substantially from PAPs in that it adds limited amounts of nucleotides, readily utilizes CTP, and is specific for its tRNA substrate; therefore, a comparison with its binding pocket would be less informative.

The ability of an NTR to utilize both UTP and UDP as well as ADP and ATP does not have a precedent. However, assays showing the inability of PAPs to incorporate NDPs seem confined to the *E. coli*, cytosolic mammalian PAPII, and vaccinia virus polymerases (August *et al.*, 1962; Nevins and Joklik, 1977). Purified PAP I from HeLa cell extracts, though admittedly of a different class of NTRs than PAP4, is able to utilize ADP, but only 7% as efficiently as ATP (Nevins and Joklik, 1977). Furthermore, with the proper specificity factors, ADP is as good a substrate as ATP for AAUAAA-directed polyadenylation by mammalian PAPI (Lakota and Nelson, 1991). Concerning the ability of PAP4 to utilize more than one NTP, in this respect it resembles *E. coli* PAPI (Yehudai-Resheff and Schuster, 2000) in its relaxed nucleotide specificity *in vitro*.

PNPase depletion affects polyadenylation in the chloroplast but not in the mitochondria.

PNPase silencing resulted in an almost total loss of polyadenyation in *Chlamydomonas* chloroplasts. The residual activity observed as poly(A) tails on cloned cDNAs could be accounted for by the 10% or more remaining PNPase expression in PNPi3. I tentatively conclude, therefore, that as in *Synechocystis* and spinach chloroplasts, PNPase acts both to polyadenylate transcripts, and is at least partially responsible for their subsequent decay. However, the *atpB* tails that have been observed in *Chlamydomonas* chloroplasts are more homogeneous than those reported in spinach chloroplasts and *Synechocystis* (Lisitsky *et al.*, 1996; Rott *et al.*, 2003). This could be explained by either a difference in the catalytic properties of PNPase itself, or in the ratios of available nucleotides in the three different systems.

PNPase depletion did not affect the population of either type of tails for the mitochondrial *cox1* transcript. In contrast, depletion of mitochondrial PNPase in *Arabidopsis* had a profound effect on the transcript population, resulting in the stabilization of maturation byproducts and noncoding and chimeric transcripts. These stabilized RNAs were obtained by virtue of their polyadenylated 3' termini (Holec *et al.*, 2006). Therefore, rather than resulting in an absence of tails, as observed in the *Chlamydomonas* chloroplast, PNPase depletion in plant mitochondria allowed for the presence of more normally destabilizing tails, indicating that in at least one plant's mitochondria, PNPase functions mainly as an exonuclease. The enzyme responsible for polyadenylation in plant mitochondria is not known.

The human mitochondrial PNPase is localized to the intermembrane space, where presumably it would not come in contact with RNA (Chen *et al.*, 2006). Nevertheless, in HeLa cells with stable silencing of PNPase, long poly(A) tails at the ends of *COX1* mRNA were abolished, and tails on *ND3* and *ND5* mRNAs were lengthened (Slomovic and Schuster, 2008). It was therefore hypthothesized that PNPase can influence polyadenylation indirectly by altering the size of the ATP pool available for a PAP or other polymerase, since ATP depletion also affected tail length (Slomovic and Schuster, 2008). Therefore, even though the human mitochondria has a PNPase, it is unlikely to directly polyadenylate transcripts. Thus, in general, PNPase may not be a mitochondrial polyadenylation enzyme, despite its role in chloroplast polyadenylation.

The Chlamydomonas *mitochondrial U-rich tails share similarities and differences with other U-containing tails*

My analysis of oligonucleotide tails on mitochondrial transcripts revealed that short, U-rich tails are present along with poly(A) tails in *Chlamydomonas* mitochondria. Unlike the situation in trypanosome and human mitochondria, *Chlamydomonas* mitochondrial tails are far from homogeneous, being a mostly A/U combination with over twice as much U as A. The only other place this sort of tail has been identified was on RNAs of the Epstein-Barr virus after miRNA cleavage; a non-encoded UA-tract of a pattern similar to that described in the Results was inserted immediately prior to the poly(A) tail (Shen and Goodman, 2004). U-rich tracts were also observed in the same location on RNA3 from the beet necrotic yellow vein virus (Jupin *et al.*, 1990). Otherwise, when U tails are found, they are usually more homogeneous. Mitochondrial poly(U) tails have been observed in trypanosomes, added to guide RNAs necessary for RNA editing by RET1 Terminal Uridyltransferase (TUTase; Blum *et al.*, 1990), and in human mitochondria when PNPase is silenced (Slomovic and Schuster, 2008). Additionally, since the likely mechanism of UTP–stimulated decay of polyadenylated transcripts is the addition of U to the end of the tail by RET1 (Ryan and Read, 2005), the A-U tail generated by this pathway would have a poly(A) tract followed by poly(U), rather than the mixture that I observed.

A summary of the sequence evidence for post-transcriptional uridylation of RNA (Rissland and Norbury, 2008) makes it apparent that although non-template-dependent uridylation is not unusual, it is usually discovered serendipitously. Current knowledge of plant mitochondrial poly(A) tails arises from experiments utilizing a dT_{17-18}-adapter primer (Lupold *et al.*, 1999;

Gagliardi and Leaver, 1999; Gagliardi *et al.*, 2001; Kuhn and Binder, 2002), rather than the dCdT-adaptor with G-tailed RNA that was necessary to observe the U-rich tails in *Chlamydomonas* mitochondria. This raises the possibility that a heretofore unknown U-rich tail population may be present in plant mitochondria.

The two types of tails in Chlamydomonas *mitochondria suggest the presence of multiple mitochondrial polymerizing enzymes*

Since distinct types of tails can be added to the same stretch of *cox1* mRNA in *Chlamydomonas*, it is likely that two enzymes, or enzyme forms, are responsible for the activities. Such a situation is already known to be the case in both human and trypanosome mitochondria, where two types of poly(A) tails (long and short) are observed in addition to the poly(U) tails described above. In the human mitochondria, silencing PNPase and PAP (hmPAP) both result in changes to tails, but when both enzymes were co-silenced, a class of short poly(A) tails was still present, indicating the presence of yet another polymerase (Slomovic and Schuster, 2008). The same thing appears to be true in trypanosome mitochondria. Upon silencing of the mitochondrial kPAP2, the composition of 3' terminal tails on the *RPS12* transcript, but not on others, was altered to include more frequently interspersed U's. This suggests the presence of multiple polymerizing enzymes of variable nucleotide and mRNA substrate specificity (Kao and Read, 2007).

A contrasting case is that of Star-PAP, also called U6-TUT, which is one enzyme with two very distinct activities. This enzyme was first characterized as a uridyltransferase purified from a HeLa cell extract, which was highly specific for its U6 noncoding RNA substrate (Trippe *et al.*, 2006).

Star-PAP was later found to act as a PAP that was stimulated in the presence of phosphatidylinositol-4,5-bisphosphate and associated with mRNA 3' processing factors (Mellman *et al.*, 2008).

PAP4 depletion did not alter mitochondrial* cox1 *tails, but a diverse family of –A and –U adding enzymes provides additional candidates for this role.

Even though *Chlamydomonas* PAP4 is a polynucleotide polymerase *in vitro*, silencing the gene did not yield any changes in polyadenyation in either chloroplasts or mitochondria. Among the possible explanations for this result are incomplete silencing, biochemical redundancy, and a misleading result from the GFP fusion, which was carried out transiently in a heterologous system. Unfortunately, the availability of reliable gene silencing and knockout technologies is still a limitation in *Chlamydomonas* (Schroda, 2006).

As mentioned in the Introduction, another set of enzymes capable of generating poly(A) and oligonucleotide tails are the non-canonical poly(A) polymerases (ncPAPs). Since they were not included in this study, and the enzymes responsible for generating tails in mitochondria have still not been identified, this class of enzymes is worthy of further review. *Chlamydomonas* encodes nine ncPAPs, and four of these putative proteins possess predicted organellar transit peptides (Chapter 1). ncPAPs within a species are highly divergent (Martin and Keller, 2007), and members of this family may actually belong to related families of TUTs or poly(U) polymerases, which themselves diverge in sequence but may be functionally similar (Wickens and Kwak, 2008). For instance, candidate ncPAPs in multiple species' genomes, including *Arabidopsis*, were found to be poly(U) polymerases *in vivo*, although

several studies have shown that at least one of these, CID1, possesses both polyadenylation and polyuridylation activity *in vitro* (Rissland *et al.*, 2007; Kwak and Wickens, 2007). Star-PAP provides an instance where an ncPAP possesses both capabilities *in vivo*. These examples are consistent with the possibility that an ncPAP could be responsible for generating both the U-rich and poly(A) mitochondrial tails.

The function of mitochondrial polyadenylation and polyuridylation

Given that U-rich and poly(A) tails are in *Chlamydomonas* mitochondria, this raises the question of their role in RNA metabolism. Current data on poly(U) tails provide more instances where they contribute to decay than to stability (Wickens and Kwak, 2008; Rissland and Norbury, 2008), although both the tails on trypanosome mitochondrial guide RNAs and human U6 RNA are of the stabilizing variety. The fact that the tails observed in this study, both U-rich and poly(A), are found within the coding region of *cox1* is indicative of a destabilizing tail. However, the position of the gene-specific primers and the sizes of the PCR products collected would have eliminated the possibility of discovering tails on full-length transcripts that might either be stabilizing or destabilizing.

METHODS

Strains and growth conditions: For PAP4-1 expression in an *E. coli* strain containing PNPase, the construct described below was transformed into Top10 cells. The cells were grown at 37°C in LB + ampicillin (100 μg/ml) to an

O.D. of 0.8 and then induced with 0.004% arabinose and transferred to 22°C for 10 hrs.

For expression in the PNPase mutant *E. coli* ENS134-3, cells were grown in LBSP (LB medium containing 1M sorbitol and 50 mM NaPhosphate buffer, pH 7-8.5) + ampicillin (100 μg/ml) + kanamycin (50 μg/ml) at 30°C, induced as above, transferred to 25°C, and harvested after 12 hr.

For the complementation experiment, cultures of WT (Top10) and transformed and untransformed *ΔpcnB* (SK7988) were initiated in LB supplemented with 50 μg/ml thiamine at an $O.D._{600}$ of 0.09. The cells were grown for 40 min at 37°C and then induced with arabinose to a final concentration of 0.005%. After 30 min of growth at 37°C, the cells were harvested. *ΔpcnB* was a kind gift of Dr. Sidney Kushner (Univ. Georgia).

Cell wall-deficient *Chlamydomonas* (CC-849) cultures for transformation were initiated in Tris-acetate-phosphate (TAP) medium (Harris, 1989) plus 1% sorbitol under continuous light at 25°C and grown for several days until mid-log phase. They were then maintained for five more days in early to mid log phase by dilutions every 48 hrs, and were finally harvested for transformation by electroporation (described below) at a concentration 1-2 x 10^6 cells/ml.

Chlamydomonas cultures for collection of protein and RNA were initiated in TAP medium under continuous light at 25°C and grown 2-3 days until they had reached a concentration of approximately 2 x 10^6 cells/ml.

Generation of DNA constructs: To generate GFP fusions, the sequences encoding the fragment lengths described in Results were amplified from cDNA, inserted by BP Recombination into the Gateway entry vector pDONR207, and recombined into pMDC83 (Curtis and Grossniklaus, 2003), a

vector designed for N-terminal fusions with GFP, using LR Clonase (Invitrogen). The intronless *RNB2* fragment encoding amino acids 1 to 115 was amplified from *Chlamydomonas* DNA and cloned in the same manner.

The pPAP4 expression constructs were generated by inserting CDS regions 175 to 2376 (pPAP4-1) and 175 to 2817 (pPAP4-2) into pENTR (Invitrogen). Gateway LR Clonase facilitated recombination of the fragments into the pBAD-DEST49 expression vector that allows for expression of the protein with an N-terminal thioredoxin tag and a C-terminal His tag.

To produce the *PAP4* RNAi vector, PCR was used to amplify 1-171 bp of the *PAP4* coding region, corresponding to the transit peptide, and it was inserted into pENTR (Invitrogen). A double Gateway LR recombination was then used to insert this fragment in inverted orientations into pGwyRNAi, described in Chapter 2.

To generate the anti-PAP4a antibody construct, the *PAP4* cDNA fragment from 827-1142 bp of the coding region was amplified and inserted into pGEM T-easy, excised with EcoRI, and inserted into the EcoRI site of pET32a(+) (Novagen). Site-directed mutagenesis was necessary to eliminate a stop codon formed when the *PAP4* fragment was inserted at the pET32a(+) EcoRI site.

Generation of antibodies: Two PAP4 antibodies were generated, the first was adequate for identification of recombinant PAP4 (PAP4a), the second, utilizing the expression construct 4-1A, was needed to identify PAP4 in *Chlamydomonas* protein extracts (PAP4b). The PAP4a antigen in pET32a(+) was fused to N-terminal thioredoxin, His, and S tags and a C-terminal His tag. XL1-Blue cells containing the vector were grown to $O.D._{600}$ of 0.68 at 37ºC,

then induced with 1 mM IPTG for 4 hours. Cells containing the PAP4a antigen were passed through a French Press, and the lysed cells were centrifuged to pellet the antigen-containing insoluble fraction. After washing and resuspending the pellet, the PAP4a antigen was bound to nickel-nitrilotriacetic acid resin (Qiagen) and eluted as described in the manufacturer's instructions for denaturing conditions. 3 mg of eluted protein were sent to Lampire Biological Laboratories (Pipersville, PA) for antibody production in chicken using their Classic-Line Protocol.

The PAP4b antibody was generated against the entire recombinant PAP4-1, including the thioredoxin and His tags. After PAP4 expression and total protein extraction as described in the section on protein purification, 1.7 mg of soluble protein was eluted from nickel-nitrilotriacetic acid resin (elution buffer: 300 mM NaCl, 50 mM Tris pH 8, 250 mM imidazole and 7.5% glycerol), eluted from a polyacryamide gel, and used for antibody production in rabbits at Lampire Biological Laboratories using their Express-Line Protocol.

Confocal microscopy: 20 μg of each vector was used in polyethylene glycol–mediated transformation of tomato protoplasts as described (Xing *et al.*, 2001). Protoplasts were visualized 19-22 hrs post-transformation after incubation in the dye Mitotracker CMXRos (Molecular Probes) at 200 nM for 25 minutes to visualize mitochondria. Images were collected on a Leica TCS-SP5 confocal microscope (Leica Microsystems, Exton, PA USA) using a 63x water immersion objective NA 1.2. GFP and chlorophyll autofluorescence were excited with the blue argon ion laser (476 nm), and emitted light was collected from 485 nm to 550 nm for GFP and 653 nm to 695 nm for autofluorescence. Separately collected and superimposed was MitoTracker, excited with a

Diode-Pumped Solid State laser (561 nm), and collected with emitted light from 575 nm to 611 nm. Images were processed using Leica LAS-AF software (version 1.6.3 and 1.7.0) and Adobe Photoshop version 7.0 (Adobe systems). Microscopy was performed at the Plant Cell Imaging Center (PCIC) at the Boyce Thompson Institute.

Purification of PAP4: Cells were collected and lysed with a microfluidizer in lysis buffer (50 mM Tris pH7.5, 500 mM NaCl, 2 mM imidazole, 2% Triton X-100, 7.5% glycerol, 20 mM β-mercaptoethanol, and 1 EDTA-free protease inhibitor pellet per 10ml (Roche)). After removing the insoluble fraction by centrifugation, the supernatant was passed through a 0.22 micron filter and loaded onto a HisTrap column (Amersham). After washing, PAP4 was eluted with an imidazole gradient. PAP4-containing fractions were dialyzed for 2 hrs into DEPC-treated buffer E (20 mM Hepes pH 8, 60 mM KCl, 12.5 mM $MgCl_2$, 0.2 mM EDTA, and 5% glycerol), run on a HisTrap column (Amersham) and eluted with a KCl gradient. The KCl concentration of the PAP4-containing fractions was lowered by a 2 hr dialysis in buffer E, then PAP4 was purified using a MonoQ column (Amersham) and eluted with a KCl gradient. The eluate was then either concentrated 10-20 fold and frozen in aliquots, or directly dialyzed overnight in buffer D (the reaction buffer) and then frozen in aliquots. Small amounts of the concentrated PAP4 or larger amounts of the dilute PAP4 worked equally well in subsequent assays.

Activity assays: The [^{32}P]-labeled $tRNA^{Phe}$ substrate utilized in the CCAtr assays was generated from a plasmid described in (Schürer *et al.*, 2002). This plasmid and a vector encoding the full-length *E. coli* CCAtr , was a kind gift of

Dr. Heike Betat (Univ. of Leipzig, Germany) to the laboratory of Dr. Gadi Schuster (Technion University). The assay in Figure 3.4B was performed as follows: after *in vitro* transcription and ribozyme cleavage as described (Schürer *et al.*, 2002), 73 nucleotide-long [^{32}P]-labeled tRNA^{Phe} with a homogeneous 3' end was gel-purified. tRNA^{Phe} was then incubated with CTP and At1g22660 to generate the tRNA^{Phe} with C and CC 3' extensions. After phenol-chloroform extraction, this modified tRNA was used as the substrate in a reaction in buffer E, with 1 mM ATP and 120 μg PAP4 for 15 min at 25°C.

For the polyadenyation assay, 100-150 μg of PAP4 was incubated in buffer D (25 mM Tris HCl pH 8, 40 mM KCl, 0.5 mM $MnCl_2$, 0.005 mM EDTA, and 10% glycerol) with 9,000 cpm (approximately 2 ng) of [^{32}P]-labeled A_{20}, and 0.5 M NTP or NDP for 20 minutes at room temperature unless otherwise indicated. The reaction was stopped, and the RNA was purified and analyzed by PAGE as described (Stern and Gruissem, 1987).

RNA and protein extraction from *E. coli* and *Chlamydomonas*: Bacterial RNA was prepared using the Alternate Protocol described in Reddy and Gilman (2001), and quality was analyzed by the appearance of rRNA bands.

Bacterial crude protein extracts used for immunoblot analysis were prepared as follows: Cells were resuspended in 2 parts LB/ 2 parts sample buffer (2.5% SDS, 60 mM Tris pH 7.4, 15 mM EDTA, 10% glycerol, 0.14 mM β-mecaptoethanol)/1 part 6X loading buffer (60 mM Tris pH 6.8, 30% glycerol, 10% SDS, 0.6 M DTT, 0.012% bromophenol blue), incubated at 100°C for 3 min, vortexed and centrifuged to removed insoluble material.

Chlamydomonas RNA from 15 ml of culture grown as described above was extracted using Tri-Reagent (Molecular Research Center) according to

the manufacturer's instructions, but including an overnight isopropanol precipitation step at -20°C. Quality was analyzed as for *E. coli* RNA.

Chlamydomonas crude protein extracts for immunoblot analysis were prepared by collection of 15 ml of culture grown as described and resuspending cells in 100 μl 1X SDS sample buffer (2.5% SDS, 60 mM Tris pH 7.4, 15 mM EDTA, 10% glycerol, 0.14 mM β-mercaptoethanol). Samples were incubated for 4 min at 100°C, vortexed 30 sec, and centrifuged to remove insoluble material. The supernatant was transferred to a fresh tube and stored at -20°C.

***Chlamydomonas* transformation with RNAi vectors:** *Chlamydomonas* transformants of the recipient strain CC-849 generated by electroporation (Shimogawara *et al.*, 1998), were selected on TAP medium containing 12 μM 5-fluoroindole and 1.5 mM tryptophan on plates covered with a single layer of paper towels and under light.

RT-PCR and sequencing of polyribonucleotide tails: The RT-PCR used to amplify *MAA7* and actin (*IDA5*) cDNAs in the analysis of *PAP4* silencing was performed as in Chapter 2. Reverse transcription of RNA for *PAP4* amplification was performed as in Chapter 2 except that 1.5 μg of RNA was used. *PAP4* PCR was performed for 38 cycles with the primers and the annealing temperature listed in Table 3.3 using GoTaq polymerase (Promega).

For RNA tail analysis, SuperScript III Reverse Transcriptase (Invitrogen) was used to synthesize cDNA in a 20 μl reaction from 2 μg of total RNA using the dT-adapter primer (GACTCGAGTCGACATCGA$(T)_{10}$) at 45°C for 1 hr. When the dCdT-adapter primer (GACTCGAGTCGACATCGA$(C)_5(T)_8$)

was used instead, the RNA was first G-tailed as described (Komine *et al.*, 2000). 2 μl of the cDNA was used as a template in duplicate 20 μl PCR amplifications (PCR 1) using the adapter primer and an f1 primer (Table 3.3).

Table 3.3: PCR primers used in Chapter 3.

Name	Primer information		Rxn[1] Temp
	f/r[2]	Sequence	
PAP4	f	GCGCGGACCTGGTGCTTGAG	65°C
	r	GGCGGCTGCCTCATCTGCC	
adapter	r	GACTCGAGTCGACATCGA	N/A
lpp3 f1	f	CATGGAGATTAACTCAATCTAG	56°C
lpp3 f2	f	CTCAATCTAGAGGGTATTAATAATG	56°C
lpp3 f3	f	GAAAGCTACTAAACTGGTACTGG	56°C
atpB f1	f	GATGATTTACCAGAACAAGC	52°C
atpB f2	f	CAAGCATTCTACTTAGTAGG	55°C
atpB f3	f	CATTACAGAAGCTATTAG	50°C
cox1 f1	f	CCAGCCCTGGCTTTGTTGCTA	52°C
cox1 f2	f	GTCTACTTTGGTAGAGCAAGGCC	57°C
cox1 f3	f	GGTACTGGTTGGACCGCTTATC	55°C

[1]Rxn Temp refers to the annealing temperature in the PCR reaction.
[2]"f" refers to forward and "r" refers to reverse primer.

Duplicate reactions were run in the same well on a 1.5% agarose gel, the resulting smear of appropriately-sized products was excised and gel-purified with the Qiaex II gel purification kit (Invitrogen). Where distinct strong bands appeared in the nested PCR, they were found to be collections of transcripts with tails only as long as the dT primer region, and were not helpful in analysis; therefore, these bands were eliminated from the gel before purification of tailed transcripts for cloning and sequencing. 2 μl of the purified PCR 1 reaction was used as template in a nested PCR amplification (PCR 2) using the adapter primer and an f2 primer, and the product purified as for PCR 1. All of the precipitated products of PCR 2 were resuspended and TOPO-

cloned into pCR2.1 (Invitrogen), then transformed into Top10 cells. Selected colonies were analyzed by colony PCR using the gene-specific f3 primer and the adapter primer, and products examined in 2% agarose gels. Those colonies giving rise to a single discrete amplification product of >100 bp were used to obtain plasmid DNA for sequencing.

CHAPTER 4

GENOME-BASED ANALYSIS OF *CHLAMYDOMONAS REINHARDTII* EXORIBONUCLEASES AND POLY(A) POLYMERASES PREDICTS UNEXPECTED ORGANELLAR AND EXOSOMAL FEATURES*

ABSTRACT

Enzymes from several gene families modify RNA molecules at their extremities. These reactions occur in several cellular compartments, and affect every class of RNA. To assess the diversity of a subclass of these enzymes, we searched *Chlamydomonas* for open reading frames potentially encoding exoribonucleases, poly(A) polymerases, and proteins known to associate with and/or regulate them. The open reading frames were further analyzed for indications of protein localization to the nucleus, cytosol, mitochondrion, and/or chloroplast. By comparing predicted proteins with homologues in *Arabidopsis* and yeast, we derived several tentative conclusions regarding RNA 5' and 3' end metabolism in *Chlamydomonas*. First, the alga possesses only one each of the following likely organellar enzymes: polynucleotide phosphorylase, hydrolytic exoribonuclease, poly(A) polymerase and CCA-transferase, a surprisingly small complement. Second, although the core of the

* Zimmer, S. L., Fei, Z., Stern, D. B. (2008) Genome-based analysis of *Chlamydomonas reinhardtii* exoribonucleases and poly(A) polymerases predicts unexpected organellar and exosomal features. Genetics. 179: 125-136.

nuclear/cytosolic exosome decay complex is well conserved, neither nucleus-specific activators nor the cytosolic exosome activators are present. Finally, our discovery of nine non-canonical poly(A) polymerases, a divergent family retaining the catalytic domains of conventional poly(A) polymerases, leads to the hypothesis that polyadenylation may play an especially important regulatory role throughout the *Chlamydomonas* cell, stabilizing some transcripts and targeting degradation machinery to others.

INTRODUCTION

Our initial aim was to define and categorize *Chlamydomonas* enzymes involved in either elongating or trimming the 3' ends of RNAs encoded in the nuclear, mitochondrial, and chloroplast genomes. Indeed, RNA metabolism is one of the few processes occurring in all three organelles as well as the cytosol, which together represent three different endosymbiotic origins. The release of *Chlamydomonas* genome version 3 (Merchant *et al.*, 2007) – now supplemented by version 4 – gave us an opportunity to perform this analysis in a unicellular photosynthetic eukaryote, where we have focused on comparing its suite of enzymes and regulators to those found in a non-green unicellular organism – yeast – and the multicellular *Arabidopsis*. A related analysis focused on endoribonucleases, such as those of the Dicer family, is published elsewhere (Casas-Mollano *et al.*, 2008).

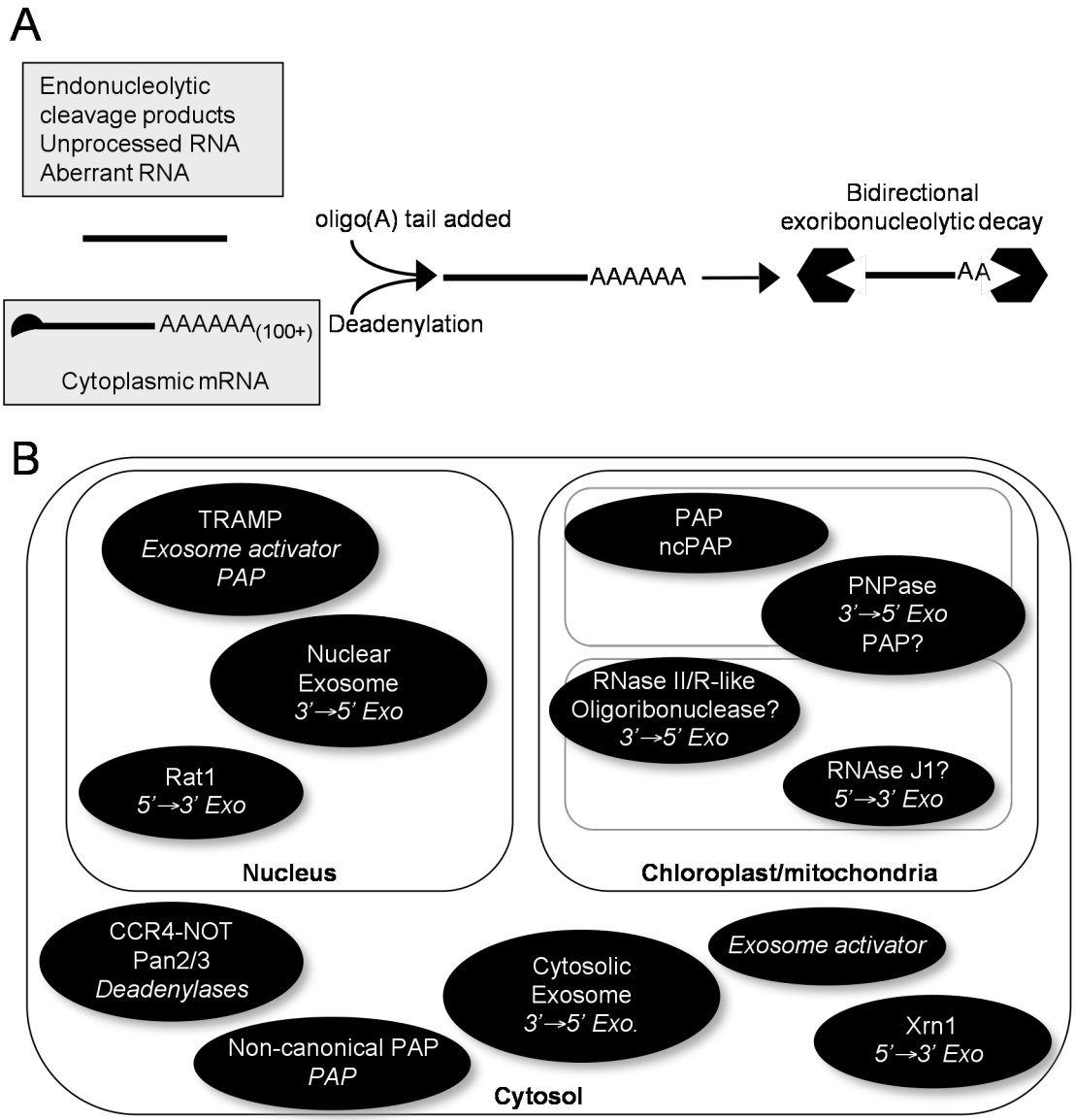

Figure 4.1: Synopsis of prokaryotic/organellar and eukaryotic exoribonucleolytic decay.
(A) Two pathways for RNA decay. At top, stimulation of decay by addition of a poly(A) tail. Below, removal of long stabilizing poly(A) tails. In both cases decay is completed by exoribonuclease activities acting from both ends of the molecule. (B) Known or suspected subcellular localization of the RNA metabolism components discussed in this paper. For nuclear and cytosolic proteins, yeast nomenclature is used. Protein names are in plain font, and their catalytic activities are in italics. For the organellar proteins, names of bacterial homologues are given.

For this work we initially reviewed all known and predicted exoribonucleases (reviewed in Carpousis *et al.*, 1999; Bollenbach *et al.*, 2004; Meyer *et al.*, 2004). Cells contain both 3' → 5' and 5' → 3' exoribonucleases (Figure 4.1), of which only the former class has been found in organelles and prokaryotes. 3' → 5' decay overcomes either secondary structure or stabilizing proteins, or acts on molecules that lack these features. Transcripts particularly vulnerable to exoribonuclease digestion include incomplete or aberrant RNAs such as premature termination products, endonucleolytic cleavage products (intermediates of RNA decay), and mRNAs that have lost their protective cap and long poly(A) tail. Conversely, 3' → 5' activity contributes to maturation of tRNAs, chloroplast mRNAs, and organellar rRNAs. A summary of most non-organellar pathways involving 3' → 5' degradation, which involve among others rRNAs, snRNAs and snoRNAs, can be found in Houseley *et al.* (2006). 5' → 3' exoribonucleases are encoded by small gene families and are involved in nuclear and cytosolic RNA decay (Newbury, 2006). In plants the family size is slightly larger, and members play a major role in RNA silencing mechanisms (Gy *et al.*, 2007). With respect to organelles, at least *Chlamydomonas* chloroplasts have a net 5' → 3' pathway (Drager *et al.*, 1999; Hicks *et al.*, 2002), but the enzymes involved are unknown. Exoribonucleases are often found in complexes, such as the bacterial degradosome and the nuclear/cytosolic exosome, which are discussed in more detail in Results. These complexes include accessory factors, including helicases and RNA-binding proteins, which were also investigated for this article.

Certain RNA-specific nucleotidyltransferase (NTR) family members were also studied, in particular polyadenylate polymerases (PAPs) and CCA-

transferases (CCAtrs), the latter of which add -CC, -A, or -CCA to the 3' ends of tRNAs (Martin and Keller, 2007). Of the PAPs, the classical nuclear version adds long tails to mRNAs, promoting nuclear export and translation. The PAP in *E. coli* is of a different NTR class, and like its chloroplast and mitochondrial counterparts is responsible for transient polyadenylation, which can increase the affinity of mRNAs or RNA fragments for the exoribonuclease polynucleotide phosphorylase (PNPase; Lisitsky *et al.*, 1997; Lisitsky and Schuster, 1999). PNPase is also a polynucleotide polymerase, although not of the NTR family. The organellar poly(A)-stimulated degradation pathway is partly related to the metabolism of nucleus-encoded mRNAs, where deadenylation of a long poly(A) tail ultimately results in a short poly(A) tail that can serve as a foothold for the exoribonuclease decay machinery, known as the exosome (Meyer *et al.*, 2004). Finally, there is a distinct family of non-canonical PAPs (ncPAPs), whose nuclear and cytosolic members have been implicated in decay-inducing, as well as stabilizing, polyadenylation (Martin and Keller, 2007), while a human mitochondrial member is responsible for addition of mRNA tails (Tomecki *et al.*, 2004).

Taking together the protein classes described above, one can infer that the structure of the major exoribonucleolytic machinery seems to be conserved in most systems. This encompasses PNPase multimers in prokaryotes and organelles, and the exosome in Archaea, the nucleus, and the cytosol. In prokaryotic and many or perhaps all organellar systems, PNPase is arranged in a ring-shaped trimer (Symmons *et al.*, 2000). The same structure is maintained in the exosome, except that the domains reside on different proteins and come together to form the core exosome (Symmons *et al.*, 2002;

Houseley *et al.*, 2006). We describe below how our findings for *Chlamydomonas* fit into these previously-established paradigms.

RESULTS [†]

Summary of relevant Chlamydomonas *proteins*

Tables 4.1 and 4.2 contain the complete collection of *Chlamydomonas* proteins likely to play a role in trimming or extending the ends of RNA molecules. Defining domains of each protein are listed, along with potential subcellular localization, whether there is EST or cDNA support, and whether the cDNA support indicates an error in the predicted protein.

Known or predicted organellar enzymes and those with no obvious yeast homologues are placed in Table 4.1. Of the 15, 10 are known or likely to be organellar based on published data, targeting experiments, or prediction software. Of these, six are from prokaryotic gene families and four are ncPAPs. Only five lack EST or cDNA support. However, only one of the protein predictions can be verified as correct with cDNA support; all others were either corrected before submission to Genbank, had to be amended before analysis, or are correct but only within a limited region of cDNA support. One amended model, the putative NTR PAP3, is unusual in that it contains a long intron which encodes, in the opposite orientation, a ubiquitin-specific protease.

[†] Zhangjun Fei, Research Scientist at the Boyce Thompson Institute, Ithaca, NY, contributed the following to these results: (1) generated the query interface for version 4.0 of the *Chlamydomonas* genome, (2) performed the HMM searches on the TimeLogic Decypher System, (3) Performed the InterProScans, and (4) constructed the phylogenetic trees.

Table 4.1: *Chlamydomonas* nucleotidyltransferases, exoribonucleases, and similar proteins for which sequence analysis suggests a role in RNA metabolism.

Protein	Gene Name	Genbank Accession[1]	Domain	Sub-cellular location[2]	cDNA support
RNAi					
MUT68	*MUT68*	ABI79451	PAP/25A core	**x**	Y
Organellar RNA decay					
PNPase	*PNP1*	ABF57675	RNase PH, KH, SI	**cp**, mt	Y
RNase II/R	*RNB2*	ABO20871	RNase II	**cp**	Y
Oligoribo nuclease	*ORN1*	EDP06341	DEDD exonuclease	NP	N
RNase J1	*RNJ1*	EU518648-EU518649[3]	RNA β-lactamase	cp	Y
PAP4	*PAP4*	EU311729	PAP/25A core	cp	Y
Suv3	*SUV3*	*142113*	DExDC helicase	mt	N
Class II NTR					
	PAP3	EDP00507[4] *206563*	PAP head domain	cp (weak)	Y
PAP (other non-canonical)					
	PAP2	EDP08764[4] *206516*	PAP/25A core	cp (strong)	Y
	PAP5	EDP08040[4] *206568*	PAP_assoc	no target	N
	PAP6	EDP01690[4] *206567*	PAP/25A core	mt (weak)	Y
	PAP7	EDP09686	PAP/25A core	n	N
	PAP8	EDP02954	PAP/25A core	cp	Y
	PAP9	EDP01828	PAP/25A core	mt	N
	PAP10	EDO99083	PAP/25A core	no target	Y

[1]Where gene model has not been deposited in Genbank, only *Chlamydomonas* version 3.1 protein ID is listed, in italics.
[2]x: cytosolic; cp: chloroplast; mt: mitochondrial; n: nucleus; NP: available sequence does not allow prediction to be made. *Chlamydomonas* locations in **bold** have experimental support. All others are predictions based on the software described in Methods.
[3]The two accession numbers represent alternative splicing variants.
[4]EST-based corrected versions of these protein predictions were constructed for targeting analysis. The corresponding *Chlamydomonas* version 3.1 protein ID is listed in italics.

Table 4.2: Putative *Chlamydomonas* orthologues of *S. cerevisiae* exoribonucleases and associated proteins

	Sc	*Chlamydomonas*		Domain	Location[2]		cDNA
		Gene ID	Genbank[1]		*Sc*	*Cr*	
Exosome complex							
Subunits with domains also found in PNPase[3]							
Archaeal Rrp41-like	Rrp41p	RNPH1	EDP01605	RNase PH	n/x		Y
	Rrp46p	RRP46	EDP03843[4] *206570*	RNase PH	n/x		Y
	Mtr3p		EDP04906	RNase PH	n/x		N
Archaeal Rrp42-like	Rrp42p	RNPH2	*205556*[4] *206571*	RNase PH	n/x		Y
	Rrp43p	RRP43	EDP05793	RNase PH	n/x		N
	Rrp45p	RNPH3	EDP06132	RNase PH	n/x		N
RNA binding	Rrp4p	RRP4	EDO97018	S1/KH	n/x		N
	Rrp40p	RRP40	EDP07280	S1/KH	n/x		Y
	Csl4p	CSL4	EDP07209	S1/zinc ribbon	n/x		Y
Other subunit							
	Rrp44p	RNB1	EDP03330	RNase II/R	n/x	**x or n**	Y
Location-specific subunits[5]							
	Rrp6p		many exos	RNase T/D	N		
	Rrp47p		none	RNA binding?	N		
	Ski7p		none	GTPase?	X		
TRAMP complex							
	Mtr4p	MTR4	EDO96924[4] *206573*	DExH-box helicase	n/x	n	Y
		HEN2	EDP01779	DExH-box helicase	n/x	-	Y
or	Trf4p	TRF4	EDP00455	PAP/25A core, PAP_assoc	N	n	Y
	Trf5p		none	PAP/25A core, PAP_assoc	N		
or	Air1p	CGLD20	EDP02869	RING Zn-finger	N	-	
	Air2p	RSZ22	EDP00877	RING Zn-finger	N		

Table 4.2 (Continued)

	Sc	*Chlamydomonas*		Domain	Location[2]		cDNA
		Gene ID	Genbank[1]		*Sc*	*Cr*	
Nuclear PAP and cytosolic deadenylases							
	PAP1	PAP1	EDP06435[4] *206508*	PAP_central	N	n	Y
	Pan2p	PAN2	EDP05128	RNase D family	X		N
	Pan3p		none	RNase D family	X		
or	Caf1p	CAF1	EDP00109	RNase CAF1	n/x		Y
	Caf1p	CAF2	EDP06748	RNase CAF1	n/x		N
or	Ccr4p	CCR4	EDO97283	Exonuclease III & leucine-rich	X		Y
	Ccr4p	CCR5	EDP04957	Exonuclease III & leucine-rich	X		N
	PARN (Human)		none	DEDD 3' exonuclease	X		
5'→3' exoribonucleases							
	Xrn1p	XRN1	*149305*	5'→3' exonuclease	X	m	Y
	Rat1p	XRN2	*206539*	5'→3' exonuclease	N	-	Y
	Xrn1p	XRN3	*149248*	5'→3' exonuclease	X	-	Y

[1]Where gene model has not been deposited in Genbank, only *Chlamydomonas* version 3.1 protein ID is listed, in italics.

[2]x: cytosol; n: nucleus; m: mitochondria; -: no subcellular location was predicted. **Bold**: location has experimental support, all others are predictions

[3]Boxes contain groups of proteins, there may be no 1:1 association

[4]EST-based corrected versions of these protein predictions were constructed for targeting analysis. The corresponding *Chlamydomonas* version 3.1 protein ID is listed in italics.

[5]Boxes contain protein models with similar domains, not necessarily homologous to the proteins listed.

Table 4.2 includes those enzymes that have been extensively studied in yeast. This comprises 15 exosome or exosome-associated enzymes, three 5' → 3' exoribonucleases, one nuclear PAP and five deadenylases. One of the 5' → 3' exoribonucleases was predicted to be mitochondrially-localized, but was included with its gene family in Table 4.2 because such a localization has no biological precedent. Of the fifteen predicted proteins with cDNA support, three were proven correct, five were incorrect and had to be amended, and partial cDNA support shows no errors in the remaining seven. The sections below discuss each of these protein classes in further detail.

Organellar RNA end-trimming and extension

Chloroplast exoribonucleolytic decay: Following endonucleolytic cleavage, 3' → 5' decay can occur from the newly-formed 3' end, a process which can be accelerated by transient polyadenylation. The enzymes and mechanisms involved are discussed in Bollenbach *et al.* (2008), and are similar to what is found in bacteria.

Poly(A) polymerases and CCA transferases: In *E. coli*, PAP1 generates the transient poly(A) tail, although PNPase, being a readily reversible enzyme, also generates A-rich tails and can substitute for PAP1 (Mohanty and Kushner, 2000a). It is still unknown whether a dedicated PAP is necessary to generate the transient poly(A) or A-rich tails observed in *Chlamydomonas*, *Arabidopsis*, spinach, and maize chloroplasts (Haff and Bogorad, 1976; Kudla *et al.*, 1996; Lisitsky *et al.*, 1996; Komine *et al.*, 2000; Walter *et al.*, 2002), or whether this role can be entirely fulfilled by PNPase, as appears to be the case in the cyanobacterium *Synechocystis* PCC6803 (Rott *et al.*, 2003).

E. coli PAP1 is a Class II NTR, as are eukaryotic and bacterial CCAtrs. Class II NTRs contain the same active domain fold as Class I NTRs, such as nuclear PAPs and archaeal CCAtrs, although the classes are otherwise divergent in sequence. Although it is difficult to utilize primary sequence to distinguish activities of members within each class, a particular Glu residue appears to be essential for the incorporation of cytosine during tRNA modification (Martin and Keller, 2004). We expected to find at least three Class II NTRs in *Chlamydomonas,* to provide CCAtrs for both the chloroplast and mitochondria and PAP for the chloroplast, but found only two, one of which possesses the distinguishing Glu. The *PAP4* gene encodes the NTR lacking the Glu, whereas the *PAP3* gene product contains the Glu, and shares very high homology with the putative *Arabidopsis* NTR At1g22660. Both *Chlamydomonas* proteins possess predicted chloroplast transit peptides. Although prediction software is not as well trained on *Chlamydomonas* proteins as on those of higher plants, if both *PAP3* and *PAP4* were chloroplast-localized, they would likely encode tRNA maturation and polyadenylation enzymes, respectively. However, this would raise the question of the source of CCA-adding activity in the mitochondria. Because in some organisms including plants CCAtrs can be dual-targeted (von Braun *et al.*, 2007), it is not unreasonable to suppose this might also be the case in *Chlamydomonas*.

Helicases: The DEAD-box helicase RhlB is present in the bacterial degradosome and stimulates the RNases therein (Coburn *et al.*, 1999; Khemici *et al.*, 2005). If chloroplast exoribonucleases operated in this context, we would anticipate finding an RhlB homologue in *Chlamydomonas*, but no such gene was located. On the other hand, tobacco VDL, a plastid protein,

does have similarity to RhlB, and its absence has severe defects on chloroplast differentiation (Wang *et al.*, 2000).

3' → 5' Exoribonucleolytic decay: *E. coli* utilizes several enzymes to perform 3'→ 5' decay, namely PNPase and the hydrolytic RNases II and R. PNPase is associated with the degradosome complex that includes RhlB, the endonuclease RNase E, and enolase, although several forms of the complex exist with alternative levels of activity (reviewed in Carpousis, 2007). In *Arabidopsis* and *Chlamydomonas* chloroplasts, PNPase depletion affects RNA stability and decay of polyadenylated transcripts, and in *Chlamydomonas* also the ability to withstand phosphorus deprivation (Walter *et al.*, 2002; Nishimura *et al.*, 2004; Yehudai-Resheff *et al.*, 2007). *Arabidopsis* RNR1, a homologue of RNase R, is required for chloroplast rRNA maturation (Bollenbach *et al.*, 2005), but also appears to be targeted to mitochondria (Perrin *et al.*, 2004).

In *Chlamydomonas*, three potential organellar 3' → 5' exoribonucleases were identified. One is the chloroplast PNPase mentioned above, and the other two are hydrolytic enzymes of the RNase II/R family, RNB1 and RNB2. To provide an experimental test of their possible organellar localization, transient expression of putative transit peptide-GFP fusions was performed. The 115 N-terminal amino acids of RNB2 localized GFP to the chloroplast, but results with RNB1 were ambiguous due to low GFP expression (Yehudai-Resheff *et al.*, 2007). Since then, higher-expressing transformants indicate that the RNB1 N-terminal 189 amino acids cannot target GFP to an organelle (data not shown). We therefore conclude that RNB1 is likely to be an orthologue of the yeast exosome subunit Rrp44, which is discussed in a later section.

5'→ 3' Exoribonucleolytic decay: As discussed in the Introduction, there is evidence of 5' → 3' exoribonucleolytic decay in *Chlamydomonas* chloroplasts. Prokaryotes do not encode canonical 5' → 3' exonucleases, although a net 5' → 3' maturation pathway is catalyzed by RNase J1 in *B. subtilis* (Mathy *et al.*, 2007). In *Chlamydomonas* chloroplasts, the enzyme responsible for 5' → 3' decay could be related to RNase J1, or might be a paralogue of a cytosolic or nuclear Xrn-type enzyme, or a dually-localized protein. As discussed in a later section, *Chlamydomonas* encodes three homologues of yeast Xrn1/Rat1 5' → 3' exoribonucleases, as well as a putative RNase J1.

Mitochondrial exoribonucleolytic decay: Mitochondrial polyadenylation, which would be expected to participate in a 3' → 5' decay pathway, is not confined to this role. While destabilizing polyadenylation is part of mitochondrial RNA decay in *Arabidopsis*, in other organisms such as humans, polyadenylation is required to complete translation termination codons and may stabilize the transcripts, as well as acting in the decay pathway. *S. cerevisiae*, in contrast, appears to have no mitochondrial polyadenylation whatsoever (reviewed in Gagliardi *et al.*, 2004; Slomovic *et al.*, 2005). Assuming that *Chlamydomonas* mtRNA does undergo polyadenylation, what enzyme is most likely to be responsible for this activity? In human mitochondria, the ncPAP hmtPAP fulfills this role (Tomecki *et al.*, 2004), and members of this family are encoded in *Chlamydomonas*, as described in the section on PAPs. Because the only two putative organellar NTRs (PAP3 and PAP4) are both predicted to be chloroplast proteins, they are not optimal candidates for either mitochondrial polyadenylation or CCAtr activity.

Yeast mtRNA decay is postulated to initiate with endonucleolytic cleavage, followed by processing by mtEXO, a complex that includes the helicase Suv3 and the exonuclease Dss1, which has several short regions of similarity to RNase II (Dmochowska *et al.*, 1995). AtSUV3, the *Arabidopsis* Suv3 homologue, has helicase activity and is located in the mitochondria (Gagliardi *et al.*, 1999); likewise, we found a *Chlamydomonas* Suv3 homologue. While a close homologue of Dss1 has been found in trypanosomes (Penschow *et al.*, 2004), the less- or unrelated proteins RNR1 and PNPase are known to have roles in RNA processing and/or decay in *Arabidopsis* mitochondria (Perrin *et al.*, 2004; Holec *et al.*, 2006). *Chlamydomonas* differs from *Arabidopsis*, though, since it appears to encode only one PNPase, already implicated in chloroplast RNA decay. Furthermore, initial experiments suggest that neither of the RNase II/R proteins, RNB1 or RNB2, is predominantly mitochondrial.

One remaining candidate for a mitochondrial exoribonuclease in *Chlamydomonas* is a predicted homologue of oligoribonuclease, ORN1, which in *E. coli* is responsible for converting oligoribonucleotides to monoribonucleotides (Ghosh and Deutscher, 1999), and is also found throughout the eukaryotes (reviewed in Zuo and Deutscher, 2001). The potential localization of the *Chlamydomonas* protein is ambiguous because the gene model is clearly incomplete, as the predicted ORF does not begin with a Met. Thus, the correctly annotated protein could include an N-terminal transit peptide.

Exoribonuclease digestion of the nuclear transcriptome - the exosome

The exosome is the basic enzymatic unit carrying out decay of nucleus-encoded and archaeal RNA, best-studied in *S. cerevisiae*, Archaea, kinetoplasts and humans, where the exosome has been reconstituted and/or crystallized (Buttner *et al.*, 2005; Liu *et al.*, 2006; Lorentzen *et al.*, 2007; Cristodero *et al.*, 2008). It has also been recently purified by TAP-tagging in *Arabidopsis* (Chekanova *et al.*, 2007). Each component of the nine or 10-subunit core exosome is necessary for cell viability in yeast and humans, and this core is common to the nuclear and cytosolic complexes, where it contains additional location-specific components. The core consists of six exonucleolytic RNase PH domain-type polypeptides, three unrelated RNA-binding proteins, and in yeast but apparently not humans, the RNase II/R family protein Rrp44 (Mitchell *et al.*, 1997; Allmang *et al.*, 1999; Liu *et al.*, 2006). The PH domain proteins fall into two groups, one more related to Rrp41 (Rrp41/Rrp46/Mtr3) and the other to Rrp42 (Rrp42/Rrp43/Rrp45). Certain members of both groups in plants and Archaea have shown 3' → 5' exonuclease activity using *in vitro* assays (Chekanova *et al.*, 2002; Lorentzen *et al.*, 2005; Hooker *et al.*, 2007), but the yeast and human orthologues do not (Liu *et al.*, 2006). The RNA-binding proteins have S1 and in some cases KH domains, and are represented in yeast by Rrp4, Rrp40 and Csl4. Curiously, the *Arabidopsis* Csl4 mutant has no growth phenotype (Chekanova *et al.*, 2007).

The situation in *Chlamydomonas* appears to mostly parallel that in yeast. When protein predictions from *Chlamydomonas* and *Arabidopsis* were searched for RNase PH domains, nine *Arabidopsis* and seven *Chlamydomonas* predicted proteins were found, although one

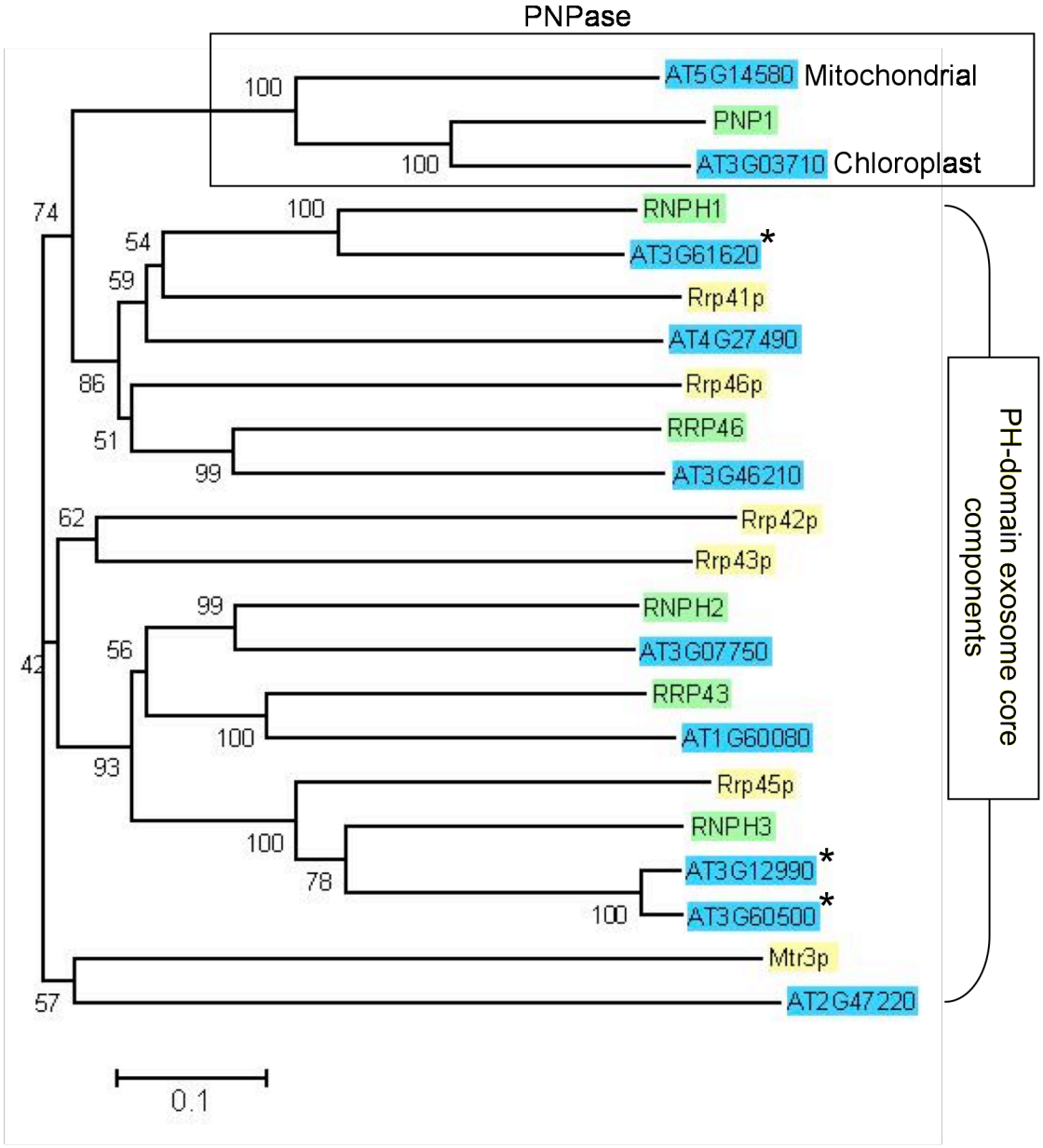

Figure 4.2: Phylogenetic analysis of *Arabidopsis* (blue), *Chlamydomonas* (green), and yeast (yellow) PH exoribonuclease domain-containing proteins.
Asterisks indicate cases where ribonuclease activity of the protein has been experimentally verified. Regarding the *Arabidopsis* gene models, Chekanova *et al.* (2007) list At4g27490 as the Mtr3 homologue, and do not identify At2g47220. They further note that At3g60500 but not At3g12990 copurify with the TAP-tagged exosome.

Chlamydomonas homologue had only weak sequence similarity with the RNase PH domain consensus, and was not analyzed further. The *Arabidopsis* and *Chlamydomonas* proteins were compared to the six PH-domain core exosome components from yeast, and the resulting relationships are shown in Figure 4.2. A separate clade is formed by the *Chlamydomonas* and *Arabidopsis* PNPase proteins, which also have PH domains. *Chlamydomonas* PNP1 is more closely related to the chloroplast than the mitochondrial isoform from *Arabidopsis*, consistent with the published data cited earlier.

With respect to the exosome subunits, two *Chlamydomonas* proteins fall into the Rrp41 group and three into the Rrp42 group. The corresponding numbers in *Arabidopsis* are four and four. This reflects in the former case a possible duplication of Rrp41 and the presence of an Mtr3 homologue, which is not found in *Chlamydomonas*. In terms of the Rrp42 group, *Arabidopsis* has a clear and probably recent duplication of Rrp45, the two of which exhibit some functional redundancy (Hooker *et al.*, 2007). While neither organism appears to encode a protein in the Rrp42/Rrp43 clade, bootstrap values suggest this may be artifactual. As presented in Figure 4.2 and Table 4.2, *Chlamydomonas* has one fewer catalytic core component than yeast (and two fewer than *Arabidopsis*). Whether an Mtr3 homologue is encoded in as-yet unsequenced DNA, or whether CrRNPH1 and CrRRP46 together fulfill the function of the Rrp41 group, remains to be established. Based on inferred active site residues (Lorentzen *et al.*, 2005), CrRNPH1 (Rrp41) is predicted to exhibit exonuclease activity, whereas Rrp46 is not. *Chlamydomonas* would thus resemble plants/Archaea more than yeast/humans in this respect.

As shown in Table 4.2, the RNA-binding components Rrp4, Rrp40 and Csl4 have a one-to-one relationship with predicted *Chlamydomonas* proteins.

Furthermore, the Rrp44 subunit could be represented by *Chlamydomonas* RNB1, which as discussed above has the requisite RNase II motifs and is apparently not organellar. Overall, the core exosome components are largely conserved, represented at present by nine *Chlamydomonas* gene models.

Other exosome and exosome-related proteins

Nuclear exosome components: In yeast, the exonuclease Rrp6 and putative RNA-binding protein Rrp47 join the core to complete the nuclear exosome (Allmang *et al.*, 1999; Mitchell *et al.*, 2003). *Chlamydomonas* homologues were not found for Rrp47 or Rrp6, a D/T family exonuclease, although several putative proteins (EDP00977, EDP01505, EDP06690, EDP08895, and EDO96190) share domains with RNase D, and thus are members of the exonuclease superfamily (Zuo and Deutscher, 2001). In contrast, *Arabidopsis* possesses three Rrp6 homologues, one of which has been implicated in degradation of nuclear polyadenylated RNA (Lange *et al.*, 2008).

TRAMP: The yeast nuclear exosome requires activation by the TRAMP complex (LaCava *et al.*, 2005). TRAMP has the dual roles of adding the short poly(A) tail to the target transcript and activating the exosome (Houseley *et al.*, 2006). It contains an ncPAP, either Trf4 or Trf5 (Houseley and Tollervey, 2006), the helicase Mtr4p (de la Cruz *et al.*, 1998), and either Air1p or Air2p (Wyers *et al.*, 2005), homologous proteins that contain a zinc-knuckle domain thought to bind RNA. The likely *Chlamydomonas* homologue of the Trf4/Trf5 proteins, CrTRF4, is discussed below along with other ncPAPs. Since yeast Mtr4 has a paralogue, Ski2, which acts in cytosolic exosome activation (Anderson and Parker, 1998), phylogenetic analysis was performed on

Chlamydomonas and *Arabidopsis* proteins with helicase domains related to those of Mtr4 and Ski2 (Figure 4.3). High bootstrap values lend confidence to the placement of two putative *Chlamydomonas* and *Arabidopsis* proteins in the Mtr4 clade. One of the *Chlamydomonas* proteins appears to be the true orthologue, with the second most closely related to the putative helicase HEN2, a plant regulator of floral homeotic genes (Western *et al.*, 2002).

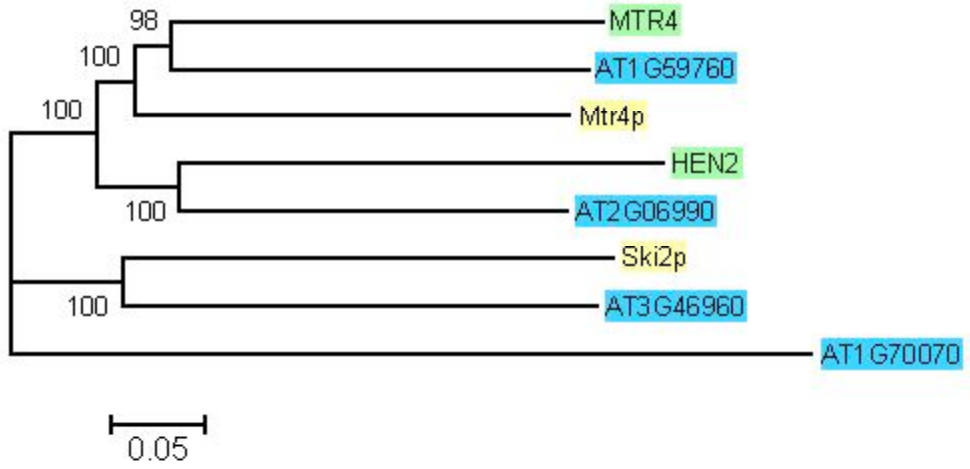

Figure 4.3: Phylogenetic analysis of *Arabidopsis* (blue), *Chlamydomonas* (green), and yeast (yellow) exosome-associated helicase proteins.

Concerning Ski2, this protein appears to have an *Arabidopsis* orthologue, however such a predicted protein is lacking in *Chlamydomonas*. Finally, a BLASTp performed with yeast Air1 and Air2 produced no hits on the translated *Chlamydomonas* genome, and no Pfam or Interpro consensus domains for the Air1 zinc-knuckle subfamily were available for domain searches. However, we did perform a search for the less specific CCHC-type

zinc finger Interpro consensus sequence and found ten predicted *Chlamydomonas* proteins, two of which are robust protein models with EST support (Table 4.2). One of these, CGLD20, belongs to the green lineage of *Chlamydomonas* genes (Merchant *et al.*, 2007). To summarize exosome accessory components, it seems likely that transient polyadenylation by a TRAMP-like complex occurs in *Chlamydomonas* nuclei, but activation of the nuclear exosome appears not to occur as it does in yeast.

Cytosolic exosome components: In addition to the core, the yeast cytosolic exosome possesses Ski7 (Araki *et al.*, 2001), but this protein is apparently lacking in *Chlamydomonas*. Ski7 contains only general domains and predicted functions, so domain-based searches of the *Chlamydomonas* databases were not performed. Furthermore, no homologues of the yeast exosome-activating complex Ski2-3-8 were found (Ski2 was discussed above).

Stabilizing poly(A) polymerase and cytosolic deadenylases: When the initial substrate for decay is cytosolic mRNA, the process begins with exoribonucleolytic digestion to remove most of the long, stabilizing poly(A) tail. Yeast possesses several deadenylation complexes, the major deadenylase being CCR4-Not and the minor deadenylase Pan2/Pan3. Deadenylation initiates decapping and following this, 5' → 3' exonucleolytic decay is possible (reviewed in Meyer *et al.*, 2004). At the same time, the shortened poly(A) tail minus its binding proteins is an ideal substrate for the cytosolic exosome, which begins degrading from the opposite (3') end. The Class I NTR PAP responsible for adding stabilizing tails to mRNA is likely encoded in *Chlamydomonas* by *PAP1*. Though the corresponding protein sequence lacks the expected nuclear localization signal, it also lacks EST support in the region where the NLS should be present, according to alignments with other

eukaryotic PAPs (Martin and Keller, 1996). Additionally, LOCTree (Nair and Rost, 2005) predicts nuclear localization based on other factors.

In terms of deadenylation components, the deadenylase domain from Caf1, one of the CCR4-Not complex deadenylases, was found in two predicted proteins, although these Caf1 homologues lack the N-terminal 100 or more amino acids found in the yeast protein. Ccr4, the other CCR4-NOT deadenylase, contains both a nuclease domain and leucine-rich repeat, but no *Chlamydomonas* predicted proteins were found with both of these features, even though two models did possess the nuclease domain. Some Ccr4-containing organisms possess additional proteins of unknown function containing the same nuclease domain but similarly lacking this repeat. Other components of the CCR4-NOT complex in yeast have unknown functions and were not investigated. One predicted protein similar to Pan2 of the minor deadenylase Pan2/Pan3 was found. The deadenylase PARN, which has been found in mammals, *Xenopus*, and *Arabidopsis* (Korner and Wahle, 1997; Copeland and Wormington, 2001; Chiba *et al.*, 2004), was not found in *Chlamydomonas*, strengthening the view that this is an enzyme specific for regulating development and stress responses in multicellular organisms.

Non-canonical poly(A) polymerases

In our search for predicted proteins containing PAP domains, we identified nine putative proteins that were not part of the traditional NTR family, but contained similar PAP catalytic domains. These ncPAPs lack RNA recognition motifs found in the NTR family members (Keller and Martin, 2002; Wang *et al.*, 2002), and have only recently begun to be characterized, initially with *Schizosaccharomyces pombe* Cid1 and Cid13 (Read *et al.*, 2002; Saitoh

et al., 2002) and *Caenorhabditis elegans* GLD2 (Wang *et al.*, 2002). The family also includes Trf4 and Trf5 of the TRAMP complex, which was mentioned above.

The *Chlamydomonas* family of nine ncPAPs is large, not as many as the 12 in *C. elegans* (Martin and Keller, 2007), but slightly exceeding the six in *S. pombe* (Stevenson and Norbury, 2006) and eight in *Arabidopsis*, and sharply contrasting with the two in *S. cerevisiae* (Trf4 and Trf5). In Tables 4.1 and 4.2, the *Chlamydomonas* ncPAPs are MUT68, TRF4, and the seven homologues listed under the heading "PAP (other non-canonical)". To attempt to establish possible orthologous relationships, we constructed several phylogenetic trees either based on global sequence alignments, or using individually or in combination the two domains found in this family, PAP/25A_core and PAP_associated. These analyses all showed that with the exception of a few closely-related proteins, there is great diversity among the ncPAPs of *Arabidopsis* and *Chlamydomonas*, whether looking within or between organisms. Bootstrap values indicated that most of the relationships are not robust and are thus not informative (data not shown). None of the *Chlamydomonas* ncPAPs appear to have arisen through relatively recent gene duplications, and in only one case is there a clear relationship between *Chlamydomonas* and *Arabidopsis* proteins, those being PAP5 and AT2G45620, neither of which has been characterized.

5'→3' exoribonucleases

S. cerevisiae contains a nuclear 5'→3' exonuclease, Rat1 (Xrn2), and a related cytosolic homologue, Xrn1 (Johnson, 1997). *Chlamydomonas* encodes three similar proteins (Table 4.2), equal to the number previously identified in

Arabidopsis (Kastenmayer and Green, 2000). All three have some level of EST support, and *XRN1* mRNA (equivalent to *Arabidopsis XRN2*) is alternatively spliced near its 5' end (David Higgs, pers. comm.), although there is no evidence that this is the case in *Arabidopsis*. None of the *Chlamydomonas* proteins contain predicted nuclear localization signals, but both splice variants of *XRN1* encode putatively mitochondrial proteins. It is possible that the mitochondrion, or perhaps the chloroplast, is now utilizing one of these proteins for decay of its own RNA, despite its absence in the pre-symbiotic organelle. A second possibility is that 5' → 3' exonuclease activity in chloroplasts is catalyzed by RNase J1, for which the *Chlamydomonas* homologue is predicted to be chloroplast-targeted, whether encoded by either of two mRNA splice variants (Table 4.1). Although RNase J1 and a related protein RNase J2 were originally characterized as endoribonucleases in *B. subtilis* (Even *et al.*, 2005), RNase J1 has been newly associated with 5' → 3' exonuclease activity (Mathy *et al.*, 2007), and ultimately accomodates both (de la Sierra-Gallay *et al.*, 2008).

DISCUSSION

Given the increasing recognition of RNA-based regulatory mechanisms, we felt it was important to identify the spectrum of RNA metabolic enzymes encoded in *Chlamydomonas*, where chloroplast RNA stability is subject to gene-specific regulation (Monde *et al.*, 2000), and where some of the earliest results related to RNA-based gene silencing were obtained (Cerutti *et al.*, 1997). Because a great variety of enzymes can modify RNA through polymerization, degradation, or covalent modification, we focused on

subgroups responsible for 5' and 3' end metabolism. Even with this restriction, the resultant protein complement is active in four subcellular compartments in photosynthetic eukaryotes, as well as in prokaryotes. The catalytic members are targeted to substrates by inherent preferences or through regulatory subunits embedded in multisubunit complexes, and some of these accessory moieties were also studied here.

Several key concepts emerged from our analysis, one being an apparent shortage with respect to the number of exoribonucleases and NTRs we believed to be necessary for RNA end metabolism in *Chlamydomonas* organelles. There are several possible reasons for this. First, there is a chance that the proteins of interest are encoded in the relatively small, unsequenced portion of the genome. Second, we may have identified the full complement of proteins, but perhaps a number of them are dual-targeted, for example PNPase, RNB2, the putative poly(A) polymerase PAP4, and/or the putative CCA-transferase PAP3. Dual-organelle targeting is difficult to predict computationally, although perhaps surprisingly common (reviewed in Millar *et al*., 2006). A third possibility is that proteins acting on the nuclear transcriptome, or their paralogues, have been recruited to the organelles to perform these functions. This may be the case with the 5' → 3' exoribonucleases, as one example. In addition, a number of the non-canonical PAPs have predicted organellar transit peptides (see below), and there is precedent for a mitochondrial PAP of this family in humans and *S. pombe* (Stevenson and Norbury, 2006). We also raised the possibility that *Chlamydomonas* homologues of oligoribonuclease and RNase J1 fulfill some of the "missing" functions.

A second general outcome of our study is that core exosome components are largely conserved in *Chlamydomonas*. Five of six PH-domain containing subunits appear to have a *Chlamydomonas* homologue, with *Arabidopsis* evincing instances of gene duplication, for example in the case of Rrp41. Concerning the other components of the core exosome, it was relatively easy to assign *Chlamydomonas* genes to the RNA-binding subunits Rrp4, Rrp40, and Csl4. Finally, targeting experiments revealed that the RNase II/R protein RNB1 is likely to be the Rrp44 homolog, which may or may not be part of the exosome in *Chlamydomonas*.

A surprising feature of the *Chlamydomonas* exosome is that unlike *S. cerevisiae*, it appears to have no cell compartment-specific components. Although putative orthologues of the Mtr4 and Trf4 enzymes of the nuclear TRAMP complex were present, the proteins utilized in yeast to activate the cytosolic exosome are apparently absent in *Chlamydomonas*. Although Ski2, the cytosolic Mtr4 paralogue, has a putative *Arabidopsis* orthologue, there does not appear to be one in *Chlamydomonas*. Additionally, the other proteins comprising the Ski2-Ski7-Ski8 complex are missing. Our conclusion is that *Chlamydomonas* either does not need to activate its cytosolic exosome, or that it has another mechanism for doing so.

A third major finding was the large family of non-canonical PAPs encoded in *Chlamydomonas*. To see if this was typical of green (chlorophyte) algae, we searched the genomes of *Ostreococcus tauri* (Derelle *et al.*, 2006) and *Volvox carteri* (http://www.jgi.doe.gov/Volvox), the latter being a close relative of *Chlamydomonas* that is nonetheless multicellular. We found evidence for only three ncPAPs in *Ostreococcus* but eight in *Volvox*,

suggesting some degree of expansion may have occurred in the order Volvocales.

The ncPAPs are found throughout the eukaryotes and contain a typical PAP catalytic domain, but otherwise lack similarity to PAPs, as well as consensus RNA-binding domains (Stevenson and Norbury, 2006). Based on our knowledge of the current pathways utilizing ncPAPs, we may speculate that *Chlamydomonas* ncPAPs play roles in both cytosolic and nuclear exosome-catalyzed decay, targeting the exosome to specific substrates. In this way, *Chlamydomonas* could also enhance the specificity of its cytosolic exosome, which as mentioned above does not appear to contain the accessory subunits found elsewhere.

An ncPAP studied in *Chlamydomonas* is MUT68, which is proposed to function in RNAi by adding a short poly(A) tail to DICER cleavage products, thus creating exosome substrates (Ibrahim *et al.*, 2006). One or more of the other ncPAPs could function like Cid1 and Cid13, polyadenylating a set of mRNAs to stabilize them, or could be involved in newly-described modification pathways involving polyuridylation (Wilusz and Wilusz, 2008). One potentially significant observation is that MUT68 and PAP6 are linked in the nuclear genome, being in the same orientation and separated by approximately 72 kb in version 4. They also are found in the same clade in various phylogenetic trees built for *Chlamydomonas* ncPAPs, with bootstrap values of 73-80 (data not shown). These facts together could reflect an ancient gene duplication, and possibly functional conservation. None of the putative *Chlamydomonas* ncPAPs, including MUT68, belong to the “Green cut” proteins present in only plant lineages (Merchant *et al.*, 2007), which could have implicated them in the chloroplast RNA decay pathways described earlier.

In summary, the ancient roots of RNA metabolism are consistent with conservation of mechanisms and individual enzymes, as we have found here in a number of cases. As is often found in genome-wide analyses, however, each organism has its peculiarities even within an otherwise conserved context. In the case of *Chlamydomonas*, this points to ncPAPs and the cytosolic exosome as particularly fruitful areas for future research, along with potential dual targeting of one or several organellar ribonucleases.

MATERIALS AND METHODS

Data resources: *C. reinhardtii* genome sequences, protein sequences (version 3.1), and EST unigene sequences were downloaded from the DOE Joint Genome Institute (JGI; http://genome.jgi-psf.org/Chlre3/). A query interface for genome versions 3.1 and 4 was implemented at the Boyce Thompson Institute (http://codequest.bti.cornell.edu/chlre). *Arabidopsis* (version 7) and *S. cerevisiae* protein sequences (updated 09/06/2007) were downloaded from TAIR (http://www.*Arabidopsis*.org) and SGD (http://www.yeastgenome.org/), respectively.

Methods: *Chlamydomonas*, *Arabidopsis* and yeast protein sequences, and *Chlamydomonas* EST unigene sequences were used to perform HMM searches against the Pfam domain database (Bateman *et al.*, 2004) with a TimeLogic Decypher system (http://codequest.bti.cornell.edu/chlre). The same sequences were also searched against the InterPro database (Mulder *et al.*, 2002) with a parallel InterProScan on the Cornell Computational Biology Service Unit MS Windows computer cluster

(http://cbsuapps.tc.cornell.edu/piprscan.aspx). Predicted proteins involved in some aspect of trimming or extending the ends of RNA were identified based on their Pfam and InterPro domains. Pfam domains utilized were 01138, 00773, 03725, 01909, 04857, 01743, and 03828. Interpro domains utilized were 003029, 001900, 011082, 011545, 001650, 001201, 002058, 002934, 004087, 001878 and 002646. To identify any genes missed by prediction programs in *Chlamydomonas* version 3.1 proteins, a subset of Pfam hidden Markov models was compared to the translated *Chlamydomonas* whole genome sequences (versions 3.1 and 4.0). For all the sequence database searches, a cutoff value of $1e^{-5}$ was used.

To predict potential mitochondrial or plastid targeting, Predotar (http://urgi.versailles.inra.fr/predotar/predotar.html; (Small *et al.*, 2004) and TargetP (http://www.cbs.dtu.dk/services/TargetP/; (Emanuelsson *et al.*, 2000) were used. This was only done if the gene model appeared complete and began with a Met codon. For nuclear localization signals, we used PredictNLS (http://cubic.bioc.columbia.edu/cgi/var/nair/resonline.pl; (Cokol *et al.*, 2000), and for proteins displaying ambiguous results, LOCTree was used (http://cubic.bioc.columbia.edu/cgi/var/nair/loctree/query; (Nair and Rost, 2005). Multiple sequence alignments were performed using ClustalW (Chenna *et al.*, 2003). Phylogenetic trees were constructed on the basis of amino acid differences (p-distance) by the Neighbor-Joining (NJ) method using the MEGA3 program (Kumar *et al.*, 2004). Robustness of the NJ trees was tested using the bootstrap method with 1000 replicates.

CHAPTER 5

FUTURE PERSPECTIVES

In this study, I used a reverse genetic approach to explore the enzymology of chloroplast poly(A)-mediated RNA decay. My investigation of one putative poly(A) polymerase, PAP4, also led me to explore the nature of mitochondrial polynucleotide tails located within the *cox1* transcript.

A major limitation of my research was an inability to reliably and stably silence candidate genes. Fortunately, our understanding and knowledge of gene silencing in *Chlamydomonas* is progressing. Several *Chlamydomonas* miRNAs have recently been characterized (Molnar *et al.*, 2007; Zhao *et al.*, 2007). Additionally, a method developed in *Arabidopsis* for utilizing native miRNAs to silence alternative targets (Schwab *et al.*, 2006) can be adapted to generate a similar *Chlamydomonas* silencing system. Our laboratory is currently developing this.

Based on data presented in Chapter 2, rigorous silencing of RNB2 and RNase J1 should yield informative data as to *Chlamydomonas* chloroplast ribonuclease activity. I suggest here that other promising targets are PAP4 and the putative organellar ncPAPs. Mitochondrial tails obtained after a more stable silencing of PAP4 should provide a definitive answer as to whether PAP4 generates either the poly(A) or the U-rich tails. The fact that these U-rich tails have not been observed as part of other decay pathways makes the discovery of the responsible enzyme more lucrative. Since the poly(U)-generating capacity of ncPAPs has only just been discovered, data obtained

from *Chlamydomonas* will be relevant to researchers studying polyuridylation in other organisms.

The function of *Chlamydomonas* mitochondrial tails should also be determined. This would include identifying tails on other transcripts, as well as determining whether tails are found at the 3' end of mitochondrial transcripts, where they may be stabilizing, as they are in humans (Slomovic *et al.*, 2005), or destabilizing, as in the mitochondria of trypanosomes and plants (Militello and Read, 2000; Gagliardi *et al.*, 2004), or only on endonucleolytic cleavage products as they are in bacteria and chloroplasts (Ingle and Kushner, 1996; Lisitsky *et al.*, 1996). The preliminary work to identify tails on the *nad3* transcript has already been done, and the tails are currently under analysis. To see if 3' terminal tails exist, designing primers near the end of transcripts for use with my current method of detection and analysis would be a convenient experimental plan. Additionally, it would not be difficult to utilize G-tailed RNA and the dCdT-adapter primer on RNA from higher plants to determine if U-rich tails are specific to *Chlamydomonas*, or a more general feature of mitochondria from green lineages.

Finally, I explored the contributions of the enzymes PNPase and PAP4 to chloroplast polyadenylation. I described in Chapter 2 how the polyadenylation and degradation activity of PNPase might be regulated by Pi, and provided experimental evidence that this might occur *in vivo*. However, the effect of P depletion on the activity of PNPase was only investigated in the context of degradation. The next step would be to ask whether an increase in polyadenylation accompanies the decreased degradation activity observed upon P depletion. Increased polyadenylation could presumably be identified by the presence of longer tails than those observed in normal conditions. These

future studies on PNPase polyadenylation under conditions of P limitation would complement the studies on its capacity to act as an exonuclease under the same circumstances.

REFERENCES

Allmang, C., Petfalski, E., Podtelejnikov, A., Mann, M., Tollervey, D., and Mitchell, P. (1999). The yeast exosome and human PM-Scl are related complexes of 3' to 5' exonucleases. Genes Dev. **13,** 2148-2158.

Amiott, E.A., and Jaehning, J.A. (2006). Mitochondrial transcription Is regulated via an ATP "sensing" mechanism that couples RNA abundance to respiration. Mol. Cell **22,** 329-338.

Anderson, J.S., and Parker, R.P. (1998). The 3' to 5' degradation of yeast mRNAs is a general mechanism for mRNA turnover that requires the SKI2 DEVH box protein and 3' to 5' exonucleases of the exosome complex. EMBO J. **17,** 1497-1506.

Araki, Y., Takahashi, S., Kobayashi, T., Kajiho, H., Hoshino, S., and Katada, T. (2001). Ski7p G protein interacts with the exosome and the Ski complex for 3'-to-5' mRNA decay in yeast. EMBO J. **20,** 4684-4693.

Asamizu, E., Nakamura, Y., Sato, S., Fukuzawa, H., and Tabata, S. (1999). A large scale structural analysis of cDNAs in a unicellular green alga, *Chlamydomonas reinhardtii*. I. Generation of 3433 non-redundant expressed sequence tags. DNA Res. **6,** 369-373.

August, J.T., Ortiz, P.J., and Hurwitz, J. (1962). Ribonucleic acid-dependent ribonucleotide incorporation. I. Purification and properties of the enzyme. J. Biol. Chem. **237,** 3786-3793.

Baginsky, S., Shteiman-Kotler, A., Liveanu, V., Yehudai-Resheff, S., Bellaoui, M., Settlage, R.E., Shabanowitz, J., Hunt, D.F., Schuster, G., and Gruissem, W. (2001). Chloroplast PNPase exists as a homo-multimer enzyme complex that is distinct from the *Escherichia coli* degradosome. RNA **7,** 1464-1475.

Balbo, P.B., and Bohm, A. (2007). Mechanism of poly(A) polymerase: structure of the enzyme-MgATP-RNA ternary complex and kinetic analysis. Structure **15,** 1117-1131.

Bannai, H., Tamada, Y., Maruyama, O., Nakai, K., and Miyano, S. (2002). Extensive feature detection of N-terminal protein sorting signals. Bioinformatics **18,** 298-305.

Barkan, A., and Goldschmidt-Clermont, M. (2000). Participation of nuclear genes in chloroplast gene expression. Biochimie **82,** 559-572.

Bateman, A., Coin, L., Durbin, R., Finn, R.D., Hollich, V., Griffiths-Jones, S., Khanna, A., Marshall, M., Moxon, S., Sonnhammer, E.L.,

Studholme, D.J., Yeats, C., and Eddy, S.R. (2004). The Pfam protein families database. Nucleic Acids Res. **32,** D138-141.

Beck, C.F. (2005). Signaling pathways from the chloroplast to the nucleus. Planta **222,** 743-756.

Beligni, M.V., and Mayfield, S.P. (2008). *Arabidopsis thaliana* mutants reveal a role for CSP41a and CSP41b, two ribosome-associated endonucleases, in chloroplast ribosomal RNA metabolism. Plant Mol. Biol. **67**, 389-401.

Bernstein, J.A., Lin, P.-H., Cohen, S.N., and Lin-Chao, S. (2004). Global analysis of *Escherichia coli* RNA degradosome function using DNA microarrays. Proc. Natl. Acad. Sci. USA **101,** 2758-2763.

Blum, B., Bakalara, N., and Simpson, L. (1990). A model for RNA editing in kinetoplastid mitochondria: "Guide" RNA molecules transcribed from maxicircle DNA provide the edited information. Cell **60,** 189-198.

Bohne, A.V., Irihimovitch, V., Weihe, A., and Stern, D.B. (2006). *Chlamydomonas reinhardtii* encodes a single sigma^{70}-like factor which likely functions in chloroplast transcription. Curr. Genet. **49,** 333-340.

Bollenbach, T.J., Tatman, D.A., and Stern, D.B. (2003). CSP41a, a multifunctional RNA-binding protein, initiates mRNA turnover in tobacco chloroplasts. Plant J. **36,** 842-852.

Bollenbach, T.J., Schuster, G., and Stern, D.B. (2004). Cooperation of endo- and exoribonucleases in chloroplast mRNA turnover. Prog. Nucleic Acid Res. Mol. Biol. **78,** 305-337.

Bollenbach, T.J., Lange, H., Gutierrez, R., Erhardt, M., Stern, D.B., and Gagliardi, D. (2005). RNR1, a 3'-5' exoribonuclease belonging to the RNR superfamily, catalyzes 3' maturation of chloroplast ribosomal RNAs in *Arabidopsis thaliana*. Nucleic Acids Res. **33,** 2751-2763.

Bollenbach, T., Schuster, G., Portnoy V, and Stern, D.B. (2008). Processing, degradation and polyadenylation of chloroplast transcripts. Topics Curr. Genet. **19,** 175-211.

Britton, R.A., Wen, T., Schaefer, L., Pellegrini, O., Uicker, W.C., Mathy, N., Tobin, C., Daou, R., Szyk, J., and Condon, C. (2007). Maturation of the 5' end of *Bacillus subtilis* 16S rRNA by the essential ribonuclease YkqC/RNase J1. Mol. Microbiol. **63,** 127-138.

Buttner, K., Wenig, K., and Hopfner, K.P. (2005). Structural framework for the mechanism of archaeal exosomes in RNA processing. Mol. Cell **20,** 461-471.

Carpousis, A.J. (2007). The RNA degradosome of *Escherichia coli*: an mRNA-degrading machine assembled on RNase E. Annu. Rev. Microbiol. **61,** 71-87.

Carpousis, A.J., Vanzo, N.F., and Raynal, L.C. (1999). mRNA degradation. A tale of poly(A) and multiprotein machines. Trends Genet. **15,** 24-28.

Casas-Mollano, J.A., Rohr, J., Kim, E., Balassa, E., Van Dijk, K., and Cerutti, H. (2008). Diversification of the core RNA interference machinery in *Chlamydomonas reinhardtii* and the role of DCL1 in transposon silencing. Genetics **179,** In Press.

Cerutti, H., Johnson, A.M., Gillham, N.W., and Boynton, J.E. (1997). Epigenetic silencing of a foreign gene in nuclear transformants of *Chlamydomonas*. Plant Cell **9,** 925-945.

Chekanova, J.A., Dutko, J.A., Mian, I.S., and Belostotsky, D.A. (2002). *Arabidopsis thaliana* exosome subunit AtRrp4p is a hydrolytic 3'-->5' exonuclease containing S1 and KH RNA-binding domains. Nucleic Acids Res. **30,** 695-700.

Chekanova, J.A., Gregory, B.D., Reverdatto, S.V., Chen, H., Kumar, R., Hooker, T., Yazaki, J., Li, P., Skiba, N., Peng, Q., Alonso, J., Brukhin, V., Grossniklaus, U., Ecker, J.R., and Belostotsky, D.A. (2007). Genome-wide high-resolution mapping of exosome substrates reveals hidden features in the *Arabidopsis* transcriptome. Cell **131,** 1340-1353.

Chen, H.W., Rainey, R.N., Balatoni, C.E., Dawson, D.W., Troke, J.J., Wasiak, S., Hong, J., McBride, H., Koehler, C.M., Teitell, M.A., and French, S.W. (2006). Mammalian PNPase is an intermembrane space ribonuclease that maintains mitochondrial homeostasis. Mol. Cell. Biol **26**, 8475-8487.

Chen, Q., Adams, C.C., Usack, L., Yang, J., Monde, R., and Stern, D.B. (1995). An AU-rich element in the 3' untranslated region of the spinach chloroplast *petD* gene participates in sequence-specific RNA-protein complex formation. Mol. Cell. Biol. **15,** 2010-2018.

Cheng, Z.F., and Deutscher, M.P. (2003). Quality control of ribosomal RNA mediated by polynucleotide phosphorylase and RNase R. Proc. Natl. Acad. Sci. USA **100,** 6388-6393.

Chenna, R., Sugawara, H., Koike, T., Lopez, R., Gibson, T.J., Higgins, D.G., and Thompson, J.D. (2003). Multiple sequence alignment with the Clustal series of programs. Nucleic Acids Res. **31,** 3497-3500.

Chiba, Y., Johnson, M.A., Lidder, P., Vogel, J.T., van Erp, H., and Green, P.J. (2004). AtPARN is an essential poly(A) ribonuclease in *Arabidopsis*. Gene **328,** 95-102.

Choquet, Y., and Wollman, F.A. (2002). Translational regulations as specific traits of chloroplast gene expression. FEBS Lett **529,** 39-42.

Coburn, G.A., and Mackie, G.A. (1996). Overexpression, purification, and properties of *Escherichia coli* ribonuclease II. J. Biol. Chem. **271,** 1048-1053.

Coburn, G.A., and Mackie, G.A. (1999). Degradation of mRNA in *Escherichia coli*: an old problem with some new twists. Prog. Nucleic Acid Res. Mol. Biol. **62,** 55-108.

Coburn, G.A., Miao, X., Briant, D.J., and Mackie, G.A. (1999). Reconstitution of a minimal RNA degradosome demonstrates functional coordination between a 3' exonuclease and a DEAD-box RNA helicase. Genes Dev. **13,** 2594-2603.

Cokol, M., Nair, R., and Rost, B. (2000). Finding nuclear localization signals. EMBO Rep. **1,** 411-415.

Copeland, P.R., and Wormington, M. (2001). The mechanism and regulation of deadenylation: identification and characterization of *Xenopus* PARN. RNA **7,** 875-886.

Cristodero, M., Bottcher, B., Diepholz, M., Scheffzek, K., and Clayton, C. (2008). The *Leishmania tarentolae* exosome: Purification and structural analysis by electron microscopy. Mol. Biochem. Parasitol. **159**, 24-29.

Curtis, M.D., and Grossniklaus, U. (2003). A gateway cloning vector set for high-throughput functional analysis of genes *in planta*. Plant Physiol. **133,** 462-469.

de la Cruz, J., Kressler, D., Tollervey, D., and Linder, P. (1998). Dob1p (Mtr4p) is a putative ATP-dependent RNA helicase required for the 3' end formation of 5.8S rRNA in *Saccharomyces cerevisiae*. EMBO J. **17,** 1128-1140.

de la Sierra-Gallay, I.L., Zig, L., Jamalli, A., and Putzer, H. (2008). Structural insights into the dual activity of RNase J. Nat. Struct. Mol. Biol. **15,** 206-212.

Deikus, G., Condon, C., and Bechhofer, D.H. (2008). Role of *Bacillus subtilis* RNase J1 endonuclease and 5' exonuclease activities in *trp* leader RNA turnover. J. Biol. Chem. **In Press**.

Deng, X.W., and Gruissem, W. (1987). Control of plastid gene expression during development: the limited role of transcriptional regulation. Cell **49,** 379-387.

Derelle, E., Ferraz, C., Rombauts, S., Rouze, P., Worden, A.Z., Robbens, S., Partensky, F., Degroeve, S., Echeynie, S., Cooke, R., Saeys, Y., Wuyts, J., Jabbari, K., Bowler, C., Panaud, O., Piegu, B., Ball, S.G., Ral, J.P., Bouget, F.Y., Piganeau, G., De Baets, B., Picard, A., Delseny, M., Demaille, J., Van de Peer, Y., and Moreau, H. (2006). Genome analysis of the smallest free-living eukaryote *Ostreococcus tauri* unveils many unique features. Proc. Natl. Acad. Sci. USA **103,** 11647-11652.

Deutscher, M.P. (1993). Promiscuous exoribonucleases of *Escherichia coli*. J. Bacteriol. **175,** 4577-4583.

Dmochowska, A., Golik, P., and Stepien, P.P. (1995). The novel nuclear gene *DSS1* of *Saccharomyces cerevisiae* is necessary for mitochondrial biogenesis. Curr. Genet. **28,** 108-112.

Donovan, W.P., and Kushner, S.R. (1986). Polynucleotide phosphorylase and ribonuclease II are required for cell viability and mRNA turnover in *Escherichia coli* K-12. Proc. Natl. Acad. Sci. USA **83,** 120-124.

Drager, R.G., Higgs, D.C., Kindle, K.L., and Stern, D.B. (1999). 5' to 3' exoribonucleolytic activity is a normal component of chloroplast mRNA decay pathways. Plant J. **19,** 521-532.

Drager, R.G., Girard-Bascou, J., Choquet, Y., Kindle, K.L., and Stern, D.B. (1998). *In vivo* evidence for 5'−3' exoribonuclease degradation of an unstable chloroplast mRNA. Plant J. **13,** 85-96.

Dreyfus, M., and Regnier, P. (2002). The poly(A) tail of mRNAs. Bodyguard in eukaryotes, scavenger in bacteria. Cell **111,** 611-613.

Duchene, A.M., Giritch, A., Hoffmann, B., Cognat, V., Lancelin, D., Peeters, N.M., Zaepfel, M., Marechal-Drouard, L., and Small, I.D. (2005). Dual targeting is the rule for organellar aminoacyl-tRNA synthetases in *Arabidopsis thaliana*. Proc. Natl. Acad. Sci. USA **102,** 16484-16489.

Emanuelsson, O., Nielsen, H., Brunak, S., and von Heijne, G. (2000). Predicting subcellular localization of proteins based on their N-terminal amino acid sequence. J. Mol. Biol. **300,** 1005-1016.

Even, S., Pellegrini, O., Zig, L., Labas, V., Vinh, J., Brechemmier-Baey, D., and Putzer, H. (2005). Ribonucleases J1 and J2: two novel endoribonucleases in *B. subtilis* with functional homology to *E. coli* RNase E. Nucleic Acids Res. **33,** 2141-2152.

Filipowicz, W., Bhattacharyya, S.N., and Sonenberg, N. (2008). Mechanisms of post-transcriptional regulation by microRNAs: are the answers in sight? Nat. Rev. Genet. **9,** 102-114.

Gagliardi, D., and Leaver, C.J. (1999). Polyadenylation accelerates the degradation of the mitochondrial mRNA associated with cytoplasmic male sterility in sunflower. EMBO J. **18,** 3757-3766.

Gagliardi, D., Perrin, R., Marechal-Drouard, L., Grienenberger, J.M., and Leaver, C.J. (2001). Plant mitochondrial polyadenylated mRNAs are degraded by a 3'- to 5'-exoribonuclease activity, which proceeds unimpeded by stable secondary structures. J. Biol. Chem. **276,** 43541-43547.

Gagliardi, D., Stepien, P.P., Temperley, R.J., Lightowlers, R.N., and Chrzanowska-Lightowlers, Z.M.A. (2004). Messenger RNA stability in mitochondria: different means to an end. Trends Genet. **20,** 260-267.

Gagliardi, D., Kuhn, J., Spadinger, U., Brennicke, A., Leaver, C.J., and Binder, S. (1999). An RNA helicase (AtSUV3) is present in *Arabidopsis thaliana* mitochondria. FEBS Lett. **458,** 337-342.

Ghosh, S., and Deutscher, M.P. (1999). Oligoribonuclease is an essential component of the mRNA decay pathway. Proc. Natl. Acad. Sci. USA **96,** 4372-4377.

Gonsalvez, G.B., Urbinati, C.R., and Long, R.M. (2005). RNA localization in yeast: moving towards a mechanism. Biol. Cell **97,** 75-86.

Green, P.J. (1994). The ribonucleases of higher plants. Ann. Rev. Plant Physiol. Plant Mol. Biol. **45,** 421-445.

Grossman, A. (2000). Acclimation of *Chlamydomonas reinhardtii* to its nutrient environment. Protist **151,** 201-224.

Grunberg-Manago, M., Ortiz, P.J., and Ochoa, S. (1956). Enzymatic synthesis of polynucleotides. I. Polynucleotide phosphorylase of *azotobacter vinelandii*. Biochim. Biophys. Acta. **20,** 269-285.

Gy, I., Gasciolli, V., Lauressergues, D., Morel, J.B., Gombert, J., Proux, F., Proux, C., Vaucheret, H., and Mallory, A.C. (2007). *Arabidopsis* FIERY1, XRN2, and XRN3 are endogenous RNA silencing suppressors. Plant Cell **19**, 3451-3461.

Haff, L.A., and Bogorad, L. (1976). Poly(adenylic acid)-containing RNA from plastids of maize. Biochemistry **15,** 4110-4115.

Hajnsdorf, E., Steier, O., Coscoy, L., Teysset, L., and Regnier, P. (1994). Roles of RNase E, RNase II and PNPase in the degradation of the *rpsO* transcripts of *Escherichia coli*: stabilizing function of RNase II and evidence for efficient degradation in an *ams pnp rnb* mutant. EMBO J. **13,** 3368-3377.

Harris, E.H. (1989). The *Chlamydomonas* Sourcebook: A comprehensive guide to biology and laboratory use. (San Diego: Academic Press).

Helliwell, C., and Waterhouse, P. (2003). Constructs and methods for high-throughput gene silencing in plants. Methods **30,** 289-295.

Herrin, D.L., and Nickelsen, J. (2004). Chloroplast RNA processing and stability. Photosynth. Res. **82,** 301-314.

Hicks, A., Drager, R.G., Higgs, D.C., and Stern, D.B. (2002). An mRNA 3' processing site targets downstream sequences for rapid degradation in *Chlamydomonas* chloroplasts. J. Biol. Chem. **277,** 3325-3333.

Holec, S., Lange, H., Kuhn, K., Alioua, M., Borner, T., and Gagliardi, D. (2006). Relaxed transcription in *Arabidopsis* mitochondria is counterbalanced by RNA stability control mediated by polyadenylation and polynucleotide phosphorylase. Mol. Cell. Biol. **26,** 2869-2876.

Hooker, T.S., Lam, P., Zheng, H., and Kunst, L. (2007). A core subunit of the RNA-processing/degrading exosome specifically influences cuticular wax biosynthesis in *Arabidopsis*. Plant Cell **19,** 904-913.

Houseley, J., and Tollervey, D. (2006). Yeast Trf5p is a nuclear poly(A) polymerase. EMBO Rep. **7,** 205-211.

Houseley, J., LaCava, J., and Tollervey, D. (2006). RNA-quality control by the exosome. Nat. Rev. Mol. Cell Biol. **7,** 529-539.

Hwang, S., Kawazoe, R., and Herrin, D.L. (1996). Transcription of *tufA* and other chloroplast-encoded genes is controlled by a circadian clock in *Chlamydomonas*. Proc. Natl. Acad. Sci. USA **93,** 996-1000.

Ibrahim, F., Rohr, J., Jeong, W.J., Hesson, J., and Cerutti, H. (2006). Untemplated oligoadenylation promotes degradation of RISC-cleaved transcripts. Science **314,** 1893.

Ingle, C.A., and Kushner, S.R. (1996). Development of an *in vitro* mRNA decay system for *Escherichia coli*: poly(A) polymerase I is necessary to trigger degradation. Proc. Natl. Acad. Sci. USA **93,** 12926-12931.

Johnson, A.W. (1997). Rat1p and Xrn1p are functionally interchangeable exoribonucleases that are restricted to and required in the nucleus and cytoplasm, respectively. Mol. Cell. Biol. **17,** 6122-6130.

Jupin, I., Bouzoubaa, S., Richards, K., Jonard, G., and Guilley, H. (1990). Multiplication of beet necrotic yellow vein virus RNA3 lacking a 3' poly(A) tail is accompanied by reappearance of the poly(A) tail and a novel short U-rich tract preceding it. Virology **178,** 281-284.

Kao, C.Y., and Read, L.K. (2007). Targeted depletion of a mitochondrial nucleotidyltransferase suggests the presence of multiple enzymes that polymerize mRNA 3' tails in *Trypanosoma brucei* mitochondria. Mol. Biochem. Parasitol. **154,** 158-169.

Kastenmayer, J.P., and Green, P.J. (2000). Novel features of the XRN-family in *Arabidopsis*: evidence that AtXRN4, one of several orthologs of nuclear Xrn2p/Rat1p, functions in the cytoplasm. Proc. Natl. Acad. Sci. USA **97,** 13985-13990.

Keller, W., and Martin, G. (2002). Gene regulation: reviving the message. Nature **419,** 267-268.

Khemici, V., Poljak, L., Toesca, I., and Carpousis, A.J. (2005). Evidence *in vivo* that the DEAD-box RNA helicase RhlB facilitates the degradation

of ribosome-free mRNA by RNase E. Proc. Natl. Acad. Sci. USA **102,** 6913-6918.

Khrebtukova, I., and Spreitzer, R.J. (1996). Elimination of the *Chlamydomonas* gene family that encodes the small subunit of ribulose-1,5-bisphosphate carboxylase/oxygenase. Proc. Natl. Acad. Sci. USA **93,** 13689-13693.

Kim, M., Christopher, D.A., and Mullet, J.E. (1993). Direct evidence for selective modulation of *psbA*, *rpoA*, *rbcL*, and 16S RNA stability during barley chloroplast development. Plant Mol. Biol. **22,** 447-463.

Kishine, M., Takabayashi, A., Munekage, Y., Shikanai, T., Endo, T., and Sato, F. (2004). Ribosomal RNA processing and an RNase R family member in chloroplasts of *Arabidopsis*. Plant Mol. Biol. **55,** 595-606.

Komine, Y., Kikis, E., Schuster, G., and Stern, D. (2002). Evidence for *in vivo* modulation of chloroplast RNA stability by 3'-UTR homopolymeric tails in *Chlamydomonas reinhardtii*. Proc. Natl. Acad. Sci. USA **99,** 4085-4090.

Komine, Y., Kwong, L., Anguera, M.C., Schuster, G., and Stern, D.B. (2000). Polyadenylation of three classes of chloroplast RNA in *Chlamydomonas reinhardtii*. RNA **6,** 598-607.

Korner, C.G., and Wahle, E. (1997). Poly(A) tail shortening by a mammalian poly(A)-specific 3'-exoribonuclease. J. Biol. Chem. **272,** 10448-10456.

Kudla, J., Hayes, R., and Gruissem, W. (1996). Polyadenylation accelerates degradation of chloroplast mRNA. EMBO J. **15,** 7137-7146.

Kuhn, J., and Binder, S. (2002). RT-PCR analysis of 5' to 3'-end-ligated mRNAs identifies the extremities of cox2 transcripts in pea mitochondria. Nucleic Acids Res **30,** 439-446.

Kumar, S., Tamura, K., and Nei, M. (2004). MEGA3: Integrated software for Molecular Evolutionary Genetics Analysis and sequence alignment. Brief Bioinform. **5,** 150-163.

Kushner, S.R. (2002). mRNA decay in *Escherichia coli* comes of age. J. Bacteriol. **184,** 4658-4665.

Kushner, S.R. (2004). mRNA decay in prokaryotes and eukaryotes: different approaches to a similar problem. IUBMB Life **56,** 585-594.

Kwak, J.E., and Wickens, M. (2007). A family of poly(U) polymerases. RNA **13,** 860-867.

LaCava, J., Houseley, J., Saveanu, C., Petfalski, E., Thompson, E., Jacquier, A., and Tollervey, D. (2005). RNA degradation by the exosome is promoted by a nuclear polyadenylation complex. Cell **121,** 713-724.

Lakota, J., and Nelson, B.D. (1991). ADP is a substrate for the AAUAAA-directed poly(A) addition reaction catalyzed by HeLa cell nuclear extracts. Eur. J. Biochem. **195,** 685-689.

Lange, H., Holec, S., Cognat, V., Pieuchot, L., Le Ret, M., Canaday, J., and Gagliardi, D. (2008). Degradation of a polyadenylated rRNA maturation by-product involves one of the three RRP6-like proteins in *Arabidopsis thaliana*. Mol. Cell. Biol**.,** MCB.02064-02007.

Lezhneva, L., and Meurer, J. (2004). The nuclear factor HCF145 affects chloroplast *psaA-psaB-rps14* transcript abundance in *Arabidopsis thaliana*. Plant J. **38,** 740-753.

Li, F., Xiong, Y., Wang, J., Cho, H.D., Tomita, K., Weiner, A.M., and Steitz, T.A. (2002). Crystal structures of the *Bacillus stearothermophilus* CCA-adding enzyme and its complexes with ATP or CTP. Cell **111,** 815-824.

Lisitsky, I., and Schuster, G. (1999). Preferential degradation of polyadenylated and polyuridinylated RNAs by the bacterial exoribonuclease polynucleotide phosphorylase. Eur. J. Biochem. **261,** 468-474.

Lisitsky, I., Klaff, P., and Schuster, G. (1996). Addition of poly(A)-rich sequences to endonucleolytic cleavage sites in the degradation of spinach chloroplast mRNA. Proc. Natl. Acad. Sci. USA **93,** 13398-13403.

Lisitsky, I., Kotler, A., and Schuster, G. (1997). The mechanism of preferential degradation of polyadenylated RNA in the chloroplast: The exoribonuclease 100RNP-polynucleotide phosphorylase displays high binding affinity for poly(A) sequences. J. Biol. Chem. **272,** 17648-17653.

Littauer, U.Z., and Kornberg, A. (1957). Reversible synthesis of polyribonucleotides with an enzyme from *Escherichia coli*. J. Biol. Chem. **226,** 1077-1092.

Littauer, U.Z., and Soreq, H. (1982). Polynucleotide Phosphorylase. In The Enzymes, P.D. Boyer, ed (New York: Academic Press, Inc.), pp. 517-553.

Liu, Q., Greimann, J.C., and Lima, C.D. (2006). Reconstitution, activities, and structure of the eukaryotic RNA exosome. Cell **127,** 1223-1237.

Lorentzen, E., Dziembowski, A., Lindner, D., Seraphin, B., and Conti, E. (2007). RNA channelling by the archaeal exosome. EMBO Rep. **8,** 470-476.

Lorentzen, E., Walter, P., Fribourg, S., Evguenieva-Hackenberg, E., Klug, G., and Conti, E. (2005). The archaeal exosome core is a hexameric

ring structure with three catalytic subunits. Nat. Struct. Mol. Biol. **12,** 575-581.

Lupold, D.S., Caoile, A.G.F.S., and Stern, D.B. (1999). Polyadenylation occurs at multiple sites in maize mitochondrial *cox2* mRNA and is independent of editing status. Plant Cell **11,** 1565-1578.

Marín-Navarro, J., Manuell, A.L., Wu, J., and P., M.S. (2007). Chloroplast translation regulation. Photosynth. Res. **94,** 359-374.

Martin, G., and Keller, W. (1996). Mutational analysis of mammalian poly(A) polymerase identifies a region for primer binding and catalytic domain, homologous to the family X polymerases, and to other nucleotidyltransferases. EMBO J. **15,** 2593-2603.

Martin, G., and Keller, W. (2004). Sequence motifs that distinguish ATP(CTP):tRNA nucleotidyl transferases from eubacterial poly(A) polymerases. RNA **10,** 899-906.

Martin, G., and Keller, W. (2007). RNA-specific ribonucleotidyl transferases. RNA **13,** 1834-1849.

Martin, G., Moglich, A., Keller, W., and Doublie, S. (2004). Biochemical and structural insights into substrate binding and catalytic mechanism of mammalian poly(A) polymerase. J. Mol. Biol. **341,** 911-925.

Mathy, N., Benard, L., Pellegrini, O., Daou, R., Wen, T., and Condon, C. (2007). 5'-to-3' exoribonuclease activity in bacteria: role of RNase J1 in rRNA maturation and 5' stability of mRNA. Cell **129,** 681-692.

Mellman, D.L., Gonzales, M.L., Song, C., Barlow, C.A., Wang, P., Kendziorski, C., and Anderson, R.A. (2008). A PtdIns4,5P2-regulated nuclear poly(A) polymerase controls expression of select mRNAs. Nature **451,** 1013-1017.

Merchant, S.S., Prochnik, S.E., Vallon, O., Harris, E.H., Karpowicz, S.J., Witman, G.B., Terry, A., Salamov, A., Fritz-Laylin, L.K., Marechal-Drouard, L., Marshall, W.F., Qu, L.-H., Nelson, D.R., Sanderfoot, A.A., Spalding, M.H., Kapitonov, V.V., Ren, Q., Ferris, P., Lindquist, E., Shapiro, H., Lucas, S.M., Grimwood, J., Schmutz, J., Cardol, P., Cerutti, H., Chanfreau, G., Chen, C.-L., Cognat, V., Croft, M.T., Dent, R., Dutcher, S., Fernandez, E., Fukuzawa, H., Gonzalez-Ballester, D., Gonzalez-Halphen, D., Hallmann, A., Hanikenne, M., Hippler, M., Inwood, W., Jabbari, K., Kalanon, M., Kuras, R., Lefebvre, P.A., Lemaire, S.D., Lobanov, A.V., Lohr, M., Manuell, A., Meier, I., Mets, L., Mittag, M., Mittelmeier, T., Moroney, J.V., Moseley, J., Napoli, C., Nedelcu, A.M., Niyogi, K., Novoselov, S.V., Paulsen, I.T., Pazour, G., Purton, S., Ral, J.-P., Riano-Pachon, D.M., Riekhof, W., Rymarquis, L., Schroda, M., Stern, D., Umen, J., Willows, R., Wilson, N., Zimmer, S.L., Allmer, J., Balk, J., Bisova, K., Chen, C.-J., Elias, M., Gendler, K., Hauser, C., Lamb, M.R., Ledford, H., Long, J.C., Minagawa, J., Page, M.D., Pan, J.,

Pootakham, W., Roje, S., Rose, A., Stahlberg, E., Terauchi, A.M., Yang, P., Ball, S., Bowler, C., Dieckmann, C.L., Gladyshev, V.N., Green, P., Jorgensen, R., Mayfield, S., Mueller-Roeber, B., Rajamani, S., Sayre, R.T., Brokstein, P., Dubchak, I., Goodstein, D., Hornick, L., Huang, Y.W., Jhaveri, J., Luo, Y., Martinez, D., Ngau, W.C.A., Otillar, B., Poliakov, A., Porter, A., Szajkowski, L., Werner, G., Zhou, K., Grigoriev, I.V., Rokhsar, D.S., and Grossman, A.R. (2007). The *Chlamydomonas* genome reveals the evolution of key animal and plant functions. Science **318,** 245-250.

Meyer, S., Temme, C., and Wahle, E. (2004). Messenger RNA turnover in eukaryotes: pathways and enzymes. Crit. Rev. Biochem. Mol. Biol. **39,** 197-216.

Militello, K.T., and Read, L.K. (2000). UTP-dependent and -independent pathways of mRNA turnover in *Trypanosoma brucei* mitochondria. Mol. Cell. Biol. **20,** 2308-2316.

Millar, A.H., Whelan, J., and Small, I. (2006). Recent surprises in protein targeting to mitochondria and plastids. Curr. Opin. Plant Biol. **9,** 610-615.

Misson, J., Raghothama, K.G., Jain, A., Jouhet, J., Block, M.A., Bligny, R., Ortet, P., Creff, A., Somerville, S., Rolland, N., Doumas, P., Nacry, P., Herrerra-Estrella, L., Nussaume, L., and Thibaud, M.C. (2005). A genome-wide transcriptional analysis using *Arabidopsis thaliana* Affymetrix gene chips determined plant responses to phosphate deprivation. Proc. Natl. Acad. Sci. USA **102,** 11934-11939.

Mitchell, P., Petfalski, E., Shevchenko, A., Mann, M., and Tollervey, D. (1997). The exosome: a conserved eukaryotic RNA processing complex containing multiple 3' to 5' exoribonucleases. Cell **91,** 457-466.

Mitchell, P., Petfalski, E., Houalla, R., Podtelejnikov, A., Mann, M., and Tollervey, D. (2003). Rrp47p is an exosome-associated protein required for the 3' processing of stable RNAs. Mol. Cell. Biol. **23,** 6982-6992.

Mohanty, B.K., and Kushner, S.R. (1999). Analysis of the function of *Escherichia coli* poly(A) polymerase I in RNA metabolism. Mol. Microbiol. **34,** 1094-1108.

Mohanty, B.K., and Kushner, S.R. (2000a). Polynucleotide phosphorylase functions both as a 3' to 5' exonuclease and a poly(A) polymerase in *Escherichia coli*. Proc. Natl. Acad. Sci. USA **97,** 11966-11971.

Mohanty, B.K., and Kushner, S.R. (2000b). Polynucleotide phosphorylase, RNase II and RNase E play different roles in the *in vivo* modulation of polyadenylation in *Escherichia coli*. Mol. Microbiol. **36,** 982-994.

Mohanty, B.K., and Kushner, S.R. (2003). Genomic analysis in *Escherichia coli* demonstrates differential roles for polynucleotide phosphorylase

and RNase II in mRNA abundance and decay. Mol. Microbiol. **50,** 645-658.

Mohanty, B.K., Maples, V.F., and Kushner, S.R. (2004). The Sm-like protein Hfq regulates polyadenylation dependent mRNA decay in *Escherichia coli*. Mol. Microbiol. **54,** 905-920.

Molnar, A., Schwach, F., Studholme, D.J., Thuenemann, E.C., and Baulcombe, D.C. (2007). miRNAs control gene expression in the single-cell alga *Chlamydomonas reinhardtii*. Nature **447,** 1126-1129.

Monde, R.A., Schuster, G., and Stern, D.B. (2000). Processing and degradation of chloroplast mRNA. Biochimie **82,** 573-582.

Mudd, E.A., Sullivan, S., Gisby, M.F., Mironov, A., Kwon, C.S., Chung, W.I., and Day, A. (2008). A 125 kDa RNase E/G-like protein is present in plastids and is essential for chloroplast development and autotrophic growth in *Arabidopsis*. J. Exp. Bot.

Mulder, N.J., Apweiler, R., Attwood, T.K., Bairoch, A., Bateman, A., Binns, D., Biswas, M., Bradley, P., Bork, P., Bucher, P., Copley, R., Courcelle, E., Durbin, R., Falquet, L., Fleischmann, W., Gouzy, J., Griffith-Jones, S., Haft, D., Hermjakob, H., Hulo, N., Kahn, D., Kanapin, A., Krestyaninova, M., Lopez, R., Letunic, I., Orchard, S., Pagni, M., Peyruc, D., Ponting, C.P., Servant, F., and Sigrist, C.J. (2002). InterPro: an integrated documentation resource for protein families, domains and functional sites. Brief Bioinform. **3,** 225-235.

Murakami, S., Kuehnle, K., and Stern, D.B. (2005). A spontaneous tRNA suppressor of a mutation in the *Chlamydomonas reinhardtii* nuclear *MCD1* gene required for stability of the chloroplast *petD* mRNA. Nucleic Acids Res. **33,** 3372-3380.

Nair, R., and Rost, B. (2005). Mimicking cellular sorting improves prediction of subcellular localization. J. Mol. Biol. **348,** 85-100.

Nevins, J.R., and Joklik, W.K. (1977). Isolation and partial characterization of the poly(A) polymerases from HeLa cells infected with vaccinia virus. J Biol. Chem. **252,** 6939-6947.

Newbury, S.F. (2006). Control of mRNA stability in eukaryotes. Biochem. Soc. Trans. **34,** 30-34.

Nishimura, Y., Kikis, E.A., Zimmer, S.L., Komine, Y., and Stern, D.B. (2004). Antisense transcript and RNA processing alterations suppress instability of polyadenylated mRNA in *Chlamydomonas* chloroplasts. Plant Cell **16,** 2849-2869.

Penschow, J.L., Sleve, D.A., Ryan, C.M., and Read, L.K. (2004). TbDSS-1, an essential *Trypanosoma brucei* exoribonuclease homolog that has pleiotropic effects on mitochondrial RNA metabolism. Eukaryot. Cell **3,** 1206-1216.

Pepe, C.M., Maslesa-Galic, S., and Simons, R.W. (1994). Decay of the IS10 antisense RNA by 3' exoribonucleases: evidence that RNase II stabilizes RNA-OUT against PNPase attack. Mol. Microbiol. **13,** 1133-1142.

Perrin, R., Meyer, E.H., Zaepfel, M., Kim, Y.J., Mache, R., Grienenberger, J.M., Gualberto, J.M., and Gagliardi, D. (2004). Two exoribonucleases act sequentially to process mature 3'-ends of *atp9* mRNAs in *Arabidopsis* mitochondria. J. Biol. Chem. **279,** 25440-25446.

Portnoy, V., and Schuster, G. (2006). RNA polyadenylation and degradation in different Archaea; roles of the exosome and RNase R. Nucleic Acids Res. **34,** 5923-5931.

Portnoy, V., and Schuster, G. (2008). *Mycoplasma gallisepticum* as the first analyzed bacterium in which RNA is not polyadenylated. FEMS Microbiol. Lett. **283,** 97-103.

Raynal, L.C., Krisch, H.M., and Carpousis, A.J. (1998). The *Bacillus subtilis* nucleotidyltransferase is a tRNA CCA-adding enzyme. J. Bacteriol. **180,** 6276-6282.

Read, R.L., Martinho, R.G., Wang, S.W., Carr, A.M., and Norbury, C.J. (2002). Cytoplasmic poly(A) polymerases mediate cellular responses to S phase arrest. Proc. Natl. Acad. Sci. USA **99,** 12079-12084.

Reddy, K.J., and Gilman, M. (2001). Preparation of bacterial RNA. Curr. Protoc. Mol. Biol. **Chapter 4,** Unit 4.4.

Régnier, P., and Arraiano, C.M. (2000). Degradation of mRNA in bacteria: emergence of ubiquitous features. Bioessays **22,** 235-244.

Rissland, O.S., and Norbury, C.J. (2008). The Cid1 poly(U) polymerase. Biochim. Biophys. Acta **1779,** 286-294.

Rissland, O.S., Mikulasova, A., and Norbury, C.J. (2007). Efficient RNA polyuridylation by noncanonical poly(A) polymerases. Mol. Cell Biol. **27,** 3612-3624.

Rodermel, S., Haley, J., Jiang, C.Z., Tsai, C.H., and Bogorad, L. (1996). A mechanism for intergenomic integration: abundance of ribulose bisphosphate carboxylase small-subunit protein influences the translation of the large-subunit mRNA. Proc. Natl. Acad. Sci. USA. **93,** 3881-3885.

Rohr, J., Sarkar, N., Balenger, S., Jeong, B.R., and Cerutti, H. (2004). Tandem inverted repeat system for selection of effective transgenic RNAi strains in *Chlamydomonas*. Plant J. **40,** 611-621.

Rott, R., Drager, R.G., Stern, D.B., and Schuster, G. (1996). The 3' untranslated regions of chloroplast genes in *Chlamydomonas reinhardtii*

do not serve as efficient transcriptional terminators. Mol. Gen. Genet. **252,** 676-683.

Rott, R., Zipor, G., Portnoy, V., Liveanu, V., and Schuster, G. (2003). RNA polyadenylation and degradation in cyanobacteria are similar to the chloroplast but different from *Escherichia coli*. J. Biol. Chem. **278,** 15771-15777.

Ryan, C.M., and Read, L.K. (2005). UTP-dependent turnover of *Trypanosoma brucei* mitochondrial mRNA requires UTP polymerization and involves the RET1 TUTase. RNA **11,** 763-773.

Saha, D., Prasad, A.M., and Srinivasan, R. (2007). Pentatricopeptide repeat proteins and their emerging roles in plants. Plant Physiol. Biochem. **45,** 521-534.

Saitoh, S., Chabes, A., McDonald, W.H., Thelander, L., Yates, J.R., and Russell, P. (2002). Cid13 is a cytoplasmic poly(A) polymerase that regulates ribonucleotide reductase mRNA. Cell **109,** 563-573.

Salvador, M.L., Klein, U., and Bogorad, L. (1993). Light-regulated and endogenous fluctuations of chloroplast transcript levels in *Chlamydomonas*. Regulation by transcription and RNA degradation. Plant J. **3,** 213-219.

Schein, A., Sheffy-Levin, S., Glaser, F., and Schuster, G. (2008). The RNase E/G-type endoribonuclease of higher plants is located in the chloroplast and cleaves RNA similarly to the *E. coli* enzyme. RNA **Epub ahead of print**.

Schroda, M. (2006). RNA silencing in *Chlamydomonas*: mechanisms and tools. Curr. Genet. **49,** 69-84.

Schroda, M., Beck, C.F., and Vallon, O. (2002). Sequence elements within an HSP70 promoter counteract transcriptional transgene silencing in *Chlamydomonas*. Plant J. **31,** 445-455.

Schroda, M., Vallon, O., Wollman, F.A., and Beck, C.F. (1999). A chloroplast-targeted heat shock protein 70 (HSP70) contributes to the photoprotection and repair of photosystem II during and after photoinhibition. Plant Cell **11,** 1165-1178.

Schürer, H., Lang, K., Schuster, J., and Mörl, M. (2002). A universal method to produce *in vitro* transcripts with homogeneous 3' ends. Nucleic Acids Res. **30,** e56.

Schuster, G., Timberg, R., and Ohad, I. (1988). Turnover of thylakoid photosystem II proteins during photoinhibition of *Chlamydomonas reinhardtii*. Eur. J. Biochem. **177,** 403-410.

Schwab, R., Ossowski, S., Riester, M., Warthmann, N., and Weigel, D. (2006). Highly specific gene silencing by artificial microRNAs in *Arabidopsis*. Plant Cell **18,** 1121-1133.

Shen, B., and Goodman, H.M. (2004). Uridine addition after microRNA-directed cleavage. Science **306,** 997.

Shimogawara, K., Fujiwara, S., Grossman, A., and Usuda, H. (1998). High-efficiency transformation of *Chlamydomonas reinhardtii* by electroporation. Genetics **148,** 1821-1828.

Slomovic, S., and Schuster, G. (2008). Stable PNPase RNAi silencing: its effect on the processing and adenylation of human mitochondrial RNA. RNA **14,** 310-323.

Slomovic, S., Laufer, D., Geiger, D., and Schuster, G. (2005). Polyadenylation and degradation of human mitochondrial RNA: The prokaryotic past leaves its mark. Mol. Cell. Biol. **25,** 6427-6435.

Slomovic, S., Portnoy, V., Liveanu, V., and Schuster, G. (2006a). RNA polyadenylation in prokaryotes and organelles; Different tails tell different tales. Crit. Rev. Plant Sci. **25,** 65-77.

Slomovic, S., Laufer, D., Geiger, D., and Schuster, G. (2006b). Polyadenylation of ribosomal RNA in human cells. Nucleic Acids Res. **34,** 2966-2975.

Small, I., Peeters, N., Legeai, F., and Lurin, C. (2004). Predotar: A tool for rapidly screening proteomes for N-terminal targeting sequences. Proteomics **4,** 1581-1590.

Stern, D.B., and Gruissem, W. (1987). Control of plastid gene expression: 3' inverted repeats act as mRNA processing and stabilizing elements, but do not terminate transcription. Cell **51,** 1145-1157.

Stern, M.J., Ames, G.F.-L., Smith, N.H., Robinson, E.C., and Higgin, C.F. (1984). Repetitive extragenic palindromic sequences: A major component of the bacterial genome. Cell **37,** 1015-1026.

Stevenson, A.L., and Norbury, C.J. (2006). The Cid1 family of non-canonical poly(A) polymerases. Yeast **23,** 991-1000.

Symmons, M.F., Jones, G.H., and Luisi, B.F. (2000). A duplicated fold is the structural basis for polynucleotide phosphorylase catalytic activity, processivity, and regulation. Structure Fold Des. **8,** 1215-1226.

Symmons, M.F., Williams, M.G., Luisi, B.F., Jones, G.H., and Carpousis, A.J. (2002). Running rings around RNA: a superfamily of phosphate-dependent RNases. Trends Biochem. Sci. **27,** 11-18.

Tomecki, R., Dmochowska, A., Gewartowski, K., Dziembowski, A., and Stepien, P.P. (2004). Identification of a novel human nuclear-encoded mitochondrial poly(A) polymerase. Nucleic Acids Res. **32,** 6001-6014.

Tomita, K., and Weiner, A.M. (2002). Closely related CC- and A-adding enzymes collaborate to construct and repair the 3'-terminal CCA of tRNA in *Synechocystis sp*. and *Deinococcus radiodurans*. J. Biol. Chem. **277,** 48192-48198.

Trippe, R., Guschina, E., Hossbach, M., Urlaub, H., Luhrmann, R., and Benecke, B.J. (2006). Identification, cloning, and functional analysis of the human U6 snRNA-specific terminal uridylyl transferase. RNA **12,** 1494-1504.

Vanacova, S., and Stef, R. (2007). The exosome and RNA quality control in the nucleus. EMBO Rep. **8,** 651-657.

Vance, C.P., Uhde-Stone, C., and Allan, D.L. (2003). Phosphorus acquisition and use: critical adaptations by plants for securing a nonrenewable resource. New Phytologist **157,** 423-447.

von Braun, S.S., Sabetti, A., Hanic-Joyce, P.J., Gu, J., Schleiff, E., and Joyce, P.B. (2007). Dual targeting of the tRNA nucleotidyltransferase in plants: not just the signal. J. Exp. Bot. **58,** 4083-4093.

Walter, M., Kilian, J., and Kudla, J. (2002). PNPase activity determines the efficiency of mRNA 3'-end processing, the degradation of tRNA and the extent of polyadenylation in chloroplasts. EMBO J. **21,** 6905-6914.

Wang, L., Eckmann, C.R., Kadyk, L.C., Wickens, M., and Kimble, J. (2002). A regulatory cytoplasmic poly(A) polymerase in *Caenorhabditis elegans*. Nature **419,** 312-316.

Wang, Y., Duby, G., Purnelle, B., and Boutry, M. (2000). Tobacco VDL gene encodes a plastid DEAD box RNA helicase and is involved in chloroplast differentiation and plant morphogenesis. Plant Cell **12,** 2129-2142.

West, S., Gromak, N., Norbury, C.J., and Proudfoot, N.J. (2006). Adenylation and exosome-mediated degradation of cotranscriptionally cleaved pre-messenger RNA in human cells. Mol. Cell **21,** 437-443.

Western, T.L., Cheng, Y., Liu, J., and Chen, X. (2002). *HUA ENHANCER2*, a putative DExH-box RNA helicase, maintains homeotic B and C gene expression in *Arabidopsis*. Development **129,** 1569-1581.

Wickens, M., and Kwak, J.E. (2008). Molecular biology. A tail tale for U. Science **319,** 1344-1345.

Wilusz, C.J., and Wilusz, J. (2008). New ways to meet your (3') end oligouridylation as a step on the path to destruction. Genes Dev. **22,** 1-7.

Wostrikoff, K., and Stern, D. (2007). Rubisco large-subunit translation is autoregulated in response to its assembly state in tobacco chloroplasts. Proc. Natl. Acad. Sci. USA **104,** 6466-6471.

Wyers, F., Rougemaille, M., Badis, G., Rousselle, J.C., Dufour, M.E., Boulay, J., Regnault, B., Devaux, F., Namane, A., Seraphin, B., Libri, D., and Jacquier, A. (2005). Cryptic pol II transcripts are degraded by a nuclear quality control pathway involving a new poly(A) polymerase. Cell **121,** 725-737.

Xing, T., Malik, K., Martin, T., and Miki, B.L. (2001). Activation of tomato PR and wound-related genes by a mutagenized tomato MAP kinase kinase through divergent pathways. Plant Mol. Biol. **46,** 109-120.

Yamaguchi, K., Beligni, M.V., Prieto, S., Haynes, P.A., McDonald, W.H., Yates, J.R., 3rd, and Mayfield, S.P. (2003). Proteomic characterization of the *Chlamydomonas reinhardtii* chloroplast ribosome. Identification of proteins unique to the 70S ribosome. J. Biol. Chem. **278,** 33774-33785.

Yang, J., and Stern, D.B. (1997). The spinach chloroplast endoribonuclease CSP41 cleaves the 3' untranslated region of *petD* mRNA primarily within its terminal stem-loop structure. J. Biol. Chem. **272,** 12784-12880.

Yang, J., Schuster, G., and Stern, D.B. (1996). CSP41, a sequence-specific chloroplast mRNA binding protein, is an endoribonuclease. Plant Cell **8,** 1409-1420.

Yehudai-Resheff, S., and Schuster, G. (2000). Characterization of the *E.coli* poly(A) polymerase: nucleotide specificity, RNA-binding affinities and RNA structure dependence. Nucleic Acids Res. **28,** 1139-1144.

Yehudai-Resheff, S., Hirsh, M., and Schuster, G. (2001). Polynucleotide phosphorylase functions as both an exonuclease and a poly(A) polymerase in spinach chloroplasts. Mol. Cell. Biol. **21,** 5408-5416.

Yehudai-Resheff, S., Zimmer, S.L., Komine, Y., and Stern, D.B. (2007). Integration of chloroplast nucleic acid metabolism into the phosphate deprivation response in *Chlamydomonas reinhardtii*. Plant Cell **19,** 1023-1038.

Zhao, T., Li, G., Mi, S., Li, S., Hannon, G.J., Wang, X.J., and Qi, Y. (2007). A complex system of small RNAs in the unicellular green alga *Chlamydomonas reinhardtii*. Genes Dev. **21,** 1190-1203.

Zilhao, R., Cairrao, F., Regnier, P., and Arraiano, C.M. (1996). PNPase modulates RNase II expression in *Escherichia coli*: implications for mRNA decay and cell metabolism. Mol. Microbiol. **20,** 1033-1042.

Zimmer, S. L., Fei, Z., and Stern, D. B. (2008). Genome-based analysis of *Chlamydomonas reinhardtii* exoribonucleases and poly(A) polymerases

predicts unexpected organellar and exosomal features. Genetics **179**, 125-136.

Zuo, Y., and Deutscher, M.P. (2001). Exoribonuclease superfamilies: structural analysis and phylogenetic distribution. Nucleic Acids Res. **29,** 1017-1026.